รายงานวิจัยฉบับสมบูรณ์

Project Title : Synthesis and characterization of ligands bearing ferrocene and/or anthracene-adduct moieties for catalysis

(ชื่อโครงการ) การสังเคราะห์และการพิสูจน์โครงสร้างของลิแกนด์ที่มีเฟอร์โรซีนและแอนทราซีนแอดดักเป็นองค์ประกอบสำหรับการเร่งปฏิกิริยา

โดย
ผู้ช่วยศาสตราจารย์ เอกสิทธิ์ สมสุข
ภาควิชาเคมี คณะวิทยาศาสตร์ มหาวิทยาลัยมหิดล

18 กรกฎาคม 2552

สัญญาเลขที่ RMU4980050

รายงานวิจัยฉบับสมบูรณ์

Project Title : Synthesis and characterization of ligands bearing ferrocene and/or anthracene-adduct moieties for catalysis

(ชื่อโครงการ) การสังเคราะห์และการพิสูจน์โครงสร้างของลิแกนด์ที่มีเฟอร์โรซีนและแอนทราซีนแอดดักเป็นองค์ประกอบสำหรับการเร่งปฏิกิริยา

โดย
ผู้ช่วยศาสตราจารย์ เอกสิทธิ์ สมสุข
ภาควิชาเคมี คณะวิทยาศาสตร์ มหาวิทยาลัยมหิดล

สนับสนุนโดยสำนักงานกองทุนสนับสนุนการวิจัยและสำนักงานคณะกรรมการการอุดมศึกษา
(ความเห็นในรายงานนี้เป็นของผู้วิจัย สกว.ไม่จำเป็นต้องเห็นด้วยเสมอไป)

รูปแบบ Abstract (บทคัดย่อ)

Project Code : RMU4980050

(รหัสโครงการ)

Project Title : Synthesis and characterization of ligands bearing ferrocene and/or anthracene-adduct moieties for catalysis

(ชื่อโครงการ) การสังเคราะห์และการพิสูจน์โครงสร้างของลิแกนด์ที่มีเฟอร์โรซีนและแอนทราซีนแอดดักเป็นองค์ประกอบสำหรับการเร่งปฏิกิริยา

Investigator : Asst. Prof. Ekasith Somsook, Department of Chemistry, Faculty of Science, Mahidol University

(ชื่อนักวิจัย) ผศ. ดร. เอกสิทธิ์ สมสุข ภาควิชาเคมี คณะวิทยาศาสตร์ มหาวิทยาลัยมหิดล

E-mail Address : scess@mahidol.ac.th

Project Period : July 19, 2006 – July 18, 2009

(ระยะเวลาโครงการ) 19 ก.ค. 2549 – 18 ก.ค. 2552

ABSTRACT

In this research, ligands containing ferrocene moieties have been designed for Suzuki-Miyaura coupling reactions and atom transfer radical polymerization. Nanoparticles stabilized by ferrocene-containing ligands were successfully synthesized and characterized by many techniques. Ligand-supported Pd catalysts were utilized in the Suzuki-Miyaura cross-coupling reactions to improve the conversion and selectivity. In addition to coupling reactions, the atom transfer radical polymerization (ATRP) of methyl methacrylate (MMA) catalyzed by copper-tripodal complexes with ferrocene moieties (CuX/ TRENFcImine, X=Br or Cl) was investigated in order to understand the effect of redox active moieties on the performance of ATRP catalysts. The highly active and less controlled polymerization was probably caused by the electronic effect rather than the steric effect from ferrocene moieties resulted to the higher and lower in the activation and deactivation steps, respectively. The polydispersity was improved by the addition of $CuBr_2$ but the rates of polymerization became slower at this system.

KEYWORDS: Nanocatalysis, Suzuki-Miyaura cross-coupling. Atom transfer radical polymerization (ATRP), Ferrocene, Tripodal ligand.

บทคัดย่อ

ในงานวิจัยนี้ ได้ทำการศึกษาปฏิกิริยาการจับคู่และการสังเคราะห์พอลิเมอร์แบบการถ่ายโอนอะตอมอนุมูลอิสระโดยใช้ตัวเร่งปฏิกิริยาที่มีเฟอร์โรซีนเป็นองค์ประกอบ ได้ทำการสังเคราะห์วัสดุนาโนที่ถูกทำให้คงตัวด้วยลิแกนด์ที่มีเฟอร์โรซีนและได้ทำการพิสูจน์เอกลักษณ์โดยหลายๆ เทคนิค ได้นำตัวเร่งปฏิกิริยาที่มี Pd ไปใช้ในปฏิกิริยาการจับคู่ต่างกันเพื่อเพิ่มประสิทธิภาพของปฏิกิริยา นอกจากนี้ ได้ทำการสังเคราะห์พอลิเมอร์แบบการถ่ายโอนอะตอมอนุมูลอิสระโดยมีตัวเร่งปฏิกิริยาเป็นสารเชิงซ้อนของทองแดงกับลิแกนด์ไตรโปดอลที่มีเฟอร์โรซีนเป็นองค์ประกอบ วบคุมยังไม่ดีเป็นผลมาจากอิเล็คทรอนิกมากกว่าการเกะกะของหมู่เฟอร์โรซีน มีผลให้ขั้นไปข้างหน้าเร็วกว่าขั้นย้อนกลับ การปรับปรุงดัชนีการกระจายตัวของพอลิเมอร์ทำได้โดยการเติม

KEYWORDS: การเร่งปฏิกิริยาแบบนาโน การจับคู่ต่างกันแบบ Suzuki-Miyaura การพอลิเมอร์ไรเซชันแบบถ่านโอนอะตอมอนุมูลอิสระเฟอร์โรซีน ลิแกนด์สามขา

Part I

Synthesis and Catalytic Activities of Nanoparticles Stabilized by Ligand with Ferrocene Moiety

Abstract

Ferricinium ions were formed in the preparation of gold nanoparticles using 2-ferrocenylbenzothiazole as a reducing reagent as observed by electron paramagnetic resonance (EPR) spectroscopy. In contrast, an EPR signal of ferricinium was not observed in silver nanoparticles using 2-ferrocenylbenzothiazole as a reducing reagent and also in gold and silver nanoparticles using 2-phenylbenzothiazole as a reducing reagent. Citric acid was used to stabilize ferricinium ions formed in the reaction as the aggregation rate of nanoparticles slightly decreased. The average particle size is 30 nm as characterized by transmission electron microscope (TEM). The rates of nanoparticles formation and aggregation were observed by UV-visible spectroscopy. The blue shift of wavelengths was observed in the formation of gold nanoparticles reduced by 2-ferrocenylbenzothiazole while no wavelength shifting was observed in the formation of silver nanoparticles.

Introduction

Nanoparticles play an important role in many different fields. There are several methods for their preparation such as conventional method, microwave, electrospray, etc. Each of method is related to a variety of parameters. Nanoparticles interest many of researchers because they can be applied in biological and medical sciences– fluorescent biological labels[1-3], drug and gene delivery[4,5], bio detection of pathogens[6], detection of proteins[7], probing of DNA structure[8], tissue engineering[9,10], tumour destruction via heating (hyperthermia)[11], separation and purification of biological molecules and cells[12], MRI contrast enhancement[13], phagokinetic studies[14]. Moreover, the electronic device and surface enhancement Raman are also involved in the field of nanoparticles.

In this work, the gold and silver nanoparticles were prepared by uncomplicated method using benzothiazole group as a reducing ligand and citric acid was used to decrease the aggregation of the nanoparticles.

Experimental section

Chemicals

2-aminothiophenol (98%, ACROS), benzaldehyde (Polskie Odczynniki Chemiczne S.A.), ferrocenecarboxaldehyde (98%, Aldrich), $HAuCl_4 \cdot 3H_2O$ (99.9%, Sigma-Aldrich), acetonitrile (AR grade, LAB SCAN), tetrahydrofuran (AR grade, LAB SCAN), $AgNO_3$ (Merck), citric acid monohydrate ($C_6H_8O_7 \cdot H_2O$, Merck) and deionized water.

Synthetic parts

Synthesis of 2-ferrocenylbenzothiazole **(1)**

2-aminothiophenol (5 mmol, 0.6260 g) and ferrocenecarboxaldehyde (5 mmol, 1.0693 g) were mixed in the round bottom flask and used 1 mL acetonitrile as a solvent. After that, the dark brown solution occurs. The mixture was stirred 24 hours and then filtered and washed with an acetonitrile. The orange-brown solid is to be mixed with diethylether and stirred 10 minutes. The solution was filtered and evaporated. The orange solid was dried under vacuum and purified by column chromatography (silica gel 60, 5% EtOAc/Hexane). Anal. Found: C, 63.94; H, 4.12; N, 3.88. Calc. for $C_{17}H_{13}NSFe$: C, 63.94; H, 4.07; N, 4.38. ^{1}H NMR ($CDCl_3$, 300 MHz) 7.89 (*d*, 1H, *J* = 9.0 Hz), 7.75 (*d*, 1H, *J* = 9.0 Hz), 7.36 (*t*, 1H, *J* = 6.0 Hz), 7.25 (*t*, 1H, *J* = 6.0 Hz), 4.94 (*brs*, 2H), 4.43 (*brs*, 2H), 4.09 (*brs*, 5H). ^{13}C NMR ($CDCl_3$, 75 MHz) δ 168, 154, 135, 126, 124, 122, 121, 71, 70, 69. ESI-Mass m/z 320.0223 $[M+H]^+$. FTIR (KBr) 3449, 1655, 1527, 1441, 1422, 814, 761, 726, 499, 485. Melting point 95-97 °C.

Synthesis of 2-phenylbenzothiazole **(2)**

2-aminothiophenol (5 mmol, 0.6260 g) and ferrocenaldehyde (5 mmol, 0.5307 g) were mixed in the round bottom flask and used 25 mL acetonitrile as a solvent. The mixture was refluxed 24 hours. The yellow solution was evaporated and purified by column chromatography (silica gel 60, 5% EtOAc/Hexane). Anal. Found: C, 74.51; H, 4.35; N, 6.29. Calc. for $C_{13}H_9NS$: C, 73.91; H, 4.26; N, 6.63. ^{1}H NMR ($CDCl_3$, 300 MHz) 7.99 (*brd*, 1H, *J* = 6.0 Hz), 7.96 (*brd*, 2H, *J* = 3.0 Hz) 7.77 (*d*, 1H, *J* = 6.0 Hz), 7.37 (*brt*, 4H, *J* = 6.0 Hz), 7.26 (*t*, 1H, *J* = 6.0 Hz). ^{13}C NMR ($CDCl_3$, 75 MHz) δ 168, 154, 135, 134, 131, 129, 127, 126, 125, 123, 122. ESI-Mass m/z 211.0541 $[M+H]^+$. FTIR (KBr) 3449, 3065, 1509, 1479, 1434, 1314, 1225, 1071, 963, 767, 730, 667, 623. Melting point 92-94 °C.

Chart 1. Structures of the benzothiazole **(1)** and **(2)**

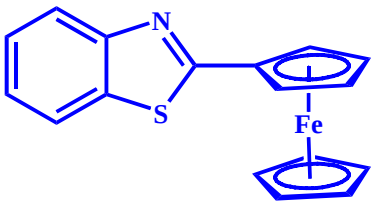

2-ferrocenylbenzothiazole **(1)**

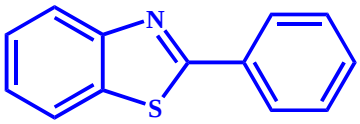

2-phenylbenzothiazole **(2)**

Preparation of nanoparticles

In a synthesis of gold nanoparticles, $HAuCl_4 \cdot 3H_2O$ in THF (1 mM, 1.5 mL) and 2-ferrocenylbenzothiazole **(1)** in THF (1 mM, 1.5 mL) were mixed and stirred vigorously, the solution became to purple indicating the formation of gold nanoparticles. To study the effect of the stabilizing agent, the experimental procedure was repeated by the above method and also a 1 mM (1.5 mL) of citric acid in THF was added into the mixture. The color of solution still occurred in purple. For the investigation of 2-phenylbenzothiazole **(2)**, the preparation of gold nanoparticles is similar to 2-ferrocenylbenzothiazole **(1)**. During the process, the color of the solution appeared yellow in both before and after the addition of citric acid.

The preparation of silver nanoparticles was used in the same method as gold nanoparticles. The solution using the 2-ferrocenylbenzothiazole **(1)** gave an orange whereas the 2-phenylbenzothiazole **(2)** showed a colorless solution.

* Silver dissolved in water.

Table 1. The components for gold and silver nanoparticles preparation.

Nanoparticle	Metal	Substituented group	Stabilizer
(a)	Au^{3+}	ferrocenyl	-
(b)	Au^{3+}	ferrocenyl	citric acid
(c)	Au^{3+}	phenyl	-
(d)	Au^{3+}	phenyl	citric acid
(e)	Ag^{+}	ferrocenyl	-
(f)	Ag^{+}	ferrocenyl	citric acid
(g)	Ag^{+}	phenyl	-
(h)	Ag^{+}	phenyl	citric acid

Spectroscopies

The ligand purities were examined by using ^{1}H NMR and ^{13}C NMR spectroscopy (Bruker, 300 MHz and 75 MHz respectively) with a concentrated solution of ligands dissolved in chloroform-d. UV-visible spectroscopic measurements were carried out with a HEWLETT PACKARD 8453 spectrometer and an automatic voltage stabilizer series-101. The paramagnetic compounds were measured by electron paramagnetic resonance (EPR) spectroscopy (Bruker, E500). In TEM measurements, the samples were prepared by dropping the particles that dissolved in THF onto a 300-mesh formvar coated copper grid and the solvent was evaporated at ambient pressure and temperature; the images were acquired for each sample with a Tecnai G2 Sphera transmission electron microscope (TEM) operated at 80 kV.

Results and discussion

TEM measurements

Transmission electron microscopy (TEM) has been used to measure the nanoparticle core dimensions. Figure 1 shows the TEM micrographs for the gold and silver nanoparticles.

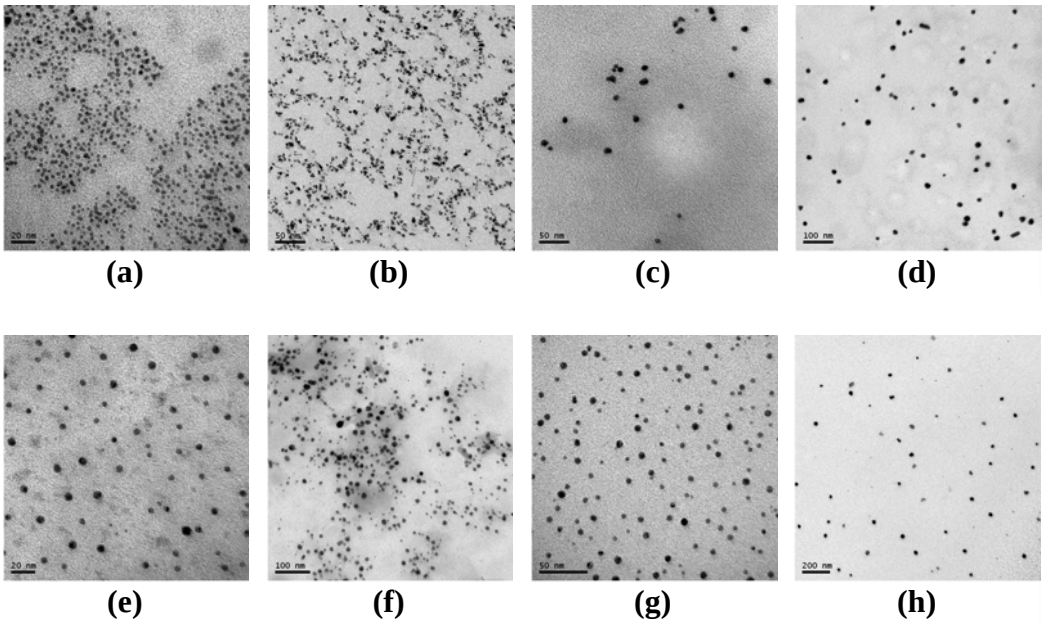

Figure 1. (a-d) show the TEM micrographs of gold nanoparticles; the representative scale bar indicate for 20 nm (a), 50 nm (b and c), and 100 nm (d): (e-h) show the TEM micrographs of silver nanoparticles; the representative scale bar indicate for 20 nm (e), 100 nm (f), 50 nm (g), and 200 nm (h).

The particles sizes were determined and summarized in the Table 2. In case of AuNPs using ligand 1, the particles are smaller than AgNPs in the same system due to the ligand size. The NPs with citric acid are larger than without citric acid.

Table 2. The summary results of gold and silver nanoparticles.

Nanoparticle	Average size (nm)	Std. Dev (nm)	Number
(a)	2.38	0.99	641
(b)	4.84	1.99	714
(c)	10.40	1.90	22
(d)	15.70	4.21	56
(e)	4.14	1.73	75
(f)	8.80	3.72	304
(g)	4.19	1.84	143
(h)	23.80	8.75	60

EPR measurements

Electron paramagnetic resonance (EPR) has been used to measure the characteristic peak of the paramagnetic compound. The ferricinium ions signal, obtained in THF solution, was observed especially in AuNPs using complex 1 as a ligand at 9.5 GHz, g = 2.01. It consists of a singlet signal. The ferrocenyl group can reduce Au(III) to be Au(I). Figure 2 indicates the kinetic EPR spectra of the increased ferricinium ions signal in the AuNPs(a) and (b).

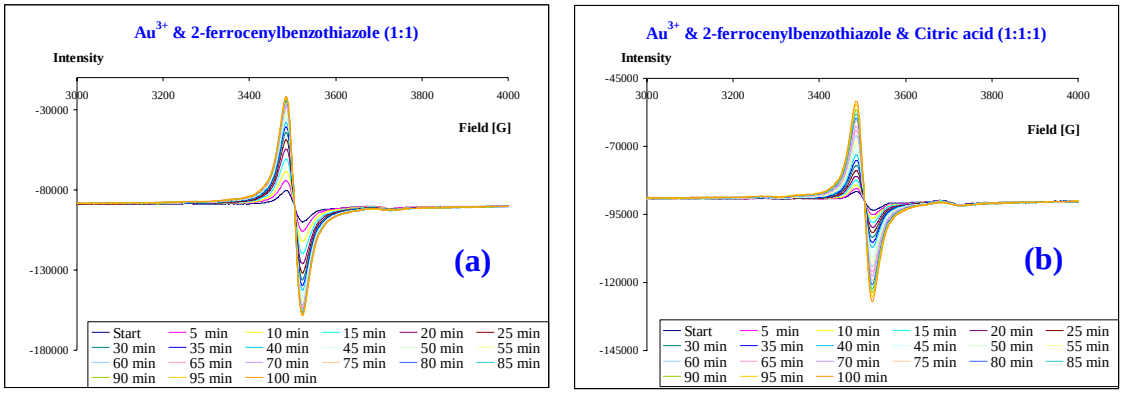

Figure 2. The EPR spectra of ferricinium ions in THF at 298 K generated by the reduction of: (a) 100:100 µL of Au^{3+} (1 mM) and 2-ferrocenylbenzothiazole (1mM) in THF (g = 2.01), (b) 100:100:100 µL of Au^{3+} (1 mM), 2-ferrocenylbenzothiazole (1 mM) and citric acid (1 mM) in THF (g = 2.01).

The rate of ferricinium ions in Figure 3(a) shows an explonential increase while Figure 3(b) is a straight line. The intensities plot as shown in Figure 3.

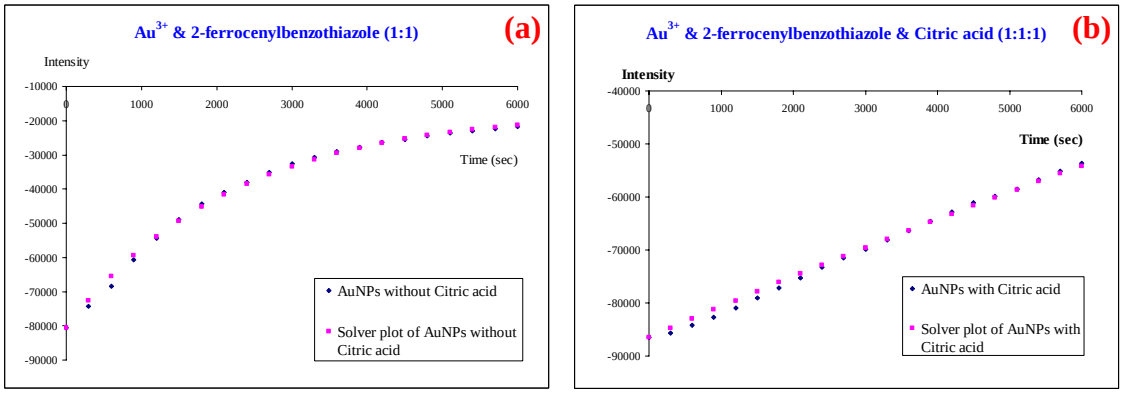

Figure 3. Graph plot between the intensity of ferricinium ions versus time (sec): (a) 100:100 µL of Au^{3+} (1 mM) and 2-ferrocenylbenzothiazole (1 mM) in THF, (b) 100:100:100 µL of Au^{3+} (1 mM), 2-ferrocenylbenzothiazole (1 mM) and citric acid (1 mM) in THF.

From the solver plot, the formation of ferricinium ions is slightly decreased when the citric acid was added (kinetic rate: (a); 4.51 x 10^{-4} sec^{-1} and (b); 3.26 x 10^{-5} sec^{-1}), so the citric acid can reduce the ferricinium ions formation in the AuNPs. In the case of AuNPs, reduced by phenylbenzothiazole and all AgNPs were not observed in EPR signal of reducing ligands.

UV-visible spectroscopy

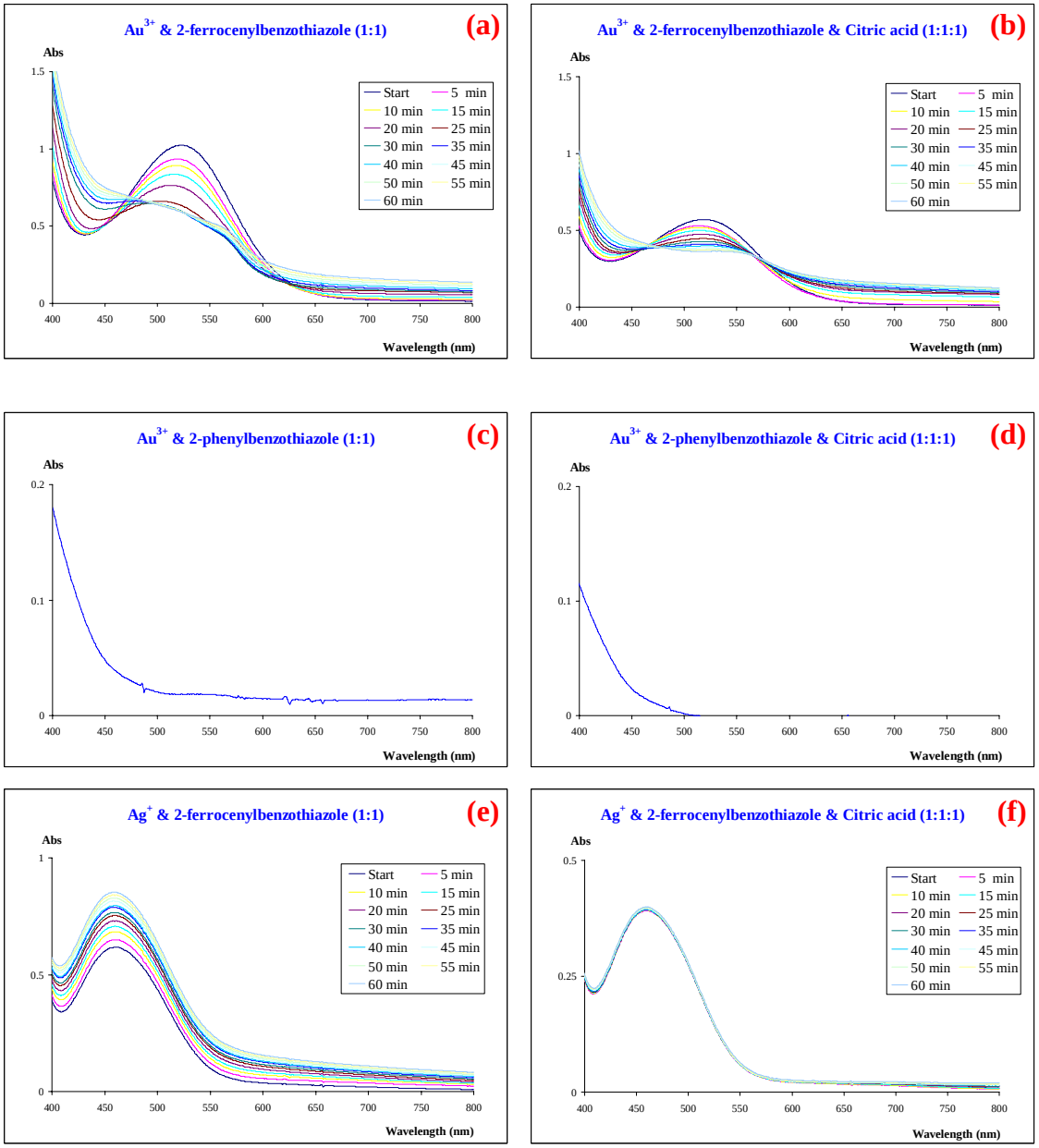

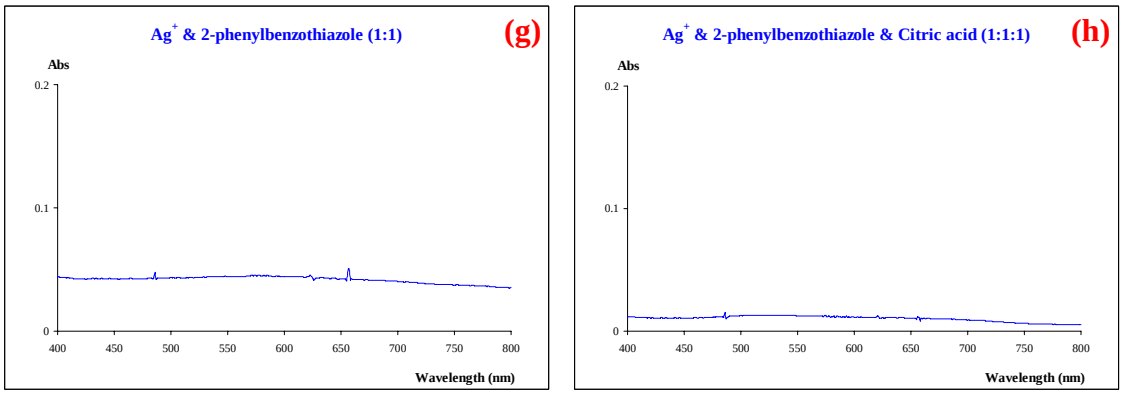

Figure 4. The UV-visible spectra of gold (a-d) and silver (e-h) nanoparticles.

Figure 4(a) shows the blue shift of wavelength that occurs in the formation of gold nanoparticles with ferrocenylbenzothiazole ligand. When the citric acid was added into the mixture, Figure 4(b), the rate of the aggregation is slightly decreased.

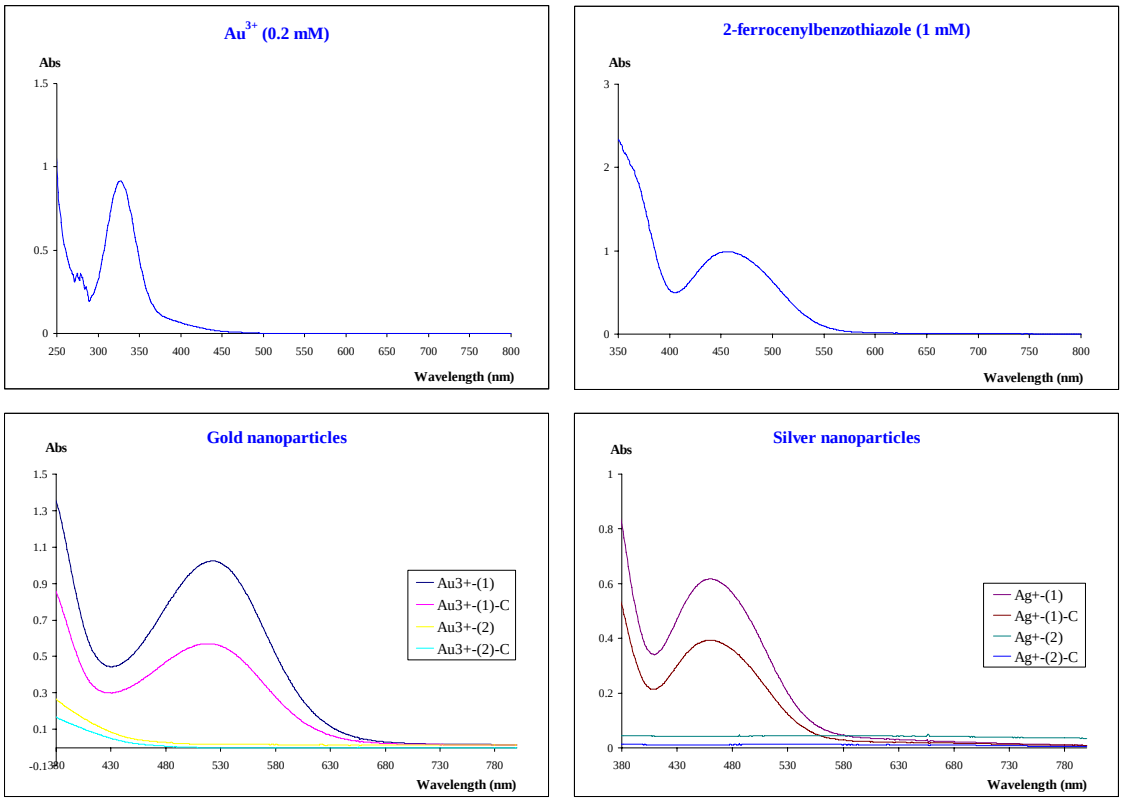

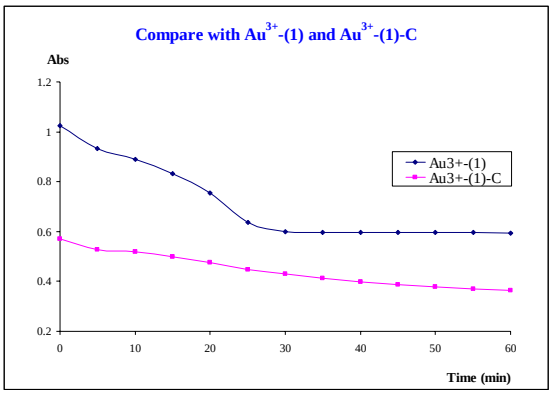

Homocoupling of ferroceneboronic and phenylboronic acid catalyzed by AuNPs

The catalytic activities of AuNPs were examined toward homocoupling of ferroceneboronic acid (Table 3) and phenylboronic acid (Table 4) in water under aerobic conditions. After the reaction at ambient temperature for 24 hrs, the product 2, 3, 5 and 6 were obtained.

Table 3. Homocoupling of ferroceneboronic acid in water, catalyzed by AuNPs

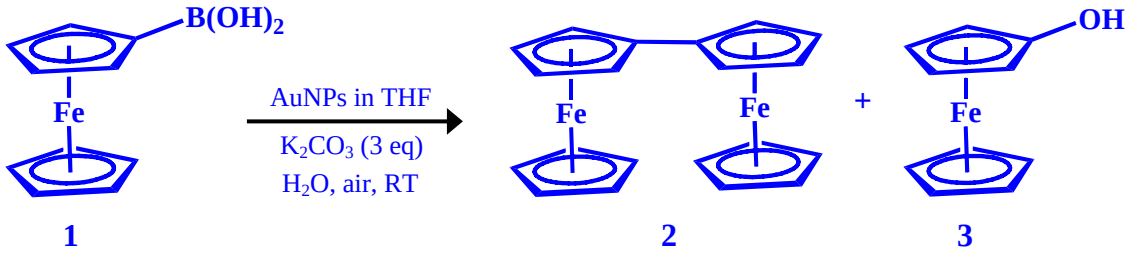

Entry	Catalyst	Yield (%)		
		1	2	3
1	A	trace	>99	trace
2	B	trace	47.38	52.62
3	C	trace	>99	trace
4	D	trace	>99	trace
5	E	trace	>99	trace
6	F	trace	>99	trace

Table 4. Homocoupling of phenylboronic acid in water, catalyzed by AuNPs

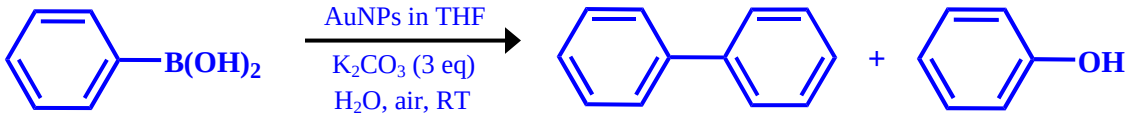

4 **5** **6**

Entry	Catalyst	Yield (%)		
		4	**5**	**6**
7	A	82.98	11.62	5.40
8	B	35.27	46.31	18.42
9	C	80.22	17.65	2.12
10	D	90.30	9.04	0.66
11	E	74.90	14.98	10.12
12	F	69.68	20.90	9.42

Conclusion

The AuNPs and AgNPs can be prepared successfully by conventional method under mild condition.

References

[1] Bruchez M, Moronne M, Gin P, Weiss S, Alivisatos AP, *Science*, **1998**, *281*, 2013-2016.

[2] Chan WCW, Nie SM, *Science*, **1998**, *281***,** 2016-2018.

[3] Wang S, Mamedova N, Kotov NA, Chen W, Studer J, *Nano Letters*, **2002**, *2***,** 817-822.

[4] Mah C, Zolotukhin I, Fraites TJ, Dobson J, Batich C, Byrne BJ, *Mol Therapy*, **2000**, *1***,** S239.

[5] Panatarotto D, Prtidos CD, Hoebeke J, Brown F, Kramer E, Briand JP, Muller S, Prato M, Bianco A, *Chemistry&Biology*, **2003**, *10***,** 961-966.

[6] Edelstein RL, Tamanaha CR, Sheehan PE, Miller MM, Baselt DR, Whitman LJ, Colton RJ, *Biosensors Bioelectron*, **2000**, *14***,** 805-813.

[7] Nam JM, Thaxton CC, Mirkin CA, *Science*, **2003**, *301*, 1884-1886.

[8] Mahtab R, Rogers JP, Murphy CJ, *J Am Chem Soc*, **1995**, *117***,** 9099-9100.

[9] Ma J, Wong H, Kong LB, Peng KW, *Nanotechnology***, 2003**, *14***,** 619-623.

[10] de la Isla A, Brostow W, Bujard B, Estevez M, Rodriguez JR, Vargas S, Castano VM, *Mat Resr Innovat*, **2003**, *7***,** 110-114.

[11] Yoshida J, Kobayashi T, *J Magn Magn Mater*, **1999**, *194***,** 176-184.

[12] Molday RS, MacKenzie D, *J Immunol Methods*, **1982**, *52***,** 353-367.

[13] Weissleder R, Elizondo G, Wittenburg J, Rabito CA, Bengele HH, Josephson L, *Radiology*, **1990**, *175***,** 489-493.

[14] Parak WJ, Boudreau R, Gros ML, Gerion D, Zanchet D, Micheel CM, Williams SC, Alivisatos AP, Larabell CA, *Adv Mater*, **2002**, *14***,** 882-885.

Part II

Effect of Ferrocene Substituents and Ferricinium Additive on the Properties of Polyaniline Derivatives and Catalytic Activities in the Suzuki-Miyaura Cross-Coupling Reaction

ABSTRACT

Poly(aniline-*co*-*m*-ferrocenylaniline) and ferricinium-doped poly(aniline-*co*-*m*-ferrocenylaniline) were synthesized by using a conventional chemical oxidative polymerization. The as-prepared polymers were then characterized by UV-Visible spectroscopy, electron paramagnetic resonance (EPR), nuclear magnetic resonance (NMR), thermal gravimetric analysis (TGA) and differential scanning calorimetric (DSC) analysis, cyclic voltammetry (CV), and vibrating sample magnetometry (VSM).

Increasing of the percentages of *m*-ferrocenylaniline in the polymers resulted to a blue shift of UV-Vis absorption spectra and lower decomposition temperatures. The thermal stability of copolymers is improved by the addition of ferricinium. NMR spectra confirmed the presence of ferrocene moieties or ferricinium in the polymers. Broader EPR spectra indicated the loss of conjugation and crystallinity of copolymers. The CV measurements showed that the electron withdrawing power of ferrocene moieties could lead to the decreasing of electron delocalization. The VSM results showed that as-prepared polymers were soft magnetic materials with very low magnetization. Poly(*m*-ferrocenylaniline)-supported Pd catalysts were utilized in the Suzuki-Miyaura cross-coupling reactions to improve the conversion and selectivity.

KEYWORDS: Polyaniline; *m*-ferrocenylaniline; ferricinium; Suzuki-Miyaura cross-coupling.

1. Introduction

It is of special interest to investigate the incorporation of nanostructures into polymers for practical applications in materials science and catalysis.[1-3] The hybrid nanocomposites based on organic polymers can be fabricated with various inorganic nanoparticles to create new materials with improvements in their properties for serving various functions.[4-6] The *in-situ* nanoparticle synthesis[7,8] is a highly powerful method to produce inorganic nanoparticle/polymer composites with such silica,[9] titania,[10] gold[11] and palladium[12] in various polymers. The surface of nanoparticles is modified in this method to improve the catalytic activity and selectivity due to the dispersion of nanoparticles in polymers. Moreover, polymers play an important role to prevent the particles from their aggregation.[8] It is generally accepted that the efficiency of the nanoparticles catalyst is dependent on the catalytic system and reversible redox cycles. The catalytic activity can be chemically tuned with the redox property of appropriate ligands or polymers. In past years, there have been few studies investigating the polymer-supported transition metal catalysts for catalysis in both academic and industrial laboratories. Therefore, the development of polymer-supported metal catalysts for catalysis is discussed in this research.

Since the discover that conjugated polymers can be made to conduct electricity, a tremendous amount of research has been carried out in the field of conducting polymers.[13,14] Polyaniline (PANI) is currently an excellent example of the most widely studied conducting polymers which can be synthesized and processed by the oxidative polymerization of aniline in an aqueous acid solution with ease, either by using an electrochemical method or by using a chemical oxidant for polymerization,[15,16] offering

considerable promise for commercialization due to its easy synthetic method, controllable doping levels through the acidic or basic condition, high stability, non-solubility in many organic solvents and water, and unique properties.[13,14] Bulk polyaniline has been studied for many potential applications including lightweight battery electrode,[17] electromagnetic shielding devices,[18] and anticorrosion coatings of steel surfaces.[19-21] In order to modify the properties of polymers, substituted polyanilines can be made by adding various functional groups to the backbone of the polymers. In another way, it is possible to modify PANI by incorporating external dopants bounding to the polymer backbone.[22] A wide range of copolymers produced from aniline and other aniline derivatives has been reported. There have been studies using a variety of ring-substituted anilines, such as anilineboronic acid,[23] *m*-aminophenol,[24] and butylthioaniline,[25] using the conventional chemical or electrochemical oxidative polymerization with aniline to obtain the desired properties of the polymer while maintaining the overall conjugation of the polyaniline.

In several years, a wide variety of cross-coupling methodologies have been developed and cross-coupling reactions have emerged as the most powerful and useful synthetic tools.[26,27] Of the great majority of cross-coupling reactions, metal-catalyzed cross-coupling reactions have been extensively employed for the preparation of compounds in a wide range of areas of such medical chemistry, metal-ligand catalysts, and molecular recognition. Using transition-metal catalysts, the advantage of the cross-coupling reaction occurs at lower temperature under a mild condition[27-29] in which the most active catalysts used are based on Ni and Pd complexes.[26-33] Pd is one of the most useful transition metal catalyst for carbon-carbon cross-coupling reactions.[27] It is now accepted that Suzuki-Miyaura reactions involving the formation of carbon-carbon bonds

have become the most important method in organic chemistry, as they present the key steps in the building of more complex molecules from simple precursors. The Suzuki-Miyaura cross-coupling reaction of aryl halides with arylboronic acids is a fundamental transformation in modern organic synthesis and offers a powerful method for the formation of the aryl-aryl bond.[26] Due to difficulties in separating the Pd catalyst and ligand from the final product and recycling the catalyst, its use is limited in homogeneous reaction systems. Therefore, the solid-supported Pd catalysts have been studied to develop for synthesis under air- and moisture-stable heterogeneous systems by immobilizing ligand-free Pd(0) particles on various media, such as carbon,[34] silica[34] and chitosan.[35] Palladium nanoparticles in the presence of conjugated conductive polyaniline as a supporter have been reported recently as excellent catalysts[36] in the cross-coupling reaction. Due to its good environmental stability and interesting redox properties, PANI was used as a redox-active supporter in the redox reactions catalyzed by the palladium transition metal without any ligand.

As it can be easily oxidized and reduced reversibly, ferrocene and its derivatives have been attractive for tuning novel redox properties. A number of studies investigated ligands containing ferrocene covalently bonded for the metal-assisted cross-coupling reactions of aryl halides with arylboronic acids.[37,38] However, there has no report on the study of the conventional chemical oxidative copolymerization of functional ferrocenyl groups bonded on the polymer backbone for employing in the Suzuki-Miyaura cross-coupling reactions. As part of our efforts to synthesize a novel conjugated polymer, herein polyanilines based on the ferrocene moiety extended on the polymer backbone were synthesized, and their properties were investigated to improve the catalytic

activities. The aim of this work was therefore to prepare and characterize poly(aniline-*co*-*m*-ferrocenylaniline)(s) and ferricinium-doped poly(aniline-*co*-*m*-ferrocenylaniline)(s), and to investigate the Suzuki-Miyaura cross-coupling activities of the nanocomposites of the conjugated PANI and poly(*m*-ferrocenylaniline)-supported Pd(0) catalysts in toluene. The as-prepared samples were characterized by UV-visible spectroscopy, electron paramagnetic resonance (EPR), nuclear magnetic resonance (NMR), thermal gravimetric analysis (TGA) and differential scanning calorimetric (DSC) analysis, cyclic voltammetry (CV), and vibrating sample magnetometry (VSM).

2. Experiment

2.1 Chemicals

The starting chemicals used in this experiment were analytical graded reagents and consist of aniline (Panreac), ferrocene (Merck), *m*-nitroaniline (Merck), tin metal (Merck), concentrated hydrochloric acid (Merck), concentrated sulfuric acid (Merck), sodium hydroxide (Merck), ammoniumperoxydisulfate (Merck), sodium nitrite (Fluka), sodium sulfate crystals (Carlo Erba), and diethylether (Lab Scan). Aniline monomer was distilled under the reduced pressure, and it was stored at 4 ^{o}C before use. Deionized (R≥18.2 MΩ-cm) water was obtained from Nanopure® Analytical Deionaization Water. All the above chemicals were used as received without further purification. The procedure for the synthesis of polyaniline was based on the literature.[14]

2.2 Synthesis of poly(aniline-co-m-ferrocenylaniline)

The synthesis of *m*-ferrocenylaniline was based on the reduction of *m*-ferrocenylnitrobenzene by Sn/HCl. In a 50-mL Erlenmeyer flask, a mixture of aniline

(5.4869 mmol, 0.5 mL, 0.511 g) and *m*-ferrocenylaniline (5 mol% of aniline) was added into a solution of a 7 mL of 1 M H_2SO_4. Repeat the above procedure with the different molar ratios of *m*-ferrocenylaniline at 10, 15 and 20% with respect to aniline. The mixture solution was then stirred at ambient conditions until solid monomer dissolved completely. After that, a required amount of 1 g of ammoniumperoxydisulfate dissolved in a 2 mL of deionized water was added dropwise into the solution. The copolymerization was allowed to proceed for 24 hrs. A fine dark red powder was obtained and filtered, and then washed with deionized water. Finally, the polymer product was dried in vacuum.

2.3 Synthesis of ferricinium-doped polyaniline

In a 50-mL Erlenmeyer flask, aniline (5.4869 mmol, 0.5 mL, 0.511 g) was added into a 7 mL of a 1 M H_2SO_4, then a 1 g of ammoniumperoxydisulfate dissolved in a 2 mL of deionized water was added dropwise into the solution while stirring continuously. During the formation of polyaniline, the ferricinium ion (2.7435 mmol, 0.51039 g) which was prepared by mixing ferrocene in 0.5 mL of concentrated H_2SO_4 was also added into the solution. The polymerization was allowed to proceed for 24 hrs at ambient conditions. A fine dark blue-green powder was obtained and filtered, and then washed with de-ionized water to remove impurities. The ferricinium-doped polyaniline was dried in vacuum.

2.4 Synthesis of ferricinium-doped poly(aniline-co-m-ferrocenylaniline)

In a 50-mL Erlenmeyer flask, a mixture of aniline (5.4869 mmol, 0.5 mL, 0.511 g) and *m*-ferrocenylaniline (5 mol% of aniline) was added into a 7 mL of 1 M H_2SO_4. The mixture was stirred at ambient conditions until the solid monomer dissolved

completely. Repeat the above procedure with the different molar ratios of *m*-ferrocenylaniline at 10, 15 and 20% with respect to aniline. After that, 1 g of ammoniumperoxydisulfate in a 2 mL of deionized water was added dropwise into the solution. During the formation of copolymer, the ferricinium ion (2.7435 mmol, 0.51039 g) was then added. The polymerization was allowed to proceed for 24 h. A fine dark orange powder was obtained and filtered and washed with deionized water. The polymer product was dried under vacuum.

2.5 Preparation of nanocomposites of polymer-supported Pd catalysts

The palladium/polymer nanocomposites for Suzuki-Miyaura cross-coupling reactions were synthesized by combining palladium(II) acetate (0.01 mmol, 2.2449 mg) with polyaniline or poly(aniline-*co*-*m*-ferrocenylaniline) (0.1 mmol) in a 5 mL of toluene. The mixture was allowed with stirring at room temperature under a closed system for 24 hrs. The nanocomposites were separated and washed with water and then toluene. The isolated solid was dried in vacuum and then kept for Suzuki-Miyaura cross-coupling reactions.

2.6 Suzuki-Miyaura cross-coupling reactions

After the reaction as described above, arylbromide (0.5 mmol), and arylboronic acid (0.5 mmol) were mixed into a 10 mL of toluene. A solid of potassium hydroxide (2 mmol, 112.22 mg) and the nanocomposites of polymer-supported Pd catalysts of polyaniline or poly(aniline-*co*-*m*-ferrocenylaniline) were added to the reaction mixture. Then, the reaction was refluxed for 20 hrs. After the completing of the reaction, palladium/polymers nanocomposites can be easily recovered by filtration, and then filtrant was dried under vacuum. These heterogeneous catalysts can be reusable for the

Suzuki-Miyaura cross-coupling reactions. The combined organic extracts were dried over Na_2SO_4 crystals, and evaporated in vacuum to give a crude product. The crude product was purified with column chromatography on silica gel eluted with 0, 10% EtOAc/Hexane (v/v) as eluents to give the biphenyl product. The isolated product was characterized by GC/MS or ^{1}H NMR.

3. General Characterization

3.1 Visible spectroscopy

The visible absorbance spectra of the sample solution were monitored over the range of 400-800 nm using a HP-8453 Hewlett Packard UV-Visible scanning spectrophotometer with the path length of the quartz cell at 10 mm. A required amount of 5 mg of samples was dissolved in dimethyl sulfoxide (DMSO). The spectra of samples were measured by using DMSO as a reference.

3.2 Electron Paramagnetic Resonance (EPR) spectroscopy

The EPR measurements were performed in a ground sample in a quart tube. A Bruker (E-500 Bruker) was used to operate at a frequency of 9.86 GHz, and the modulation amplitude used was set at 1.0 G. The microwave power for the EPR measurements of the poly(aniline-*co*-*m*-ferrocenylaniline)(s) was set at 20 mW. The temperature dependence of the EPR signal intensities of the poly(aniline-*co*-*m*-ferrocenylaniline)(s) in a solid state was measured at 298 K.

3.3 Nuclear Magnetic Resonance (NMR) spectroscopy

All samples of polyaniline, poly(aniline-*co*-*m*-ferrocenylaniline) and ferricinium-doped poly(aniline-*co*-*m*-ferrocenylaniline) were examined by using ^{1}H NMR

spectroscopy (300 and 500 MHz Avance Bruker) with a concentrated solution dissolved in dimethyl sulfoxide-d_6 and chloroform-*d* (for *m*-ferrocenylaniline).

3.4 Thermal analysis

The dry samples were measured by using thermal gravimetric analysis (TGA) and differential scanning calorimetric (DSC) analysis with the TA instrument-2960 SDT simultaneous analyzer. A dry sample was placed into an alumina crucible for TGA/DSC and heated from 30 ^{o}C to 700 ^{o}C with increasing temperature rate of 10 ^{o}C min^{-1} under a flowing argon gas at 100 cm^{3} min^{-1}.

3.5 Cyclic Voltammetry (CV)

An AUTOLAB-30 electrochemical analyzer was used to carry out the cyclic voltammetric measurements. In all cases, three electrodes was employed, consisting of working electrode and Pt wire serving as a counter electrode and the Ag/AgCl (saturated 3 M KCl) serving as the reference electrode. The electrochemical experiments were carried out at 25 $^{\circ}$C.

3.6 Vibrating sample magnetometry (VSM)

The coercivities (*Hc*), the remanent magnetizations (*Mr*) and the saturation magnetizations (*Ms*) of the as-prepared samples were performed by using the vibrating sample magnetometer (Lakeshore, Model 4500). The magnetic parameters (*Hc*, *Mr* and *Ms*) of each sample were determined from the hysteresis loops produced by the VSM. The saturation magnetization was reached at an applied field of 7 kOe. The data of magnetization as a function of the applied field were plotted and also employed for calculation.

4. Results and Discussion

Poly(aniline-*co*-*m*-ferrocenylaniline) was readily synthesized in diluted sulfuric acid at different molar ratios of *m*-ferrocenylaniline at 5, 10, 15, 20, and 100% by using ammonium peroxydisulfate as an oxidant. The structure of poly(aniline-*co*-m-ferrocenylaniline) is proposed as shown in Scheme 1 where A^- is an anion, Fc is a ferrocenyl substituent on the aromatic ring. The incorporation of *m*-ferrocenylaniline in the polymer chain is generally random and dependent on the molar ratios of monomers used in the preparation of poly(aniline-*co*-*m*-ferrocenylaniline). Therefore, It can be expected that the higher molar ratio used, the more *m*-ferrocenylaniline incorporated in the structure of the copolymer backbone. Likewise, ferricinium-doped poly(aniline-*co*-*m*-ferrocenylaniline) was prepared in diluted sulfuric acid with ferricinium as an external dopant at different molar ratios *m*-ferrocenylaniline at 5, 10, 15, 20, and 100% with respect to aniline by using ammonium peroxydisulfate as an oxidant. The added ferricinium cations during the formation of the copolymers may chemically linked anions with the electrostatic force in the polymer chain. The structure of the ferricinium-doped poly(aniline-*co*-*m*-ferrocenylaniline) is proposed as shown in Scheme 2.

4.1 Visible Spectroscopy

The colorful solutions of poly(aniline-*co*-*m*-ferrocenylaniline) in DMSO were observed: green for polyaniline, blue-green for 5 and 10 % molar ratios and orange for 15 and 20% molar ratios of *m*-ferrocenylaniline to aniline. Visible spectra of the copolymers were recorded over the range of 400-800 nm as shown in Figure 1. Polyaniline exhibits the green color of the emeraldine base form showing only one band at 620 nm due to a π-π^* transition of the conjugated ring system[39,40] and the

intramolecular transition between the quinoid and benzenoid units in the structure of polyaniline.[41] For the 5% molar ratios, the strong absorption peak is shifted to a lower wavelength at 570 nm. It can be seen that the blue shift of absorption bands of the copolymers was observed as the molar ratios of *m*-ferrocenylaniline were increased. For 15 and 20% molar ratios of *m*-ferrocenylaniline, the visible spectra showed a strong absorption band at 500 nm which is a characteristic band of ferrocene moieties.

In order to study the influence of the external dopant of ferricinium ions to the absorption bands of copolymers, the visible spectra of ferricinium-doped copolymers in DMSO were also monitored. As shown in Figure 2, the solution of polymers exhibited two colors: (i) blue-green for ferricinium-doped polyaniline and (ii) orange for ferricinium-doped poly(aniline-*co*-*m*-ferrocenylaniline). The visible spectrum of ferricinium-doped polyaniline showed two absorption bands: (i) the first region of absorption peaks is very broad over the wavelength of 550-700 nm, which is similar to characteristics of polyaniline as described above,[39,40] and (ii) the second region is located at about 500 nm which is a character of ferrocene obtaining from the reduction from ferricinium ions to ferrocene by polyaniline. Only one absorption band of ferricinium-doped poly(aniline-*co*-*m*-ferrocenylaniline) was observed at about 500 nm due to the ferrocenyl groups on the polymer backbone and ferrocene from the reduction of ferricinium by polyaniline.

4.2 Electron Paramagnetic Resonance (EPR) Spectroscopy

The characteristic EPR spectra of solid polyaniline derivatives were recorded at the operating frequency of 9.86 GHz at 298 K. Figure 3 shows that the intensities of EPR spectra of polyaniline derivatives were decreased gradually when increasing the

percentages of *m*-ferrocenylaniline monomers in the structural backbone of poly(aniline-*co*-*m*-ferrocenylaniline). The asymmetry and line width of EPR spectra may be caused by the nature of the copolymer structure which is strongly dependent on the molar ratios of *m*-ferrocenylaniline to aniline. The g-values of copolymers were 2.0032, 2.0035, 2.0038, and 2.0039 corresponding to 5, 10, 15 and 20% molar ratio of *m*-ferrocenylaniline to aniline, respectively whereas the g-value of polyaniline is 2.0031. Therefore, the g-values of poly(aniline-*co*-*m*-ferrocenylaniline) were similar to the one of polyaniline. The g-factor value is dependent on the electronic structure of species in order to be able to move the electron through the molecule.[24] According to the g-value obtained from the EPR measurements, it can be described that the added *m*-ferrocenylaniline had a minimal influence on the paramagnetic properties of poly(aniline-*co*-*m*-ferrocenylaniline). The decreasing intensities of EPR spectra of the copolymers may be due to the disordered polymer structure and the conjugation may be disrupted by the ferrocene moieties on the main chain of the copolymers.[14]

EPR spectra of ferricinium-doped poly(aniline-*co*-*m*-ferrocenylaniline) were recorded under the same conditions as those measurements of the copolymers. Figure 4 shows clearly that the addition of ferricinium ions as an external dopant affects strongly to the changes in the EPR signal intensities of the-synthesized copolymers. The results indicated that the electron states of the ferricinium-doped poly(aniline-*co*-*m*-ferrocenylaniline) are more localized. It is obvious that the difference from the undoped copolymers is caused by the addition of ferricinium ions into the reaction mixture during the preparation of polymers. The g-values are 2.0034 for all ferricinium-doped

copolymers. The g-values indicated that the electronic structures of all poly(aniline-*co*-*m*-ferrocenylaniline)(s) were similar and close to the g-value of a free electron (2.0036).

4.3 Nuclear Magnetic Resonance (NMR) Spectroscopy

^{1}H NMR spectra of paramagnetic polyaniline and polyaniline derivatives can be observed in DMSO- d_6 with a numbers of scans as shown in Figure 5. The characteristic ^{1}H NMR spectrum of polyaniline and polyaniline derivatives with a triplet peak (1:1:1) was usually observed in the region of δ 7.1-6.9 ppm.[42] This peak is assigned to the aromatic protons in the main chain of polyaniline. Polyaniline is easily oxidized and reduced reversibly.[14] Therefore, paramagnetic ferricinium can be observed on a ^{1}H NMR spectrum by the reduction to ferrocene by polyaniline. The chemical shift of ferrocene is generally observed at δ 4.1 ppm.[43] A huge broad singlet peak at δ 3.5 ppm is assigned to water in DMSO-d_6. In the studied polymers, the chemical shits of ferrocene moieties in the main chain of polymers and ferricinium additives were observed in the region of δ 4.2-4.0 ppm. The chemical shift of ferricinium in ferricinium-doped polyaniline was observed at δ 4.15 ppm as a sharp singlet peak. In the ferrocene region, two major peaks of ferricinium-doped poly(aniline-*co*-*m*-ferrocenylaniline) were observed at δ 4.1 and 4.0 ppm and assigned to species from additive ferricinium and ferrocene moieties in the main chain of polymers, respectively. In summary, ^{1}H NMR spectroscopy can be used to confirm the presence of ferrocene moieties and ferricinium additive in the copolymers.

4.4 Thermal analysis

In order to determine the thermal stabilities of the samples, the thermal gravimetric analysis (TGA) and differential scanning calorimetric (DSC) analysis were carried out. TGA technique provides the information about the temperature-dependent

weight loss of the sample. Meanwhile, the DSC method involves recording phase-specific changes or transformations of the sample during heating, and analyzing the heat flow.[44] Table 1 shows the TGA/DSC data obtained from the poly(aniline-*co*-*m*-ferrocenylaniline)(s) and poly(*m*-ferrocenylaniline). As can be seen, the polymers started to lose weight at around 100 ^{o}C due to the vaporization of the adsorbed water from samples.[23] Each product contains an appreciable amount of absorbed water which leads to a weight loss about 7-9 % of initial weight. Meanwhile, the polymer chain begins to degrade over the temperature 200^{o}C. The DSC for the polymers showed a strong endothermic transition of evaporation of adsorbed water at the range of 80-110^{o}C. In the second peak, a slow rate of the weight loss of polymers occurred in a wide range of 200 to 400^{o}C is assigned to the removal of remaining H_2SO_4 in samples. This range of the weight loss of the copolymers is quite similar to that of polyaniline. The decomposition temperature of polyaniline is in the range of 270-370^{o}C.[45,46] The total weight loss of the copolymers was in a range of 16-33 % of initial weight. In DSC results, the exothermic peak was divided into two parts. The first exothermic peak between 260-290 ^{o}C was caused by the H_2SO_4 deprivation and the second exothermic peak about 500 ^{o}C was caused by the polymer chain degradation. The decomposition of polymer was not observed above 600 ^{o}C.

From the weight loss and decomposition temperature obtained, in general, the thermal stability of the polymer is dependent on the dopant and the nature of structure of the polymer backbone.[23] The ferrocene moieties, which covalently bonds to the polymer backbone, are an electron withdrawing group.[47] It is believed that the ferrocene moiety plays a key role for increasing the oxidizing potential of polymers. Similarly, its steric

group may affect in thermal stabilities of the polymers. The decomposition temperatures of poly(aniline-*co*-*m*-ferrocenylaniline)(s) had a trend to occur at the lower temperature as increasing the percentage of *m*-ferrocenylaniline.

Table 2 shows the TGA/DSC data obtained from the ferricinium-doped poly(aniline-*co*-*m*-ferrocenylaniline)(s) and ferricinium-doped poly(*m*-ferrocenylaniline). The decomposition patterns of ferricinium-doped copolymers were similar to the one of undoped copolymers. From the TGA results shown in Table 2, it shows clearly that the weight loss patterns of the polymers were quite similar in all samples. The higher thermal stabilities of the doped samples can be described that the backbone of poly(aniline-*co*-*m*-ferrocenylaniline)(s) and poly(*m*-ferrocenylaniline) was stabilized by the added external dopant of ferricinium ions with the electrostatic interactions to anions attached to the polymer backbone.

4.5 Electrochemical oxidation analysis

Polyaniline is electrically conductive in its emeraldine oxidation state when doped with a salt that the imine nitrogens on the polymer backbone are protonated. Dopants can be added in any desired quantity until all imine nitrogens are doped, simply by controlling the pH and the dopant acid solution.[13,14] In order to compare the conductivity, the undoping and doping processes of the added ferrocenium ions were investigated by CV measurements.

In this study, all electrochemical experiments were performed in a single component cell with three electrode compositions. The counter and reference electrodes were a Pt wire and a Ag/AgCl electrode in saturated KCl, respectively. Meanwhile, the supporting electrolyte was an aqueous solution of a 0.1 M KCl. Due to the obtained

products were in the form a solid powder, it is rather difficult to prepare a working electrode from as-prepared samples. In our first attempt, the electrochemical measurement was performed by the deposition of samples onto a glassy carbon electrode and the current signal from the CV measurement was not observed. The working electrode was, however, successfully prepared by the formation of a composite electrode, containing carbon powder, sample and mineral oil serving as a binder in the ratio of 50: 40: 10 by weight.[48]

Polyaniline and poly(aniline-co-m-ferrocenylaniline)

In the CV measurements, the experiments were carried out by using repeated potential cycling between -0.1 and 0.8 V. The Figure 8 shows the CVs at the scan rate of a 5 mVs^{-1} of the polyaniline and poly(aniline-*co*-*m*-ferrocenylaniline) at the different molar ratios of *m*-ferrocenylaniline. Figure 6 shows clearly that the oxidation current of poly(aniline-*co*-*m*-ferrocenylaniline) decreases with the increasing of the percentage of *m*-ferrocenylaniline. For 5% *m*-ferrocenylaniline by molar ratio, the redox behavior of the copolymer is quite similar to the one of polyaniline. The potential peaks were broad due to the major component of carbon powder in the working electrode. The peak current of poly(aniline-*co*-*m*-ferrocenylaniline) was decreased quickly for 10 % *m*-ferrocenylaniline by molar ratio. It can be described that the steric hindrance to the conjugated length of the polymer and the electron withdrawing power of ferrocene moieties from the aromatic rings could lead to the decreasing the electron delocalization.[49] Therefore, the electrons were more localized at the paramagnetic centers. However, the current was increased greatly with the increasing of the percentage of *m*-ferrocenylaniline. Similar to ferrocene, the Figure 8b shows that the copolymers

exhibit single oxidation and reduction waves in the range of 0-1 V. In this work, the oxidation and reduction potentials were located around 0.48 and 0.33 V, respectively. It was proposed that these potentials of the as-synthesized poly(aniline-*co*-*m*-ferrocenylaniline)(s) obtained the CV data were caused from the redox process of ferrocenyl moieties[50] as a part of the structure of poly(aniline-*co*-*m*-ferrocenylaniline)(s). Therefore, ferrocene and its derivatives are attractive for tuning the redox properties which it can be oxidized and reduced reversibly.[51]

Polyaniline and poly(aniline-co-m-ferrocenylaniline) doped with ferricinium ion

Figure 7 shows that the resulting products obtained from the CV measurements exhibit the redox behavior similarly to the undoped condition. The Figure 7a shows that the peak potential of ferricinium-doped polyaniline obtained is still broad. However, figure 7b shows clearly that the peak current of ferricinium-doped poly(aniline-*co*-*m*-ferrocenylaniline) was decreased quickly for 5% *m*-ferrocenylaniline by molar ratio. However, the currents were increased greatly with the increasing of percentage of *m*-ferrocenylaniline for 10, 15 and 20% by molar ratio to aniline. The oxidation and reduction potentials were the same as the undoped condition. All CV voltammograms display chemically reversible ferrocene/ferricinium redox waves.[50] This was suggested that the ferrocene moieties of copolymers in all samples showed the similar redox potentials due to the lack of direct interactions between the metal center.[52] Compared with the undoped condition, the results showed the higher currents of poly(aniline-*co*-*m*-ferrocenylaniline)(s) were observed. The higher current of poly(aniline-*co*-*m*-ferrocenylaniline)(s) was enhanced by the addition of the external dopant of ferricinium.

4.6 Vibrating Sample Magnetometry (VSM)

The VSM measurements of samples were measured in samples dried by incubating in an oven at 50^{o}C for 48 hrs. In this work, a required amount (approximately 20 mg) of the dry sample was vibrated in a magnetic field at 300 K. The saturation magnetizations were derived from the VSM measurements by cycling the field from -7 kOe to 7 kOe. The electron localization effects of the magnetic states in the polyaniline copolymers have been investigated by several studies due to their interesting magnetic behaviors. For example, Kahol and coworkers described that the ring-substituted derivative of polyaniline copolymer such as poly(aniline-*co*-methylaniline) increased electron localization compared to polyaniline.[53] The Figure 8 indicated that, from the hysteresis loops, all samples of the as-prepared poly(aniline-*co*-*m*-ferrocenylaniline) were soft magnetic materials because the magnetization values obtained from the final products were very low in the range from -0.06 to 0.02 emu/g. We found that when increasing the molar ratio of *m*-ferrocenylaniline used in the copolymerization, the magnetic behavior from the band gap of hysteresis loops tended to increase the electron localization of the as-prepared poly(aniline-*co*-*m*-ferrocenylaniline)(s).

4.7 Cross-coupling of aryl bromides and arylboronic acids

The general features of the catalytic cycles for Suzuki-Miyaura cross-coupling reactions are currently well understood and involved in the oxidative addition-transmetallation-reductive elimination sequence.[26,27] Polymers stabilized colloidal palladium nanoparticles have been reported as the catalysts for the Suzuki-Miyaura cross-coupling reactions.[54] In this study, the Suzuki-Miyaura cross-coupling reactions of aryl bromides and arylboronic acids were catalyzed heterogeneous Pd nanocatalysts based on

the dispersion of Pd/polymer nanocomposites. Kantam and coworkers reported a new way to decrease or disappear of the Pd catalyst by the polyaniline-supported palladium complex for Suzuki-Miyaura cross-coupling reactions in water.[36] It has been established that the nature of the ligands has a great influence on the oxidation addition rate of Pd(0) catalysts. Therefore, ferrocene moieties on the main chain of polymers were expected to accelerate the rate of electron transfer to achieve a higher conversion and yield.

The Suzuki-Miyaura cross-coupling reactions of 4-bromotoluene with arylboronic acids were catalyzed by poly(*m*-ferrocenylaniline)-stabilized palladium nanocatalysts under a basic condition at room temperature (Scheme 3). The cross-couplings catalyzed by palladium nanocatalysts stabilized by polyaniline were used as a reference. The catalytic studies of Suzuki-Miyaura cross-coupling reactions were summarized in the Table 3. For the entries 1 and 2, the poly(*m*-ferrocenylaniline) experiments gave excellent conversion and yield percentages than the polyaniline experiments. The entries 3 and 4 showed comparable results for both ligands. It can be described that the rate of reactions in the entries 1 and 2 may be low due to the electron and steric effects with polyaniline ligands. Due to the steric effect of methyl group on biphenyl ring, the yield increases from entry 2, 3 and 4 corresponding to *o*-, *m*- and *p*- substituted benzene ring, respectively. Therefore, ferrocene moieties on the main chain of poly(*m*-ferrocenylaniline) accelerated the rate of reaction by increasing the rate of electron transfer. However, for the entries 3 and 4, no significant effects of ferrocene moieties on the catalytic activities were observed. It should be noted that the electrons are less delocalized if the percentage of *m*-ferrocenylaniline is increased based on the EPR data. The less electron delocalization may make conjugated polymers less useful in the

conductivity. However, it probably showed a better stabilization to the substrate or the transition state to accelerate the rate of reaction.

5. Conclusions

The novel polyaniline derivatives were prepared by the copolymerization of aniline and *m*-ferrocenylaniline monomers. The copolymers of poly(aniline-*co*-*m*-ferrocenylaniline)(s) and the ferricinium-doped poly(aniline-*co*-*m*-ferrocenylaniline)(s) were synthesized by using a conventional chemical oxidative polymerization. The molar ratio of *m*-ferrocenylaniline and aniline, had influences directly on the chain structure, optical properties, thermal stabilities, redox properties, and magnetic properties of copolymers. When increasing a molar ratio of *m*-ferrocenylaniline, the visible spectra of copolymers had a tendency to shift to the lower wavelength (blue shift). The thermal analysis indicated that the decomposition temperatures of copolymers were decreased with the increasing of the *m*-ferrocenylaniline due to the electron withdrawing power of ferrocene moieties on the polymer backbone. Furthermore, the steric effect of the ferrocenyl substitution also affected the ability of the copolymers to form crystalline regions. The thermal stability of copolymers is improved by the addition of an external dopant. The EPR data showed that the loss of conjugation and crystallinity of copolymers was due to the functional ferrocenyl substituents. The results of CV measurements show that withdrawing electrons from the aromatic rings of ferrocenyl groups could lead to the decreasing of the electron delocalization, probably due to the interference of the reversibility of the electron transfer rate. The VSM results showed the copolymers were soft magnetic materials with a very low magnetization. Poly(*m*-

ferrocenylaniline)-stabilized Pd(0) catalysts were used in the Suzuki-Miyaura cross-coupling reactions of 4-bromotoluene with arylboronic acids in toluene. The poly(*m*-ferrocenylaniline)-stabilized Pd(0) catalyst was found to be an excellent effective catalyst.

Acknowledgements

This research was supported by the Center for Innovation in Chemistry: Postgraduate Education and Research Program in Chemistry (PERCH-CIC), the Thailand Research Fund (TRF) and the Faculty of Science, Mahidol University.

References

(1) Xu, J.; Wang, J.; Mitchell, M.; Mukherjee, P.; Jeffries-El, M.; Petrich, J. W.; Lin, Z. *J. Am. Chem. Soc.* **2007**, *129*, 12828-12833.

(2) Sen, T.; Sebastianelli, A.; Bruce, I. J. *J. Am. Chem. Soc.* **2006**, *128*, 7130-7131.

(3) Ding, Y.; Chen, M.; Erlebacher, J. *J. Am. Chem. Soc.* **2004**, *126*, 6876-6877.

(4) Beecroft, L. L.; Ober, C. K. *Chem. Mater.* **1997**, *9*, 1302-1317.

(5) Yi, D. K.; Lee, S. S.; Ying, J. Y. *Chem. Mater.* **2006**, *18*, 2459-2461.

(6) Saxena, A.; Tripathi, B. P.; Shahi, V. K. *J. Phys. Chem. B* **2007**, *111*, 12454-12461.

(7) Mallick, K.; Witcomb, M. J.; Dinsmore, A.; Scurrell, M. S. *Langmuir* **2005**, *21*, 7964-7967.

(8) Ajayan, P. M.; Schadler, L. S.; Braun, P. V. *Nanocomposite science and technology*; Wiley-VCH: Weinheim, 2003.

(9) Hsiue, G.-H.; Kuo, W.-J.; Huang, Y.-P.; Jeng, R.-J. *Polymer* **2000**, *41*, 2813-2825.

(10) Strohm, H.; Lobmann, P. *Chem. Mater.* **2005**, *17*, 6772-6780.

(11) Weber, R.; Grotkopp, I.; Stettner, J.; Tolan, M.; Press, W. *Macromolecules* **2003**, *36*, 9100-9106.

(12) Schweizer, S.; Becht, J. M.; LeDrian, C. *Org. Lett.* **2007**, *9*, 3777-3780.

(13) Skotheim, T. A.; Reynolds, J. R. *Handbook of conducting polymers: Conjugated polymers, processing and applications*; 3 ed.; CRC press: New York, 2007.

(14) Skotheim, T. A.; Reynolds, J. R. *Handbook of conducting polymers: Conjugated polymers, theory, synthesis, properties, and characterization*; 3 ed.; CRC press: New York, 2007.

(15) Macdiarmid, A. G.; Chiang, J. C.; Richter, A. F.; Epstein, A. J. *Synthetic Met.* **1987**, *18*, 285-290.

(16) Rappoport, Z. *The chemistry of anilines*; Wiley & Sons: New Jersey, USA, 2007.

(17) Ryu, K. S.; Jeong, S. K.; Joo, J.; Kim, K. M. *J. Phys. Chem. B* **2007**, *111*, 731-739.

(18) Trivedi, D. C.; Dhawan, S. K. *Synthetic Metals* **1993**, *59*, 267-272.

(19) Kilmartin, P. A.; Trier, L.; Wright, G. A. *Synthetic Met.* **2002**, *131*, 99-109.

(20) Fahlman, M.; Jasty, S.; Epstein, A. J. *Synthetic Met.* **1997**, *85*, 1323-1326.

(21) Lu, W.-K.; Elsenbaumer, R. L.; Wessling, B. *Synthetic Met.* **1995**, *71*, 2163-2166.

(22) Han, C. C.; Lu, C. H.; Hong, S. P.; Yang, K. F. *Macromolecules* **2003**, *36*, 7908-7915.

(23) Yu, I.; Deore, B. A.; Recksiedler, C. L.; Corkery, T. C.; Abd-El-Aziz, A. S.; Freund, M. S. *Macromolecules* **2005**, *38*, 10022-10026.

(24) Mu, S.; Chen, C. *J. Phys. Chem. B* **2007**, *111*, 6998-7002.

(25) Han, C. C.; Hong, S. P.; Yang, K. F.; Bai, M. Y.; Lu, C. H.; Huang, C. S. *Macromolecules* **2001**, *34*, 587-591.

(26) Diederich, F.; Stang, P. J. *Metal-catalyzed cross-coupling reactions*; Wiley-VCH: New York, 1998.

(27) Miyaura, N.; Suzuki, A. *Chem. Rev.* **1995**, *95*, 2457-2483.

(28) Roglans, A.; Pla-Quintana, A.; Moreno-Manas, M. *Chem. Rev.* **2006**, *106*, 4622-4643.

(29) Corbet, J. P.; Mignani, G. *Chem. Rev.* **2006**, *106*, 2651-2710.

(30) Tang, Z. Y.; Hu, Q. S. *J. Org. Chem.* **2006**, *71*, 2167-2169.

(31) Tang, Z. Y.; Hu, Q. S. *J. Am. Chem. Soc.* **2004**, *126*, 3058-3059.

(32) Felpin, F. X. *J. Org. Chem.* **2005**, *70*, 8575-8578.

(33) Bei, X.; Turner, H. W.; Weinberg, W. H.; Guram, A. S.; Petersen, J. L. *J. Org. Chem.* **1999**, *64*, 6797-6803.

(34) Yin, L. X.; Liebscher, J. *Chem. Rev.* **2007**, *107*, 133-173.

(35) Yi, S.-S.; Lee, D.-H.; Sin, E.; Lee, Y.-S. *Tetrahedron Lett.* **2007**, *48*, 6771-6775.

(36) Kantam, M. L.; Roy, M.; Roy, S.; Sreedhar, B.; Madhavendra, S. S.; Choudary, B. M.; De, R. L. *Tetrahedron* **2007**, *63*, 8002-8009.

(37) Yu, S.-B.; Hu, X.-P.; Deng, J.; Huang, J.-D.; Wang, D.-Y.; Duan, Z.-C.; Zheng, Z. *Tetrahedron Lett.* **2008**, *49*, 1253-1256.

(38) Kwong, F. Y.; Chan, K. S.; Yeung, C. H.; Chan, A. S. C. *Chem. Commun.* **2004**, *20*, 2336-2337.

(39) Shah, A.-u.-H. A.; Holze, R. *Synthetic Met.* **2006**, *156*, 566-575.

(40) Amaya, T.; Saio, D.; Hirao, T. *Tetrahedron Lett.* **2007**, *48*, 2729-2732.

(41) Pruneanu, S.; Veress, E.; Marian, I.; Oniciu, L. *J. Mater. Sci.* **1999**, *34*, 2733-2739.

(42) Zhang, J.; Shan, D.; Mu, S. *Polymer* **2007**, *48*, 1269-1275.
(43) Dogan, O.; Koyuncu, H. *J. Organomet. Chem.* **2001**, *631*, 135-138.
(44) Brown, M. E. *Introduction to thermal analysis*; Kluwer: New York, 2001.
(45) Zeng, X.-R.; Ko, T.-M. *Polymer* **1998**, *39*, 1187-1195.
(46) Lu, X.; Tan, C. Y.; Xu, J.; He, C. *Synthetic Met.* **2003**, *138*, 429-440.
(47) Petersen, R.; Foucher, D. A.; Tang, B.-Z.; Lough, A.; Raju, N. P.; Greedan, J. E.; Manners, I. *Chem. Mater.* **1995**, *7*, 2045 - 2053.
(48) Lee, H. Y.; Goodenough, J. B. *J. Solid State Chem.* **1999**, *144*, 220-223.
(49) Xu, Y.; Dai, L.; Chen, J.; Gal, J.-Y.; Wu, H. *Euro. Polym. J.* **2007**, *43*, 2072-2079.
(50) Shi, J.; Tong, B.; Zhao, W.; Shen, J.; Zhi, J.; Dong, Y.; Haussler, M.; Lam, J. W. Y.; Tang, B. Z. *Macromolecules* **2007**, *40*, 5612-5617.
(51) Sayed, A. M. E.; Yamasaki, S.; Yamauchi, A. *J. Appl. Polym. Sci.* **2008**, *107*, 1678-1685.
(52) Stone, D. L.; Smith, D. K.; McGrail, P. T. *J. Am. Chem. Soc.* **2002**, *124*, 856-864.
(53) Kahol, P. K.; Pendse, V.; Pinto, N. J.; Traore, M.; Stevenson, W. T. K.; McCormick, B. J.; Gundersen, J. N. *Phys. Rev. B* **1994**, *50*, 2809.
(54) Schulz, J.; Schulz, J. r.; Patin, H. *Chem. Rev.* **2002**, *102*, 3757-3778.

Part III

Effect of Ferrocene Moieties on Copper-Based Atom Transfer Radical Polymerization of Methyl Methacrylate

ABSTRACT

The atom transfer radical polymerization (ATRP) of methyl methacrylate (MMA) catalyzed by copper-tripodal complexes with ferrocene moieties (CuX/ TRENFcImine, X=Br or Cl) was investigated in order to understand the effect of redox active moieties on the performance of ATRP catalysts. The CuBr/TRENFcImine system was highly active with 82% conversion in 2 hours. However, the polymerization became slower at the higher molar ratio of monomer to catalyst. The polydispersity was broad and the initiation efficiency was relatively low. The highly active and less controlled polymerization was probably caused by the electronic effect rather than the steric effect from ferrocene moieties resulted to the higher and lower in the activation and deactivation steps, respectively. The polydispersity was improved by the addition of

$CuBr_2$ but the rates of polymerization became slower at this system. The effect of the halide groups on the ATRP showed that the CuBr/TRENFcImine system exhibited the faster rate of polymerization than the CuCl/TRENFcImine system. The higher molar ratio of monomer to catalyst had no significant effects for the CuCl/TRENFcImine system. However, the trace of water in the $CuCl_2.2H_2O$ system shifted to a higher molecular weight.

KEYWORDS: Atom transfer radical polymerization (ATRP), Ferrocene, Tripodal ligand.

1. Introduction

Atom transfer radical polymerization (ATRP) [1, 2] is one of controlled/living radical polymerization (CRP) processes with rapid growing in the past decade due to the successful polymerization with controlled molecular weight, well-defined compositions, architectures, and functionalities of polymers [3-8]. In the general process of ATRP (Scheme 1), a radical (R•) and a metal complex at the higher oxidation state ($X\text{-}M_t^{n+1}$) were generated by the transfer of halogen (X) from an alkyl halide initiator (R-X) to the lower oxidation state of the metal complex (M_t^n). Then the radical is propagating with the consumption of monomers (with rate constants k_p) and it is somehow deactivated by reacting with the oxidized complex to transform to the original active catalyst and oligomeric alkyl halide, this process repeats itself (with rate constants k_{act} and k_{deact}) and the molecular weights of polymers are controlled in this process to obtain high molecular weight and narrow molecular weight distribution. The ATRP process is involved in the chemical exchange between the metal catalyst active species and the oxidized metal complex deactivated species, therefore the catalyst (including transition metals and ligands) in ATRP plays a crucial role in the catalytic pathway. A successful ATRP required a fast activation/deactivation equilibrium with small k_{act} and large k_{deact} to control the polymerization. As a wide variety of transition metal complexes used in the ATRP system such as copper [9], iron [10], nickel [11], ruthenium [12], rhenium [13], molybdenum [14], and osmium [15] with suitable ligands such as multidentate amines has been reported.

Ligands play a great role in ATRP to tune the activity of the metal center and to solubilize the metal salts. The examples of highly active ATRP catalysts are that

copper(I) bromide with tetradentate ligands with such as CuBr/*tris*[2-(*N*,*N*-dimethylamino)ethyl]amine (Me_6TREN) [16] and CuBr/*tris*(2-pyridylmethyl)amine (TPMA) [17] form highly active ATRP catalysts which are much more active than the original CuBr/bipyridine system. The ligand structure greatly influences the effectiveness of the catalyst. A linear correlation between the redox potential of copper complexes and the logarithmic of apparent rate constant (k_p^{app}) has been reported for the ATRP in aqueous media [18]. The performance of more active and stable ATRP catalysts is based on the electron transfer processes [19]. Nevertheless, the redox potential of the metal complex is an important parameter to be considered in the design of new catalysts.

The objective of this study was to modulate the redox potential of the metal center of ATRP catalyst based on the redox properties of ferrocene to obtain high reactivity and dynamics for the atom transfer process due to the fast electron transfer process. Tripodals with ferrocene moieties were well-characterized in the study of electron communication among ferrocene centers [20, 21]. In this study, we report the effect of ferrocene moieties on the reactivities of atom transfer radical polymerization catalyzed by copper-tripodal complexes.

2. Experimental section

2.1. Materials and Equipment.

Methyl methacrylate (MMA) (99%, Fluka) was vacuum distilled before use. (1-bromoethyl)benzene (97%, Acros organics), (1-chloroethyl)benzene (97%, Acros

organics), CuBr (97%, Riedel-de Haën), $CuBr_2$ (99%, J.T. Baker Chemical Co.), CuCl (98%, Merck) and $CuCl_2.2H_2O$ (97%, Fluka chemika) were used without purification. The starting materials for tripodal ligand were purchased as follows: ferrocene carboxaldehyde (98%, Aldrich) and *tris*(2-aminoethyl)amine - TREN (98%, Fluka). All solvents were purchased as AR grade. NMR spectra were collected on a 300 MHz Bruker AVANCE spectrometer. ESI-MS spectra were recorded on a Bruker Data Analysis Esquire-LC mass spectrometer, equipped with an electrospray source.

2.2 Synthesis of tripodal ligand (TRENFcImine)

Tripodal ligand (TRENFcImine) was prepared as shown in Scheme 2 with a moderate yield. The synthesis was performed under ambient condition at room temperature.

The following was adapted from literature [20, 21]. A mixture of tris(2-aminoethyl)amine (1.0038 g, 6.8641 mmol) and ferrocene carboxaldehyde (4.0694 g, 16.670 mmol) with a small amount of acetonitrile was stirred overnight at room temperature. The orange precipitate was obtained and then filtered off and washed with acetonitrile and dried under vacuum. The tripodal *tris*imine ligand was obtained in a yield of 78% (3.9278 g, 5.3484 mmol).

ESI-MS, m/z: 735.3 [M+H]. ^{1}H NMR (300MHz, CD_3OD): δ(ppm) 2.78 (*t*, 6H, 3(N-C*H*$_2$CH$_2$-)), 3.49 (*t*, 6H, 3(N-CH$_2$C*H*$_2$-)), 4.09 (*s*, 15 H, Fc), 4.36 (*m*, 6H, Fc), 4.54 (*m*, 6H, Fc), 8.02 (*s*, 3H, *H*C=N).

2.3 Polymerization

The polymerization of methyl methacrylate was carried out under dry argon in a dried Schlenk flask equipped with a magnetic stirring bar. The Schlenk flask was charged with the required amount of ligand and metal halide catalyst sealed with a rubber septum, then evacuated-backfilled with argon for three times. After methyl methacrylate monomer was added via a syringe, three cycles of freeze-pump-thaw were performed to remove oxygen and then degassed solvents were added with an argon–purged syringe. The solution mixture was stirred for 10-15 minutes at room temperature and immersed in an oil bath preheated to the desired temperature and stirred for 10 minutes at desired temperature. Finally an initiator was added to start the polymerization. After a given time, the reaction was quenched with tetrahydrofuran (THF) and the reaction mixture was cooled to room temperature. The obtained polymer solution was passed over an alumina column to remove the catalyst. THF was removed by evaporation and ligand residues in the polymer product were washed with an excess amount of methanol. The final polymer product was dried under vacuum and used for the kinetic studies.

2.4 Polymer characterization

The yield percentage of the polymerization was determined gravimetrically by weighing the dried polymer. The molecular weight and polydispersity index of polymer products (relative to polystyrene standards calibration) were measured using a Waters 150-CV GPC equipped with PLgel 10 μm mixed B 2 columns (MW resolving range = 500-10,000,000) and refractive index detector, using THF as the eluent at 30 °C with the flow rate 1.0 mL/min. .

2.5 Conformer Search

The model structures of Cu(I)-TRENFc(*cis*-Imine) and Cu(I)-TRENFc(*trans*-Imine) were generated by the Conformer Search Module of CERIUS^2 (version 4.9) using the Universal force field [22]. The starting structure of each model was randomly generated and minimized by CERIUS^2. Free rotation torsion angles of each model were randomly varied over 360^o in the conformer searching. A total of 200 minimized conformers for each model were obtained. Then the overlay of minimized conformers was performed by CERIUS^2.

3. Results and discussion

3.1. Polymerizations of MMA with tripodal ligand/CuBr catalyst

Multidentate nitrogen-based ligands are the most effective ligands in copper-based ATRP and Me_6TREN is the best active ATRP ligand among the tripodal ligand architecture [23]. A steric hindered ligand usually promotes a much slower and less controlled polymerization [16]. Even though a ferrocene moiety is bulkier than a methyl group, the redox active property of ferrocene moieties is expected to facilitate the electron transfer process in the ATRP and enhance the catalytic activities. It should be recalled that the polymerization of MMA catalyzed by CuBr/Me_6TREN in toluene was not much successful with less than 10% initiation [23], even though the controlled polymerization was achieved in a highly polar solvent [24]. In this study, the CuBr/TRENFcImine system was tested in toluene, a common nonpolar solvent for polymerization, for the ATRP of MMA using 1-bromoethyl benzene (PEBr) as an

initiator at 90 ^{o}C (entries 1-5, Table 1). No significant amount of polymers was obtained after polymerization with the stand-alone ligand or CuBr/TRENFcImine system for 35 minutes at 90 ^{o}C. Figure 1 shows a kinetic plot of the % conversion versus time, showing that the monomer conversion increases with time, and the rate of reaction is relatively fast (82% conversion in 2 hours) indicating that this catalytic system is highly active and the slower rate of polymerization due to the steric hindrance ligand can be overcome with the facilitation of electron transfer from ferrocene moieties. Figure 2 shows a plot of $\ln([M]_o/[M]_t)$ versus time for the homogeneous ATRP of MMA in 60% (v/v) toluene. The linearity of $\ln([M]_o/[M]_t)$ versus time was observed with a k_{obs} of 2.3 x 10^{-4} s^{-1} (Figure 2, label A), suggesting that the polymerization was first-order with respect to monomer and the concentration of growing radicals remained constant all over the reaction [25]. The number average molecular weight, M_n from GPC is not observed with the linear increase in M_n versus monomer conversion (as required for the living polymerization). It is possibly due to the inefficiency of the initiation step. However all M_n results in Table 1 (entries 1-5) show that the M_n is increasing with the monomer conversion and reaction times. The polymerizations of MMA under the condition of [monomer]:[initiator]:[metal catalyst]:[ligand] = 100:1:1:1 at 90 °C gave a broad molecular weight distribution (M_w/M_n in the range of 1.63-2.11). This is probably due to the faster and slower rates in the activation and deactivation steps, respectively. Therefore $CuBr_2$ was added as the additive to increase the rate of the deactivation step. The results are shown in Table 1 (entries 6-10), it is apparent that the addition of $CuBr_2$ leads to the improvement of the polydispersity index (lower M_w/M_n) with the slower rate of polymerization. The addition of $CuBr_2$ increased the concentration of Cu(II) species

and then the concentration of dormant species (R-X) was increased. Therefore, the radical coupling termination was suppressed resulting lower M_w/M_n (in the range of 1.49-1.67) (Eq. (1) and Eq. (2) [26], with $K_{eq} = k_{act}/k_{deact}$, p is monomer conversion and cf. Scheme 1 for the explanation of all symbols) and the slower rate of polymerization (k_{obs} = 1.1 x 10^{-4} s^{-1}, Figure 2, label B) [16, 27]. Moreover, this system was also performed effectively at the higher concentration at 40 mol% of $CuBr_2$ with respect to CuBr (entries 11-15) leading to the lower M_w/M_n (in the range of 1.32-1.52) and the comparable rate of polymerization (k_{obs} = 1.1 x 10^{-4} s^{-1} Figure 2, label C) to the 20 mol% system. The narrow polydispersity due to the addition of $CuBr_2$ indicated that the TRENFcImine system was an efficient catalytic system for copper-based atom transfer radical polymerization even though the initiation efficiency was relatively low.

$$R_p = k_p K_{eq}[M][R\text{-}X]([Cu^{I}]/[X\text{-}Cu^{II}]) \qquad (1)$$

$$M_w/M_n = 1+(k_p[R\text{-}X]/k_{deact}[X\text{-}Cu^{II}])(2/p-1) \qquad (2)$$

3.2 Polymerizations of MMA with tripodal ligand/copper chloride catalyst

The effect of halides on the ATRP of MMA was investigated in this study (Table 2 – entries 16-20). The catalytic activity of CuCl/TRENFcImine was tested for the ATRP of MMA using 1-chloroethyl benzene (PECl) as an initiator at 90 ^{o}C in toluene. The polydispersity index of the CuCl system (entries 16-20) is slightly similar to the CuBr system (entries 1-5) while the M_n(exp) of the CuCl system is slightly higher than the CuBr system. The lower initiation efficiency is due to the stronger bond of C-Cl of the chloride system compared to the bromide system. The addition of 2 mol% of

$CuCl_2.2H_2O$ with respect to CuCl (entries 21-25) showed that the polydispersity index (M_w/M_n) was not significantly different from the CuCl system (entries 16-20) but the rate of propagation was faster (Table 2). It is possibly due to the trace of water from $CuCl_2.2H_2O$ to accelerate the rate of propagation in which the halogen transfer equilibrium is shifted from the dormant to active species [25, 28].

3.3. Effects of the monomer to catalyst ratio on the ATRP

The comparison of the ATRP of MMA at the molar ratio of the monomer to catalyst at 100:1, 100:0.5, 250:1, and 250:0.5 was investigated in this study (Table 3). This led us to determine the catalyst position in the atom transfer equilibrium and the dynamics of exchange between the dormant and active species in the ATRP process [25]. Also the catalytic activity at the higher ratio of the monomer to catalyst indicates the efficiency of the catalytic system. One of disadvantages of ATRP is that the large amount of catalyst is commonly required to achieve the polymerization control. It causes an additional cost for the amount of metal catalysts used in the polymerization. Moreover the metal residues in the final products can be a limitation for industrial applications. Table 3 shows the solution polymerization under the conditions of the CuBr and CuCl systems with different molar ratios of the monomer to catalyst. The CuBr systems (entries 26-40) show that the optimum condition with a good controlled polymerization was the 250:1:0.5 molar ratio of monomer to initiator to catalyst. The 250:1 molar ratio of monomer to catalyst resulted that the rate of polymerization (k_{obs} =

1.2 x 10^{-4} s^{-1}, Figure 2, label D) became slower and the polydispersity index (M_w/M_n) was narrower. This is probably because the rate of ATRP, M_n and M_w/M_n were dependent on the concentration of Cu(I) complexes catalyst as shown in Eq. (1) and Eq. (3) [29]. Increasing the molar ratio of the monomer to catalyst leads to the lower concentration of catalysts and slower the rate of polymerization. The CuCl systems (entries 41-45) at the 250:1 molar ratio of monomer to catalyst shows slightly broader polydispersity index with higher efficiency in the initiation step than the CuBr systems (entries 36-40).

$$M_w/M_n = 1+(2/k_{act}\,[Cu^I]t) \qquad (3)$$

3.4 Conformer search studies of copper-tripodal complexes

The conformational search was carries out by CERIUS using the Universal Force Field (UFF) to study the steric effect of Cu(I)-tripodal complexes : Cu(I)-TREN(*cis*-FcImine) and Cu(I)-TREN(*trans*-FcImine). The *cis*- and *trans*-configurations were assigned relative to the copper center. The structures and the overlay minimized structures of two models is shown in Figure 3. According to the UFF force field on CERIUS[2], the *trans*-model has a lower energy than the *cis*-model. Therefore, the TRENFcImine ligand must adopt a trans-configuration with distortion from tetrahedral geometry. Moreover, it is obvious from the overlay structures that the *trans*-FcImine model has a pore structure for the incoming ligand to enter to the copper center with less steric interactions from ferrocene moieties than the *cis*-FcImine model. The restricted rotation of C=N imine functional groups relieved the steric interactions from bulky ferrocene moieties for the incoming ligand. Hence, it is proposed here that the less controlled polymerization catalyzed by Cu(I)-TRENFcImine may not be governed by the

steric effect of ferrocene moieties. In contrast, the electronic effect resulting from the redox active ferrocene moieties in the induction the copper center to bind halides tightly might be more pronounced in the explanation of the slower rate of the deactivation step. The investigation of the electronic effect of ferrocene moieties on the atom transfer radical polymerization is in progress.

4. Conclusions

Copper-tripodal complexes with ferrocene moieties (CuX/TRENFcImine, X=Br or Cl) were employed in the ATRP of MMA. The high activity of catalysts was probably due to the facilitation of the electron transfer process of ferrocene moieties. However, this led to broader polydispersity index which could be improved effectively with the addition of $CuBr_2$ in the bromide system. The CuBr/TRENFcImine system is more active than the CuCl/TRENFcImine system. The polydispersity index of the CuBr/TRENFcImine system can be improved with the addition of $CuBr_2$. Slightly changes in the rate of polymerization and polydispersity of the CuCl/TRENFcImine were observed with increasing of the molar ratio of monomer to catalyst and the addition of $CuCl_2.2H_2O$. Trace of water in $CuCl_2.2H_2O$ accelerated the rate of propagation leading to a higher molecular weight.

Acknowledgement

This research was supported by the Center for Innovation in Chemistry: Postgraduate Education and Research Program in Chemistry (PERCH-CIC), the Thailand Research Fund (TRF-RMU4980050) and Faculty of Science, Mahidol University.

References

1. Wang JS, Matyjaszewski K. J Am Chem Soc 1995;117:5614-5615.

2. Kato M, Kamigaito M, Sawamoto M, Higashimura T. Macromolecules 1995;28:1721-1723.

3. Tsarevsky NV, Matyjaszewski K. Chem Rev 2007;107:2270-2299.

4. Matyjaszewski K, Xia J. Chem Rev 2001;101:2921-2990.

5. Patten TE, Matyjaszewski K. Acc Chem Res 1999;32:895-903.

6. Braunecker WA, Matyjaszewski K. Prog Polym Sci 2007;32:93-146.

7. Braunecker WA, Pintauer T, Tsarevsky NV, Kickelbick G, Matyjaszewski K. J Organomet Chem 2005;690:916-924.

8. Braunecker WA, Brown WC, Morelli BC, Tang W, Poli R, Matyjaszewski K. Macromolecules 2007;40:8576-8585.

9. Goodwin JM, Olmstead MM, Patten TE. J Am Chem Soc 2004;126:14352-14353.

10. O'Reilly RK, Gibson VC, White AJP, Williams DJ. J Am Chem Soc 2003;125:8450-8451.

11. Shao Q, Sun H, Pang X, Shen Q. Eur Polym J 2004;40:97-102.

12. Kamigaito M, Watanabe Y, Ando T, Sawamoto M. J Am Chem Soc 2002;124:9994-9995.

13. Kotani Y, Kamigaito M, Sawamoto M. Macromolecules 1999;32:2420-2424.

14. Maria S, Stoffelbach F, Mata J, Daran JC, Richard P, Poli R. J Am Chem Soc 2005;127:5946-5956.

15. Braunecker WA, Itami Y, Matyjaszewski K. Macromolecules 2005;38:9402-9404.

16. Inoue Y, Matyjaszewski K. Macromolecules 2004;37:4014-4021.

17. Xia JH, Matyjaszewski K. Macromolecules 1999;32:2434-2437.

18. Coullerez G, Carlmark A, Malmstrom E, Jonsson M. J Phys Chem A 2004;108:7129-7131.

19. Tsarevsky NV, Braunecker WA, Matyjaszewski K. J Organomet Chem 2007;692:3212-3222.

20. Bullita E, Casellato U, Ossola F, Tomasin P, Vigato PA, Russo U. Inorg Chim Acta 1999;287:117-133.

21. Heitzmann M, Moutet JC, Pecaut J, Reynes O, Royal G, Saint-Aman E, Serratrice G. Eur J Inorg Chem 2003;3767-3773.

22. Rappe AK, Casewit CJ, Colwell KS, Goddard WA, Skiff WM. J Am Chem Soc 1992;114:10024-10035.

23. Queffelec J, Gaynor SG, Matyjaszewski K. Macromolecules 2000;33:8629-8639.

24. Miura Y, Satoh T, Narumi A, Nichizawa O, Okamoto Y, Kakuchi T. Macromolecules 2005;38:1041-1045.

25. Ibrahim K, Yliheikkila K, Abu-Surrah A, Lofgren B, Lappalainen K, Leskela M, Repo T, Seppala J. Eur Polym J 2004;40:1095-1104.

26. Tang HD, Arulsamy N, Radosz M, Shen YQ, Tsarevsky NV, Braunecker WA, Tang W, Matyjaszewski K. J Am Chem Soc 2006;128:16277-16285.

27. Matyjaszewski K, Davis, Thomas P. Handbook of Radical Polymerization. John Wiley & Sons, Inc., Hoboken., 2002.

28. Chatterjee U, Jewrajka SK, Mandal BM. Polymer 2005;46:1575-1582.

29. Nanda AK, Matyjaszewski K. Macromolecules 2003;36:599-604.

สัญญาเลขที่ RMU4980050

โครงการ: การวิเคราะห์และการพิสูจน์โครงสร้างของลิแกนด์ที่มีเฟอร์โรซีนและแอนทราซีนแอดดักเป็นองค์ประกอบสำหรับการเร่งปฏิกิริยา

ระยะเวลาโครงการ: 19 ก.ค. 2549 – 18 ก.ค. 2552

Output

1. Thammakan, N.; **Somsook, E.*** "Synthesis and thermal decomposition of cadmium dithiocarbamate complexes" *Mater. Lett.* **2006**, *60*, 1161-1165.
2. Chairam, S.; **Somsook, E.*** "Starch Vermicelli Template for Synthesis of Magnetic Iron Oxide Nanoclusters" *J. Magn. Magn. Mater.* **2008**, *320*, 2039-2043.
3. Chaicharoenwimolkul, L.; Munmai, A.; Chairam, S.; Tewasekson, U.; Sapudom, S.; Lakliang, Y.; **Somsook, E.*** "Effect of Stabilizing Ligands Bearing Ferrocene Moieities on the Gold Nanoparticle-Catalyzed Reactions of Arylboronic Acids" *Tetrahedron Lett.* **2008**, *49*, 7299-7302.
4. Chairam, S.; Poolperm, C.; **Somsook, E.*** "Starch Vermicelli Template-Assisted Synthesis of Size/Shape-Controlled Nanoparticles" *Carbohydr. Polym.* **2009**, *75*, 694-704.
5. Chairam, S.; **Somsook, E.**; Coll, R. K.* "Enhance Thai Student Learning of Chemical Kinetics" *Res. Sci. Tech. Educ.* **2009**, *27*, 95-115.
6. Jansoon, N.; Coll, R. K.; **Somsook, E.*** "Understanding Mental Models of Dilution in Thai Students" *Int. J. Env. Sci. Educ.* **2009**, *4*, 147-168.
7. Sunsin, A.; Wisutsri, N.; Suriyarak, S.; Tienchai, R.; Jindabot, S.; Chaicharoenwimolkul, L.; **Somsook, E.*** "Effect of Ferrocene Moieties on Copper-Based Atom Transfer Radical Polymerization" *J. Appl. Polym. Sci.* **2009**, *113*, 3766-3773.

Available online at www.sciencedirect.com

SCIENCE DIRECT

Materials Letters 60 (2006) 1161 – 1165

materials letters

www.elsevier.com/locate/matlet

Synthesis and thermal decomposition of cadmium dithiocarbamate complexes

Nirawan Thammakan, Ekasith Somsook *

Department of Chemistry, Faculty of Science, Mahidol University, Rama VI Rd. Rachathewi, Bangkok 10400, Thailand

Received 22 July 2005; accepted 27 October 2005
Available online 28 November 2005

Abstract

Cadmium(II) complexes of new polydentate dithiocarbamates with benzyl or methylferrocene as substituents have been prepared. The IR spectra of the complexes suggested a bidentate coordination of dithiocarbamate ligands to the cadmium ion. The thermal properties of cadmium complexes were studied by thermogravimetric analysis (TGA) and differential scanning calorimetry (DSC). Pyrolysis of cadmium complexes was further carried out at 700 °C and the products were characterized by powder X-ray diffraction (XRD), field emission scanning electron microscopy (FESEM), and transmission electron microscopy (TEM). The pyrolysis of cadmium methylferrocene complex produced a product with nanofibers.

Keywords: Dithiocarbamate; Thermal analysis; Pyrolysis; Ferrocene; Nanofiber

1. Introduction

Cadmium dithiocarbamate complexes have been used as a precursor for the synthesis of CdS nanoparticles [1,2]. In addition, the applications of dithiocarbamate ligands have been demonstrated in the construction of new supramolecular structural motifs including polymetallic nanosized macrocycles, cryptands and catenane [3]. In this work, new dithiocarbamate ligands were readily synthesized from secondary phenyldiamine in which the substituents were benzyl or methylferrocenyl group for the formation of cadmium complexes which were coordination polymers. The thermal properties of polymers were studied by thermogravimetric analysis (TGA) and differential scanning calorimetry (DSC) and used as a precursor for the CdS preparation by pyrolysis at high temperature. The thermal decomposition products were characterized with powder X-ray diffraction, field emission scanning electron microscopy (FESEM) with energy dispersive X-ray analysis (EDX), and transmission electron microscopy (TEM).

2. Experimental

2.1. Starting materials

The synthesis of N^1, N^4-dibenzyl-1,4-phenylenediamine **2** and N^1, N^4-dimethylferrocenyl-1,4-phenylenediamine **4** was carried out by following the literature [4].

2.1.1. Synthesis of triethylammonium dithiocarbamate

Et_3N (0.08 g, 0.81 mmol) and CS_2 (0.06 g, 0.81 mmol) were added in a solution of diamine 2 (0.1 g, 0.37 mmol) in 2 mL of THF. A drop of benzene was added to the mixture. It was stirred at 0 °C for 10 min and then at room temperature for 15 h. Yellow solid was filtered off, washed with diethylether (10 mL) and dried under vacuum. (0.09 g, 28.8% yield): m.p. = 60–64 °C; MS (ESI positive ion, CH_2Cl_2) m/z: 842.8 $[M–4H]^+$; ^{1}H NMR (300 MHz, $CDCl_3$): δ = 1.34 (t, 7.3 Hz, 6H, NCH_2CH_3), 3.05 (q, 7.3 Hz, 4H, NCH_2CH_3), 4.2 (s, 2H, CH_2), 6.41 (d, 8.7 Hz, 1H, ArH), 6.69 (d, 8.7 Hz, 1H, ArH), 7.25 (m, 5H, ArH); IR (KBr pellete): ν_{max} = 3386, 2938, 2678, 2492, 1606, 1516, 1434, 1398, 1238, 1173, 1093, 1036, 819, 698, 457 cm^{-1}.

2.1.2. Synthesis of cadmium dithiocarbamate complexes, *3*

Et_3N (0.39 g, 3.82 mmol) and CS_2 (0.29 g, 3.82 mmol) were added in a solution of diamine 2 (0.5 g, 1.74 mmol) in 10 mL of

* Corresponding author. Tel.: +662 201 5123; fax: +662 354 7151.
E-mail address: scess@mahidol.ac.th (E. Somsook).

0167-577X/$ - see front matter © 2005 Elsevier B.V. All rights reserved.
doi:10.1016/j.matlet.2005.10.107

THF. The mixture was stirred for 2 h before adding more solvent to 40 mL. Then $Cd(OAc)_2 \cdot 2H_2O$ (0.51 g, 1.74 mmol) was dissolved in 4 mL of H_2O and added dropwise to the mixture. Yellow solid was precipitated out immediately and the mixture was stirred for 15 h at room temperature. The solid was filtered off, washed with CH_2Cl_2 (30 mL) and dried under vacuum. (0.056 g): IR(KBr pellete) ν_{max} = 3407, 3024, 1606, 1619, 1513, 1442, 1398, 1322, 1237, 1198, 1119, 1074, 945, 914, 747, 701, 577 cm^{-1}.

2.1.3. Synthesis of cadmium dithiocarbamate complexes, ***6***

Compound **6** was prepared using the similar method as complex **3**. (0.063 g): IR(KBr pellete) ν_{max} = 3369, 1561, 1421, 1347, 1114, 1051, 1021, 940, 675, 624 cm^{-1}.

2.1.4. Pyrolysis

Compound **3** and **6** precursors (1.5 g each) were heated to 700 °C under nitrogen atmosphere. The gray (1.13 g) and yellow (0.73 g) solid materials were obtained from compound **3** and **6**, respectively, and characterized by X-ray powder diffraction, field emission scanning electron microscopy (FESEM) with energy dispersive X-ray analysis (EDX), and transmission electron microscopy (TEM).

2.2. General measurements

2.2.1. Thermal analysis

Thermal gravimetric analysis (TGA) and differential scanning calorimetric (DSC) were performed with the TA instruments-SDT-2960 simultaneous analyzer. Samples were placed in an alumina cup and heated from 30 to 700 °C at a heating rate of 5 °C min^{-1} in a nitrogen atmosphere. A purge gas was a flowing dry nitrogen at a rate of 100 mL min^{-1}.

2.2.2. Powder X-ray diffraction (XRD)

A D8 Advance Bruker analytical X-ray system was operated at the CuKα wavelength of 1.5650 nm, 40 mA, and 40 kV. The diffraction pattern over the range of 20–70° 2θ was recorded at a scan rate of 5 s/step and step size 0.020 2θ/s.

2.2.3. Field emission scanning electron microscopy (SEM) and transmission electron microscopy (TEM)

FESEM images were recorded using a JEOL JSM-6340F attached with energy dispersive X-ray analysis (EDX). TEM images were recorded using a Philip Tecnai-20.

3. Results and discussions

3.1. Synthesis of ligands

Tetrakis(triethylammonium) bis(dithiocarbamate), a ligand with two groups of dithiocarbamates with four sulfur possible donor atoms, was obtained by a straightforward method (see Scheme 1 in Appendix A). The mass spectrum of the ligand ($[M–4H]^+$ = 842.8) was in agreement with the corresponding (tetrakis)triethylammonium bis (dithiocarbamate) in which its IR spectrum exhibited an absorption band around 1050 cm^{-1} assigned to the monodentate coordination of dithiocarbamates to triethylamine [5]. In addition, this ligand showed a stretching frequency at 2678 cm^{-1} which could be assigned to the stretching vibration of the S–H bond. Therefore, the interactions between triethylammonium cation and dithiocarbamate could be formed via hydrogen bonds. Moreover, the vibration of the C–N bond at 1470 cm^{-1} (ν(C–N) 1680–1640 cm^{-1} and ν(C–N) 1350–1250 cm^{-1}) indicated that a considerable double bond character of the C–N bond in the dithiocarbamate groups.

3.2. Synthesis of cadmium dithiocarbamate complexes

Due to the rigid and crowded structure, the obtaining products of complex **3** and **6** were not macrocycles as reported by Wong et al. [6]. They were precipitated out from THF solvent and not soluble in water, indicating that the as-prepared complexes were in a polymeric form. The lack of S–H band at 2678 cm^{-1} supported that the ligand was coordinated to cadmium via S atoms. The C–N stretching frequencies at 1442 and 1421 cm^{-1} for complex **3** and **6**, respectively, were shifted to lower frequencies comparing to the C–N frequencies at 1470 and 1475 cm^{-1} for corresponding ligands indicating the less double bond character of the dithiocarbamate complexes than the ligands. Therefore, the dithiocarbamate ligands were more likely coordinated to cadmium via a bidentate mode. The proposed structures of complex **3** and **6** are shown in Scheme 2 in Appendix A. In addition, complex **3** and **6** were also available from a starting material of tetrakis(triethylammonium) bis(dithiocarbamate).

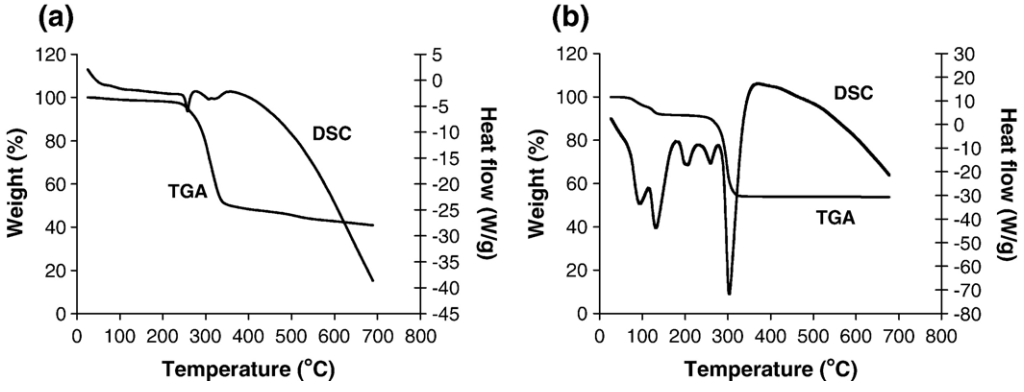

Fig. 1. TGA and DSC of (a) **3** and (b) **6**.

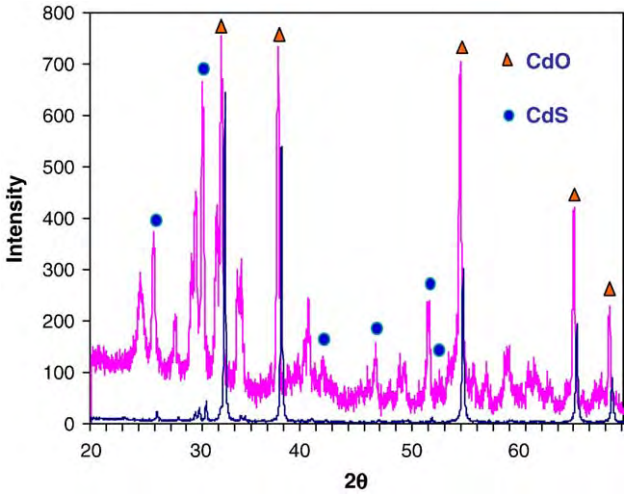

Fig. 2. XRD of the pyrolysis products from complex **3** (upper) and **6** (lower).

3.3. Thermal analysis of cadmium dithiocarbamate complexes

The thermal properties of complex **3** and **6** were studied by TGA and DSC in the temperature ranging from 20 to 700 °C under nitrogen atmosphere (Fig. 1). Their thermograms of both complexes were significantly different, probably due to the different substituents. The thermal decomposition of the cadmium methylferrocene complex **6** started at lower temperature with the loss of water immediately followed by an endothermic process (between 188.4 and 242.6 °C). At higher temperatures two steps endothermic decomposition took place, but the steps were not separated sufficiently for the individual mass losses to be identified. The cadmium benzyl complex **3** showed the decomposition in two steps. The thermal decomposition started at 249.8 °C with a small endothermic peak. Both complexes were not decomposed yet at 600 °C. It is worth noting that the lower onset temperature of the cadmium methylferrocene complex **6** is due to the methylferrocene moiety.

3.4. Pyrolysis of cadmium dithiocarbamate complexes

Based on the thermal properties, both complex **3** and **6** were further investigated by pyrolysis under nitrogen atmosphere at 700 °C. The resulting gray powder was obtained for complex **3** while the mixed colors of yellow and reddish powder was obtained for complex **6**. The XRD patterns of both pyrolysis products were different in which the product from the methylferrocene precursor exhibited a higher signal-to-noise intensity (Fig. 2). The average sizes of the nanocrystallites of the materials prepared from complex **3** and **6** were calculated to be 42 and 59 nm, respectively, as derived from Scherer's equation [7]. SEM and TEM photographs and EDX spectra of both products are shown in Figs. 3 and 4, respectively. SEM photographs of all products from the benzyl and methylferrocene precursors were significantly different in which the surface of the product from the methylferrocene precursor was covered with nanofibers where the size of fibers was estimated to be 20 nm (Fig. 3c). The formation of nanofibers was probably due to the resulting lower decomposition temperature of the methylferrocene moieties of complex **6**. In addition, two nanoscale products prepared from complex **6** were also formed with a particle size of approximately 20 nm (Fig. 3d). EDX results indicated the presence of cadmium oxide and cadmium sulfide in the residue. It should be noted that the thermal decomposition of complex **6** did not afford FeS.

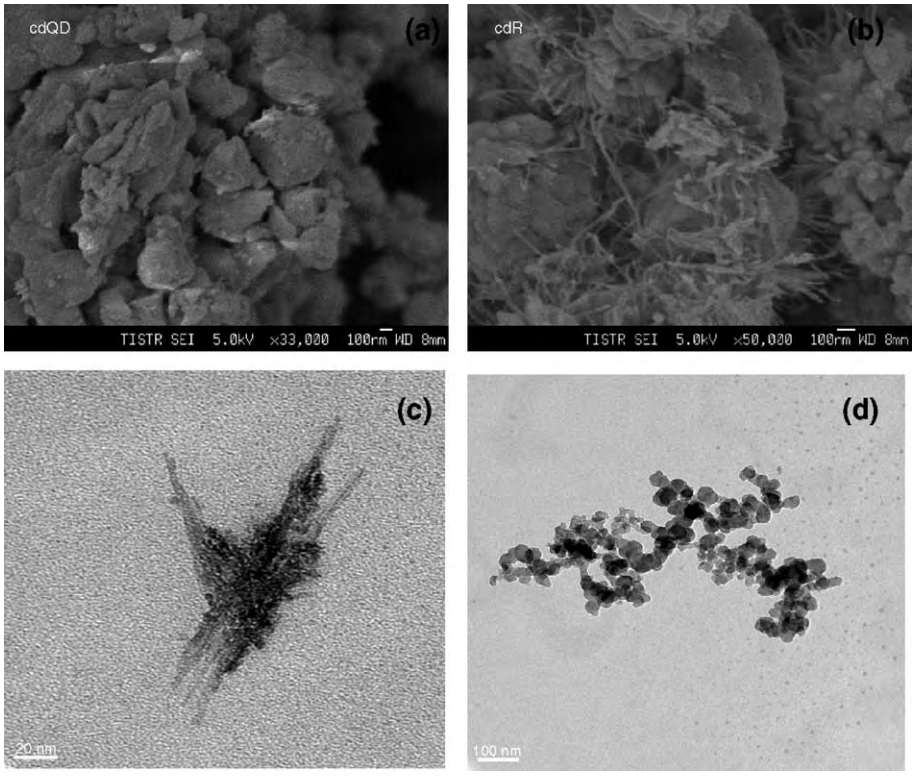

Fig. 3. (a and b) FESEM photograph of the pyrolysis products from complex **3** and **6** and (c and d) TEM photograph of the pyrolysis product from complex **6**. The bars are 100 nm for (a), (b), and (d) and 20 nm for (c).

4. Conclusion

In all complexes, the cadmium is coordinated through both sulfur atoms of the dithiocarbamate group in a bidentate fashion. The onset decomposition temperature of cadmium methylferrocene complex **6** was lower than the one of cadmium benzyl complex **3** under nitrogen atmosphere. Different products were obtained from precursors with different substituents. In this case, the cadmium methylferrocene complex **6** produced a product with nanofibers. Even though a mixture of cadmium oxide and cadmium sulfide was obtained as products, the thermal decomposition of the

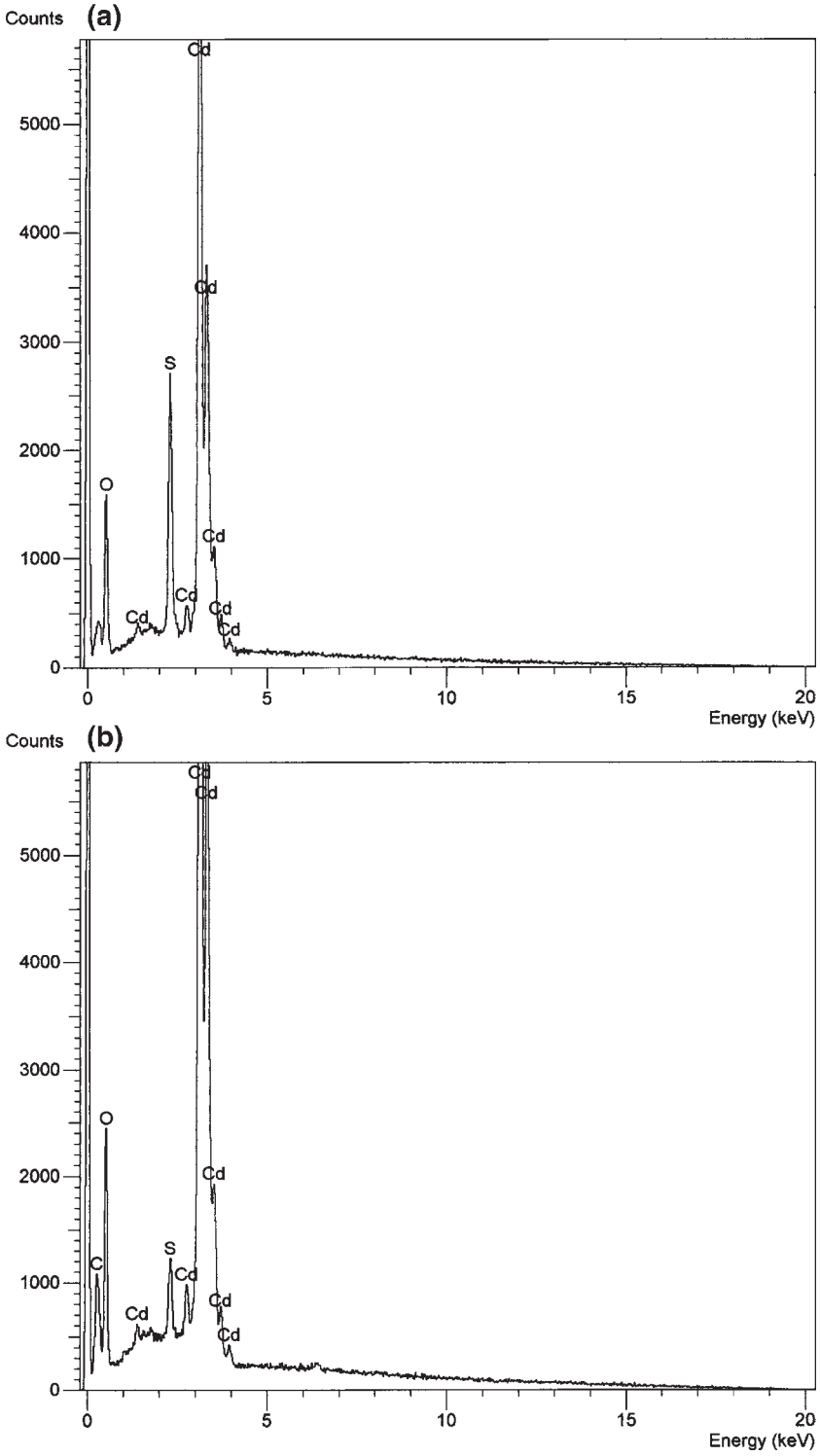

Fig. 4. EDX of the pyrolysis products from complex (a) **3** and (b) **6**.

dithiocarbamate complexes may be a useful synthetic route to obtain such compounds.

Acknowledgement

We thank Thailand Institute of Scientific and Technological Research (TISTR) for SEM measurements. This research was supported by the Postgraduate Education and Research Program in Chemistry (PERCH), the Thailand Research Fund (TRF) and the Faculty of Science, Mahidol University.

Appendix A. Supplementary data

Supplementary data associated with this article can be found, in the online version, at doi:10.1016/j.matlet.2005.10.107.

References

[1] M. Lazell, P. O'Brien, Chem. Commun. (1999) 2041.
[2] P. Yan, Y. Xie, Y.T. Qian, X.M. Liu, Chem. Commun. (1999) 1293.
[3] W.W.H. Wong, J. Cookson, E.A.L. Evans, E.J.L. McInnes, J. Wolowska, J. P. Maher, P. Bishop, P.D. Beer, Chem. Commun. (2005) 2214.
[4] A.I. Vogel, B.S. Furniss, Vogel's textbook of practical organic chemistry, Longman Scientific and Technical, 5th ed., Wiley, New York, 1989.
[5] K. Nakamoto, Infrared and Raman Spectra of Inorganic and Coordination Compounds, 5th ed., John Wiley, New York, 1997.
[6] W.W.H. Wong, D. Curiel, A.R. Cowley, P.D. Beer, Dalton Trans. (2005) 359.
[7] J.I. Langford, A.J.C. Wilson, J. Appl. Crystallogr. 11 (1978) 102.

Available online at www.sciencedirect.com
ScienceDirect
Journal of Magnetism and Magnetic Materials 320 (2008) 2039–2043
Journal of magnetism and magnetic materials
www.elsevier.com/locate/jmmm

Starch vermicelli template for synthesis of magnetic iron oxide nanoclusters

Sanoe Chairam[a], Ekasith Somsook[b,*]

[a]Institute for Innovation and Development of Learning Process, Mahidol University, Rama VI Road, Rachathewi, Bangkok 10400, Thailand
[b]Faculty of Science, Department of Chemistry, Mahidol University, Rama VI Road Rachathewi, Bangkok 10400, Thailand

Received 5 December 2007; received in revised form 26 January 2008
Available online 6 March 2008

Abstract

A novel method for fabricating magnetic iron oxide nanoparticles was achieved by using transparent vermicelli template as a new stabilizing material. The morphology of the as-prepared magnetic iron oxide deposited on the surface of vermicelli was observed as nanoclusters. The magnetization of the magnetic iron oxide nanoparticles at room temperature was decreased after carbonization at 200 °C. Therefore the thermal decomposition of iron oxide nanoparticles stabilized by starch vermicelli template yielded iron oxide/carbon nanocomposites with the soft magnetic behavior which are useful for biomedical applications.

Keywords: Magnetic iron oxide nanoparticle; Nanocluster; Starch vermicelli template

1. Introduction

Iron oxides with 16 phases are known and widespread in nature in the forms of oxides, hydroxides or oxide–hydroxides [1]. As known, nanometer-scale magnetic particles have been frequently synthesized for the nanomagnetism study due to a variety of potential applications in magnetism, catalysis, chemistry and biology [2–4].

The formation of magnetic nanoparticles has attracted considerable interest. To utilize magnetic iron oxide nanoparticles for highly sensitive magnetic nanodevices, several methods for synthesizing magnetic iron oxide nanoparticles have been developed. Among these, the solution-phase synthesis by co-precipitating of Fe^{2+} and Fe^{3+} ions in a basic media has been shown as the most effective method to prepare highly uniform magnetite (Fe_3O_4) nanoparticles in size and shape [5,6]. An alternative method is the thermal decomposition, which has been shown for the synthesis of high crystalline iron oxide nanoparticles. Many stabilizing agents with a long-chain structure [7,8] have been introduced to stabilize magnetite (Fe_3O_4) nanoparticles with the desired size. However, these compounds are highly reactive and potential environmental risks during the synthetic processes. To save the environment, biomaterials have been used as a stabilizing agent in the experimental procedures. Recently, Giri and coworkers reported the preparation of uniform sized magnetite (Fe_3O_4) nanoparticles stabilized by using phospholipids [6]. The development of new biomaterials is still a considerable challenge for *in vivo* applications. As known starch is one of the most widely used carbohydrate polymers, our interest here is the utilization of mung bean starch vermicelli as template may bring advantageous possibilities to stabilize magnetic iron oxide nanoparticles because vermicelli surface of starch which is full of polyhydroxylated functional groups [9], may assist the precipitation of the iron oxide nanoparticles on the surface of the vermicelli template.

In order to achieve the preparation of the soft magnetic materials for applications, it is required to reduce the strength of the applied magnetic field to be as small as possible. Herein, we have proposed a novel experimental procedure to prepare soft magnetite (Fe_3O_4) stabilized by mung bean starch vermicelli template after carbonization at a low temperature (200 °C). The phase transition

*Corresponding author. Tel.: +662 201 5123; fax: +662 354 7151.
E-mail address: scess@mahidol.ac.th (E. Somsook).

0304-8853/$ - see front matter © 2008 Elsevier B.V. All rights reserved.
doi:10.1016/j.jmmm.2008.02.168

temperature of the sample is performed by using thermal gravimetric analysis (TGA) and differential scanning calorimetric (DSC) measurement. The morphology of the sample was investigated by field emission scanning electron microscope (FESEM) and transmission electron microscope (TEM), respectively. To investigate the crystalline phase, the as-prepared sample was characterized by using X-ray powder diffraction (XRD). Finally, the magnetic behavior was examined by vibrating sample magnetometer (VSM).

2. Materials and experimental procedures

2.1. Materials

The starting chemicals used in this experiment were commercially analytical graded reagents. Ferrous chloride tetrahydrate ($FeCl_2 \cdot 4H_2O$, $\geqslant 99.0\%$) was purchased from Fluka (Switzerland) and used without further purification. Hydrochloric acid (HCl, 37%) and ammonium hydroxide (NH_4OH, 25%) were obtained from Labscan Asia (Thailand). Transparent mung bean starch vermicelli (100%, Kaset brand) as a stabilizing material was purchased from a local supermarket in Thailand. All glassware in this experiment were cleaned with 10% nitric (HNO_3) solution and repeatedly washed with de-ionized water obtained from Nanopure® Analytical Deionization Water with an electronic resistance $\geqslant 18.2\,M\Omega\,cm$, and dried before use.

2.2. Preparation of magnetite (Fe_3O_4) nanoparticles stabilized by vermicelli template

The method described here for synthesizing magnetite (Fe_3O_4) nanoparticles was based on the literature [1]. The controlled size of particles was prepared with the addition of mung bean vermicelli template as a stabilizing agent according to the following procedure. Typically, required amount of 1.0 g transparent mung bean vermicelli was placed into a 100 mL round-bottom flask containing 50 mL of a 0.1 M $FeCl_2$ solution. The mixture solution was stirred vigorously under the presence of air and also heated at temperature 85–90 °C by placing the thermometer for temperature control in an oil bath. To form magnetite (Fe_3O_4) nanoparticles, the pH of the mixture solution was adjusted to 12 by a diluted ammonium hydroxide solution (NH_4OH). The color of the colloidal solution was changed immediately to black. The reaction system was maintained under magnetic stirring for 30 min before cooling down to room temperature. The magnetic behavior of the precipitate was observed and removed from the solution by applying a magnetic field from the bottom of the reaction flask, and the black precipitate powder settled down. After discarding the supernatant solution, the mung bean vermicelli coated with iron oxide nanoparticles was washed several times with a diluted hydrochloric solution and de-ionized water, respectively, in order to remove impurity ions. After washing, the solution was tested until the pH was neutral (usually pH∼7). To avoid the phase transformation of the iron oxide [10], the sample is dried by incubating in an oven at 40 °C for 48 h.

2.3. Carbonization

A crucible alumina cup containing the as-prepared sample was placed in the central region of a furnace, Model 59256-P-Com Lindberg. The dry sample was carbonized at low heating temperature of 200 °C at a constant heating of $5\,^{\circ}C\,min^{-1}$. The system was maintained at this temperature for 12 h, and subsequently cooled down to room temperature at the rate of $5\,^{\circ}C\,min^{-1}$. The black precipitate powder was collected and dispersed in a solution by using an ultrasonic bath (ca. 5 min).

2.4. General characterization

The thermal properties of the dry sample were measured by using thermal gravimetric analysis (TGA) and differential scanning calorimetry (DSC) with the TA instrument-2960 SDT simultaneous analyzer. The sample was placed into an alumina crucible for TGA/DSC and heated from 30 to 700 °C with increasing temperature rate of $10\,^{\circ}C\,min^{-1}$ under a flowing argon gas at $20\,cm^3\,min^{-1}$. Scanning electron microscopy (SEM) was carried out by employing a JEOL JSM 6340F field emission scanning electron microscope (FESEM) by accelerating at a voltage of 5.0 kV. The sample was mounted on a Cu grid for SEM measurement and coated with gold to minimize charging. Transmission electron microscopy (TEM) was performed by using a Philip Tecnia G2 sphera transmission electron microscope with an acceleration voltage of 80.0 kV. The sample preparations for the TEM measurement were prepared by dispersing a drop of the sample solution on Formvar-coated Cu grids. The crystalline phase of samples was characterized by using XRD. A D8 Advance Bruker Analytic X-ray diffractometer was operated, the CuKα radiation at the wavelength of 0.15650 nm using 40 mA and 40 kV. The diffraction pattern over the range of 30–70° 2θ was recorded with the scan speed of 2 min/step and the scan rate of 0.015 2θ/s. Meanwhile, the coercivities (H_c), the remanent magnetizations (M_r) and the saturation magnetizations (M_s) of the as-prepared iron oxide nanoparticles were performed by using the vibrating sample magnetometer (VSM) and superconducting quantum interference device (SQUID) measurement (Lakeshore, Model 4500). The magnetic parameters (H_c, M_r and M_s) of each sample were determined from the hysteresis loops produced by the VSM. The saturation magnetization was reached at an applied field of 10 kOe. The magnetization data as a function of the applied field were plotted.

3. Results and discussion

3.1. Thermal analysis

The thermal properties of the iron oxide samples were examined by TGA and DSC (see Fig. 1). The major transition due to the weight loss occurs over a narrow temperature range from 282.4 to 315.8 °C. The weight loss of the sample was 67.50% from the initial amount. Meanwhile, the DSC scan shows two endothermic peaks around 58.9 and 283.3 °C, respectively. The first peak is due to the release of the absorbed water of dehydration and the second peak is obtained from a phase transition of the iron oxide change. The main endothermic effect results from the combustion process of organic compounds in the as-prepared iron oxide consuming energy at 47.8 J/g and this may involve the oxidation, in the presence of oxygen, at high temperature in the TGA experiment. Magnetite (Fe_3O_4) can be easily oxidized to maghemite (γ-Fe_2O_3), which can be further transformed into hematite (α-Fe_2O_3) at high temperature [1], which is reported by Mikhaylova [11] and Wang [12]. No weight change was observed at temperature above 400 °C.

3.2. Electron microscopy (EM) analysis

The surface morphology of the as-prepared iron oxide crystals stabilized by mung bean starch vermicelli template was examined by the FESEM measurement. The FESEM micrograph shows a large quantity of formation of nanoscale iron oxide particles of spherical nanoclusters in shape (see Fig. 2). It was clear that spherical nanoclusters with a diameter of about 200–300 nm were formed by the assembly of many small iron oxide nanoparticles. The transmission electron microscopy (TEM) was further used to examine the morphology (see Fig. 3). After using an ultrasonic treatment to disperse the as-prepared samples, the TEM micrographs exhibit a region of iron oxide nanoclusters, which was found to be similar to the FESEM

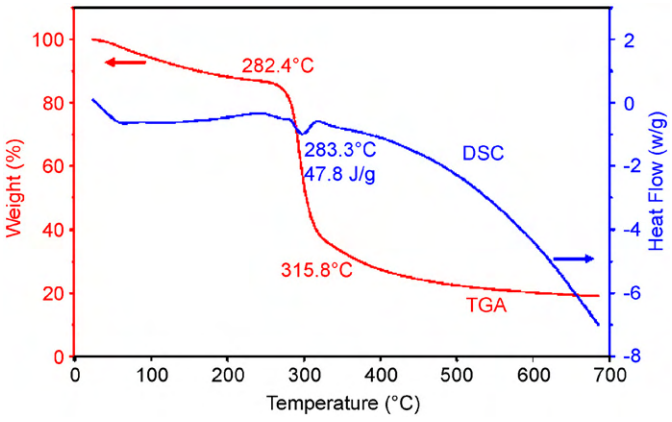

Fig. 1. Thermal analysis by using thermal gravimetric-differential scanning calorimetric (TGA-DSC) analysis of mung bean vermicelli deposited with the as-prepared magnetite (Fe_3O_4) nanoparticles.

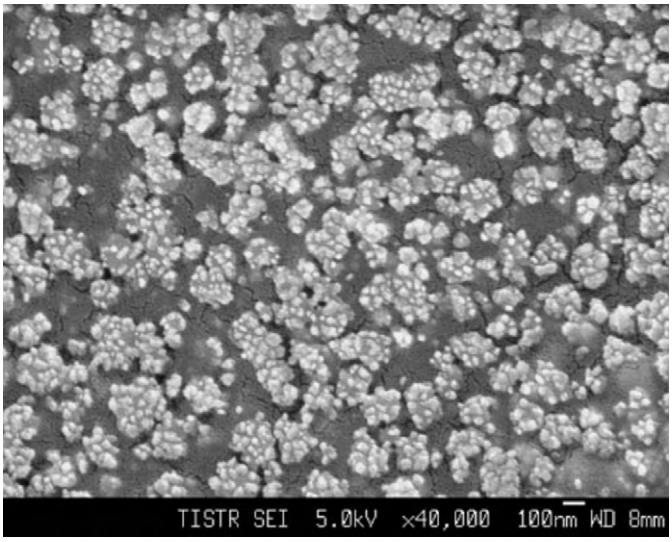

Fig. 2. The representative FESEM image of the as-synthesized iron oxide nanoparticles stabilized by mung bean vermicelli template.

results. Interestingly, it can be seen that wire-like nanoclusters with several hundred nanometers in distance were organized.

3.3. Powder X-ray diffraction (XRD) analysis

The characterization of the crystalline nature of iron oxide was carried out by using XRD analysis, which is essential for identification of the product [1,10]. The crystal structure and phase composition of the as-prepared samples was achieved by investigating the XRD patterns before and after carbonization (see Fig. 4). Before the carbonization process, the position and relative intensity of diffraction peaks from the XRD patterns of the as-prepared samples closely match with that of Fe_3O_4 powder diffraction data [1]. All peaks can be indexed closely to the cubic Fe_3O_4 nanoparticles, which are consistent with the data in the standard card (JCPDS file no. 19-629). The crystallite size of the as-prepared magnetic iron oxide nanoparticles can be calculated from the width of the representative peaks of the XRD patterns by using the Scherer's equation [13]

$$d = \frac{0.9\lambda}{B_\theta \cos \theta_B},$$

where B_θ is the width of the peak at half height and λ is the wavelength of the X-rays. θ_B is the Bragg angle. From the XRD results, the crystallite size of Fe_3O_4 nanoparticles is 14.8 nm after the carbonization. It is similar to Sun [8] who reported that high temperature reaction of the iron oxide could make smaller Fe_3O_4 nanoparticles from the larger ones.

3.4. Vibrating sample magnetometry (VSM) analysis

The saturation magnetizations were derived from the VSM measurement at room temperature by cycling the

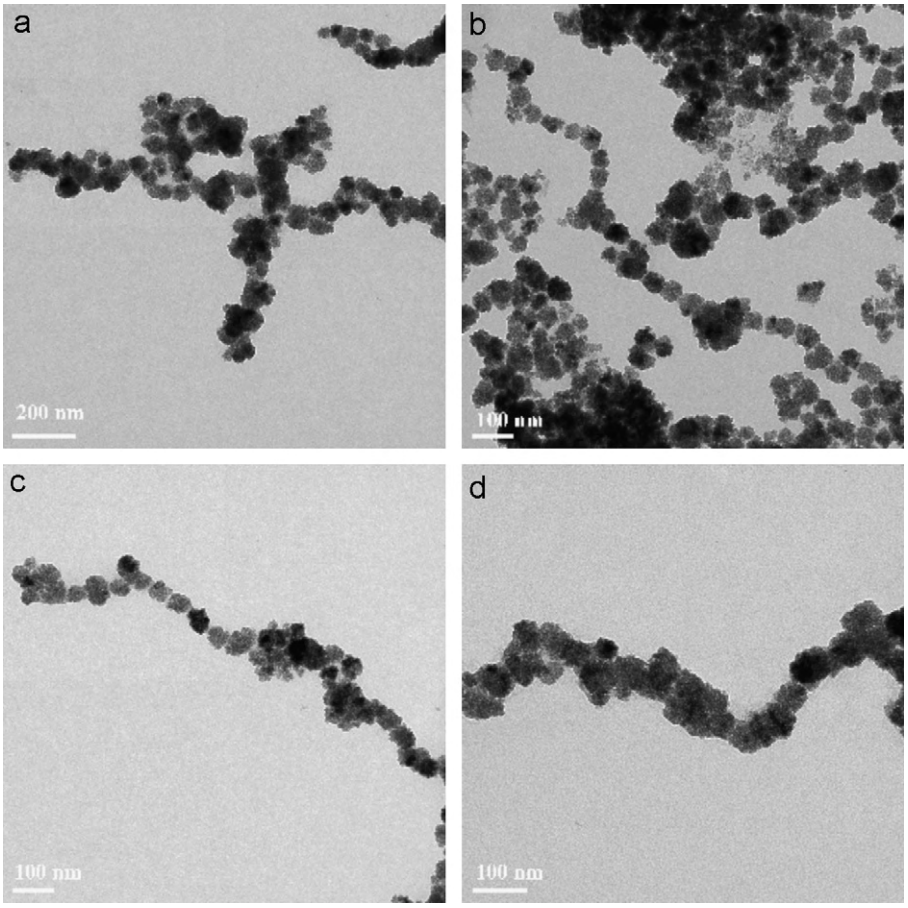

Fig. 3. Representative TEM images showing a region of a self-assembled chain of the as-prepared Fe_3O_4 nanoparticles. The bars of (a), (b), (c) and (d) correspond to 200, 100, 100 and 100 nm, respectively.

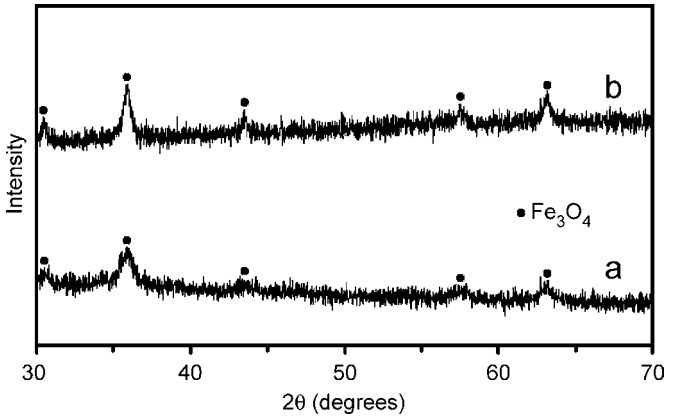

Fig. 4. XRD patterns of as-prepared iron oxide nanoparticles (a) before and (b) after carbonization. The XRD peaks for Fe_3O_4 were drawn from the JCPDS file 19-629.

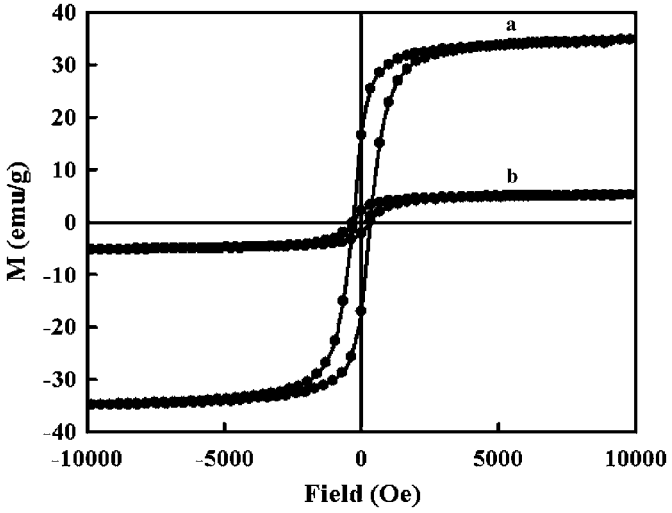

Fig. 5. Hysteresis loops at room temperature for the as-prepared iron oxide nanoparticles (a) before and (b) after carbonization.

magnetic field between −10 and 10 kOe (see Fig. 5). The saturation magnetization of the as-prepared iron oxide derived from pH 12 before carbonization was 34.8 emu/g, which is quite similar to the result reported by Wang [12]. In addition, the saturation magnetization of the final powder after carbonization was dramatically decreased to 5.1 emu/g. The saturation magnetization decreases when the crystallite size of nanoparticles is reduced as illustrated in the XRD analysis. In this case, the heating process may result to the major cracking of iron oxide nanoclusters to

iron oxide nanoparticles [14,15]. The magnetic iron oxide nanoparticles stabilized by the organic structure of starch vermicelli template was carbonized in air into black carbon, which could form the magnetic iron oxide/carbon nanocomposites. This can be also inferred that the final product after thermal decomposition was magnetically softer. The results obtained here were found to be similar to Xiong and coworkers who recently reported the magnetic properties of iron oxide/carbon nanocomposites through the formation of the polymer with magnetic iron oxide nanoparticles by heating at different temperatures to carbonize the carbon matrix [16]. They suggested that the carbonization of magnetic iron oxide nanoparticles stabilized by carbon matrix to form iron oxide/carbon nanocomposites could result in the reduction of the magnetic properties of iron oxide nanoparticles. Therefore, this is commonly employed for the reduction of magnetic properties of magnetic iron oxide nanoparticles to obtain various magnetic nanoparticles/carbon composites by the carbonization process or pyrolysis method. In addition, the coercivity of the sample, after the carbonization remains unchanged at 298 Oe. The research findings here indicate that the carbonization can be attributed to make nanoclusters to nanoparticles. This may be used as component vehicles for magnetic field-directed drug delivery of biomagnetic applications as the carbonization process can reduce the strength of the magnetic field required to obtain the magnetic behavior.

4. Conclusion

In summary, we have demonstrated a novel method for synthesizing magnetic iron oxide nanoparticles by using transparent starch vermicelli template as a new stabilizing agent. The magnetite nanoparticles can be synthesized by using the precipitation of magnetic iron oxide nanoparticles by a wet chemical method. The morphology of the as-prepared iron oxide deposited on the surface of the vermicelli was the spherical nanoclusters in the form with a diameter of about 200–300 nm. The magnetic behavior of the as-prepared products is useful for a variety of biomedical applications.

Acknowledgments

This research was supported by the Center for Innovation in Chemistry: Postgraduate Education and Research Program in Chemistry (PERCH-CIC), the Thailand Research Fund (TRF), the Thailand Toray Science Foundation (TTSF) and Faculty of Science, Mahidol University. We thank Thailand Institute of Scientific and Technological Research (TISTR) for the FESEM measurement and the Center of Nanoimaging (CNI) at the Faculty of Science, Mahidol University for the TEM measurement.

References

[1] R.M. Cornell, U. Schwertmann, The Iron Oxides: Structure, Properties, Reactions, Occurences and Uses, second ed., Wiley–VCH Verlag GmbH & Co. KGaA, Weinheim, 2003.
[2] F.Y. Cheng, C.H. Su, Y.S. Yang, C.S. Yeh, C.Y. Tsai, C.L. Wu, M.T. Wu, D.B. Shieh, Biomaterials 26 (2005) 729.
[3] B. Lindlar, M. Boldt, S. Eiden-Assmann, G. Maret, Adv. Mater. 14 (2002) 1656.
[4] S.H. Gee, Y.K. Hong, D.W. Erickson, M.H. Park, J.C. Sur, J. Appl. Phys. 93 (2003) 7560.
[5] Y. Sahoo, A. Goodarzi, M.T. Swihart, T.Y. Ohulchanskyy, N. Kaur, E.P. Furlani, P.N. Prasad, J. Phys. Chem. B 109 (2005) 3879.
[6] J. Giri, S. Guha Thakurta, J. Bellare, A. Kumar Nigam, D. Bahadur, J. Magn. Magn. Mater. 293 (2005) 62.
[7] T. Sen, A. Sebastianelli, I.J. Bruce, J. Am. Chem. Soc. 128 (2006) 7130.
[8] S. Sun, H. Zeng, D.B. Robinson, S. Raoux, P.M. Rice, S.X. Wang, G. Li, J. Am. Chem. Soc. 126 (2004) 273.
[9] T.L. Barsby, A.M. Donald, P.J. Frazier, Starch Advances in Structure and Function, The Royal Society of Chemistry, London, 2001.
[10] U. Schwertmann, R.M. Cornell, Iron Oxide in the Laboratory, VCH Verlagsgesellschaft mbH, Weinheim, 1991.
[11] M. Mikhaylova, D.K. Kim, N. Bobrysheva, M. Osmolowsky, V. Semenov, T. Tsakalakos, M. Muhammed, Langmuir 20 (2004) 2472.
[12] L. Wang, J. Luo, M.M. Maye, Q. Fan, Q. Rendeng, M.H. Engelhard, C. Wang, Y. Lin, C.-J. Zhong, J. Mater. Chem. 15 (2005) 1821.
[13] B.D. Cullity, S.R. Stock, Elements of X-ray Diffraction, Prentice-Hall, New Jersey, 2001.
[14] A.G. Roca, M.P. Morales, K.O. Grady, C.J. Serna, Nanotechnology 17 (2006) 2783.
[15] G. Kataby, T. Prozorov, Y. Koltypin, H. Cohen, C.N. Sukenik, A. Ulman, A. Gedanken, Langmuir 13 (1997) 6151.
[16] Y. Xiong, J. Ye, X. Gu, Q. Chen, J. Magn. Magn. Mater. 320 (2008) 107.

Tetrahedron Letters 49 (2008) 7299–7302

Contents lists available at ScienceDirect

Tetrahedron Letters

journal homepage: www.elsevier.com/locate/tetlet

Effect of stabilizing ligands bearing ferrocene moieties on the gold nanoparticle-catalyzed reactions of arylboronic acids

Laksamee Chaicharoenwimolkul [a], Ampaporn Munmai [b], Sanoe Chairam [b], Udomchai Tewasekson [a], Sarawut Sapudom [a], Yuthana Lakliang [c], Ekasith Somsook [a,d,*]

[a] NANOCAST Laboratory, Department of Chemistry and Center of Excellence for Innovation in Chemistry, Faculty of Science, Mahidol University, 272 Rama VI Road Rachathewi, Bangkok 10400, Thailand
[b] Institute for Innovation and Development of Learning Process, Mahidol University, 272 Rama VI Road Rachathewi, Bangkok 10400, Thailand
[c] Samsen Wittayalai School, 132/11 Rama VI Road Phayathai, Bangkok 10400, Thailand
[d] Center for Alternative Energy, Faculty of Science, Mahidol University, 272 Rama VI Road, Rachathewi, Bangkok 10400, Thailand

ARTICLE INFO

Article history:
Received 30 July 2008
Revised 2 October 2008
Accepted 8 October 2008
Available online 14 October 2008

ABSTRACT

The homocoupling reaction of phenylboronic acid and demetalation reaction of ferrocenylboronic acid was inhibited and highly active, respectively, in the presence of gold nanoparticles stabilized by ligands containing ferrocene moieties.

Nanoparticles (NPs) in catalysis have gained significant interest due to the mimicking of metal surface activation on nanoscale leading to the improvement of the efficiency and selectivity of reactions and also the recovery and recyclability of the catalysts.[1,2] Gold nanoparticles (AuNPs) have been used as catalysts in many organic transformations[3–5] due to their remarkable catalytic activities especially in the homocouplings of boronic acids.[6–8] Most of the active catalysts are based on NPs stabilized by ligands with electron transfer properties[9] or π-conjugated polymers[7] that exhibit highly reversible redox behavior. Since the discovery of ferrocene in the 1950s, this fascinating molecule, which demonstrates reversible one-electron redox reactions, has been an attractive reagent for many chemical applications.[10]

Improvement of the efficiency and selectivity of reactions catalyzed by nanocatalysts can be achieved by particle size optimization and surface modification of the nanoparticles, the latter can be carried out simply by tuning the structures of the stabilizing ligands.[11–15] In this study, the effect of ligands containing ferrocene moieties on the activities of AuNPs-catalyzed reactions of aryl boronic acids was investigated. Two substrates, phenylboronic acid (**A**) and ferrocenylboronic acid (**B**), were chosen for the reactions catalyzed by AuNPs, and two groups of stabilizing ligands, phenyl (**1**[16]) and ferrocenyl (**2**,[17] **3**, **4**,[18] **5**,[19] and **6**[20]) groups, were utilized, Figure 1.

Here, AuNPs were prepared by a simple reduction method with stabilizing ligands consisting of a ferrocene moiety. $HAuCl_4{\cdot}3H_2O$ in THF (1 mM, 1.5 mL) and ligand **2** in THF (1 mM, 1.5 mL) were mixed without any other reducing reagent and stirred vigorously.

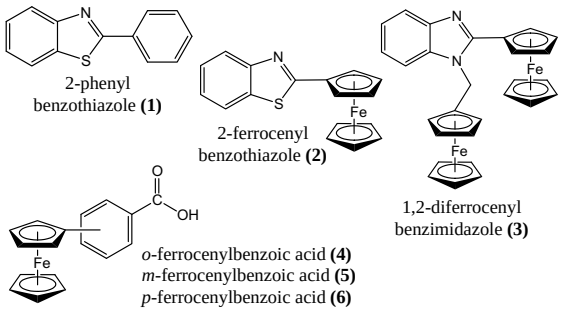

Figure 1. Stabilizing ligands in the formation of AuNPs.

The solution became red-purple indicating the formation of AuNPs; a TEM image of the AuNPs is shown in Figure 2.

Au(III) ions can be reduced to Au(0) by ferrocene-attached ligand **2** giving a product with a ferricinium moiety which can be observed by EPR spectroscopy as a singlet paramagnetic signal at $g = 2.01$. The first-order characteristic curve for ligand **2** (Fig. 3) was observed in which the rate constant was determined by fitting to a single exponential with two adjustable parameters: the rate constant and the EPR intensity at infinite time. It should be noted that no EPR signal was observed for a mixed solution of Au(III) and ligand **1**.

From Table 1, the rates of the electron transfer were dependent on the number and position of the ferrocene moieties, binding atoms, and functional groups. AuNPs with ligand **3** were probably destabilized either by the number of ferrocene moieties or by weaker interactions between the AuNPs and nitrogen atoms of the benzimidazole moiety resulting in a lower rate of ferricinium

* Corresponding author. Tel.: +66 2 201 5123; fax: +66 2 354 7151.
E-mail address: scess@mahidol.ac.th (E. Somsook).

0040-4039/$ - see front matter © 2008 Elsevier Ltd. All rights reserved.
doi:10.1016/j.tetlet.2008.10.040

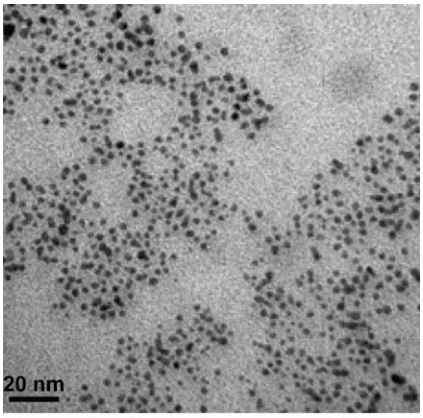

Figure 2. The TEM micrograph of gold nanoparticles stabilized by ligand **2**. The scale bar is 20 nm.

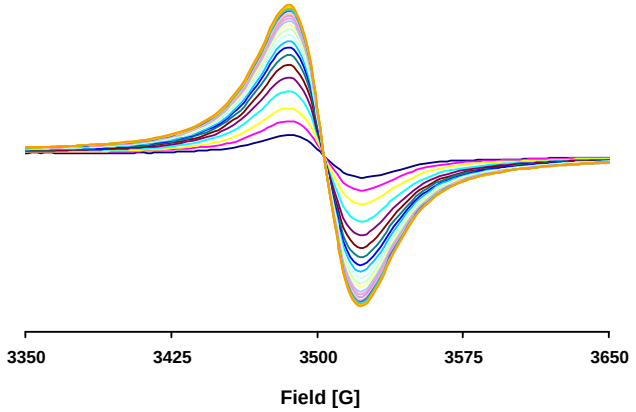

Figure 3. The kinetic EPR spectra of the ferricinium moiety generated from the reduction of Au(III) and ligand **2** were collected every 5 min for 100 min.

Table 1
The observed rate constants of ferricinium formation during the preparation of AuNPs as observed by EPR spectroscopy

Entry	Ligand	$k \times 10^4$ (s^{-1})
1	2-Ferrocenylbenzothiazole (**2**)	4.51
2	1,2-Diferrocenylbenzimidazole (**3**)	0.17
3	*o*-Ferrocenylbenzoic acid (**4**)	2.89
4	*m*-Ferrocenylbenzoic acid (**5**)	9.53
5	*p*-Ferrocenylbenzoic acid (**6**)	6.04

formation and slower electron transfer rate. Ligands **4–6** were selected to compare with the thiazole group **2** to study the binding of the carboxylic group to AuNPs. Ligand **5** showed an excellent rate of ferricinium formation due to the *meta*-effect resulting from the electron withdrawing nature of the carboxylic acid while a slower rate was observed for ligand **4**, probably due to intramolecular interactions between the ferricinium and carboxylic groups. The higher rate of ferricinium formation using the *meta*- and *para*-isomers of ferrocenylbenzoic than that with the thiazole group indicated the presence of stronger interactions between the carboxylate groups and AuNPs probably resulting from electrostatic effects.[1,2]

The C–C bond formation catalyzed by Au catalysts has been well exploited in synthetic chemistry.[21] The excellent electron transfer

Table 2
Homocoupling reactions of **A** catalyzed by Au(III) and AuNPs stabilized by ligands **1–6**[a]

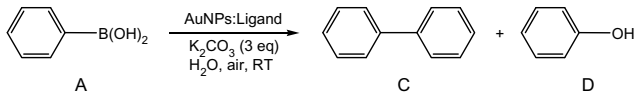

Entry	AuNPs:Ligand	Au(III) (%)	% Yield[b]		
			A	**C**	**D**
1[c]	AuNPs:**1**	4	50	33	17
2[c]	AuNPs:**2**	4	80	14	6
3[c]	AuNPs:**3**	4	79	19	2
4[d]	AuNPs:**4**	1	86	8	6
5[d]	AuNPs:**5**	1	73	16	11
6[d]	AuNPs:**6**	1	72	19	9
7[c]	Au(III)	4	54	37	9

[a] Conditions: phenylboronic acid (0.82 mmol), K_2CO_3 (2.5 mmol), 5 mL of H_2O, and 5 mL of THF, stirred for 24 h.
[b] Estimated from ^1H NMR analysis.
[c] [Au(III)] and [Ligand] = 3.13 mM.
[d] [Au(III)] and [Ligand] = 0.83 mM.

Table 3
Demetalation reactions of **B** catalyzed by Au(III) and AuNPs stabilized by ligands **1–6**[a]

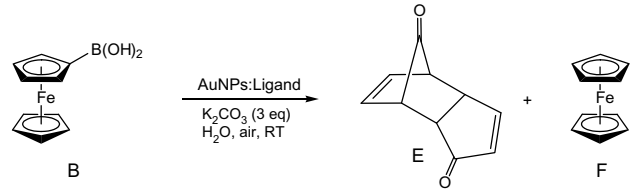

Entry	AuNPs:Ligand	Au(III) (%)	% Yield[b]		
			B	**E**	**F**
1[c]	AuNPs:**1**	7	–	47	53
2[c]	AuNPs:**2**	7	–	>99	–
3[c]	AuNPs:**3**	7	–	>99	–
4[d]	AuNPs:**4**	2	–	>99	–
5[d]	AuNPs:**5**	2	–	>99	–
6[d]	AuNPs:**6**	2	–	>99	–
7[c]	Au(III)	7	–	34	66

[a] Conditions: ferrocenylboronic acid (0.44 mmol), K_2CO_3 (1.3 mmol), 5 mL of H_2O, and 5 mL of THF, stirred for 24 h.
[b] Estimated from ^1H NMR analysis.
[c] [Au(III)] and [Ligand] = 3.13 mM.
[d] [Au(III)] and [Ligand] = 0.83 mM.

properties of ferrocene moieties were proposed here to study their activities in AuNPs-catalyzed reactions of arylboronic acids, **A** (Table 2) and **B** (Table 3), in a mixed solvent of THF/water under aerobic conditions for 24 h.

The results of the homocoupling of **A** showed similar conversions (~50%) for entries 1 and 7 (Table 2) indicating the low catalytic activity of ligand **1** while low conversions (14–28%) were observed for entries 2–6 (Table 2). It was surprising to find that the addition of stabilizing ligands containing ferrocene moieties inhibited the homocoupling of **A** even at a low %loading of Au(III).

In contrast to **A**, the AuNPs-catalyzed demetalation reactions of **B** showed excellent catalytic activities with complete conversions. Biferrocene and ferrocenyl alcohol were not observed but an unexpected dicyclopentadienone[22–24] **(E)** and ferrocene **(F)** were obtained as decomposition products. Moreover, the catalysts containing ferrocene moieties (Table 3, entries 2–6) showed excellent selectivity giving product **E**, exclusively.

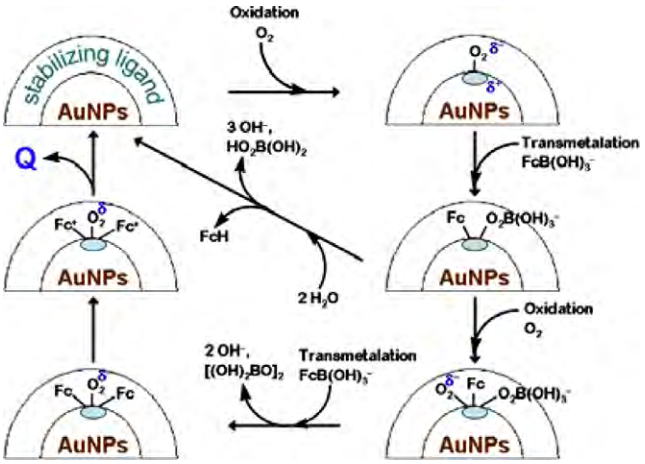

Scheme 1. Proposed mechanisms for the demetalation reaction of **B** catalyzed by AuNPs. **Q** = Fc^+–O–O–Fc^+.

The mechanisms for the reactions of **B** catalyzed by AuNPs are modified from the literature[7] and proposed as shown in Scheme 1. Initially, the oxidation by O_2 occurred on the surface of the AuNPs leading to a superoxo species. Subsequently, transmetalation of **B** produced ferrocenyl and boron peroxyl adsorbed on AuNPs in which ferrocene and boron peroxide may be partly released and then circulated back to the initial step. Next, the oxidation and 2nd-transmetalation occurred sequentially providing two ferrocenyl and a superoxo group on the AuNPs. Two ferricinium species were next formed and then bridged by the superoxo species to produce the species **Q** which was further oxidized to form dicyclopentadienone (**E**) as reported.[22–24] It should be noted that this is a rare example of the demetalation of ferrocene derivatives catalyzed by gold nanocatalysts in which a bicyclic ketone can be synthesized quantitatively on large scale with a good yield for potential applications in host-guest chemistry.

The low conversions for the homocouplings of **A** inhibited by AuNPs:**2**–**6** were further investigated in the reactions catalyzed by AuNPs stabilized by polyanilines[25] and its derivatives (**7M**–**10M**), the structures of the polymers are shown in Figure 4. In addition, ferricinium-doped polyaniline and its derivatives (**7N**–**10N**)

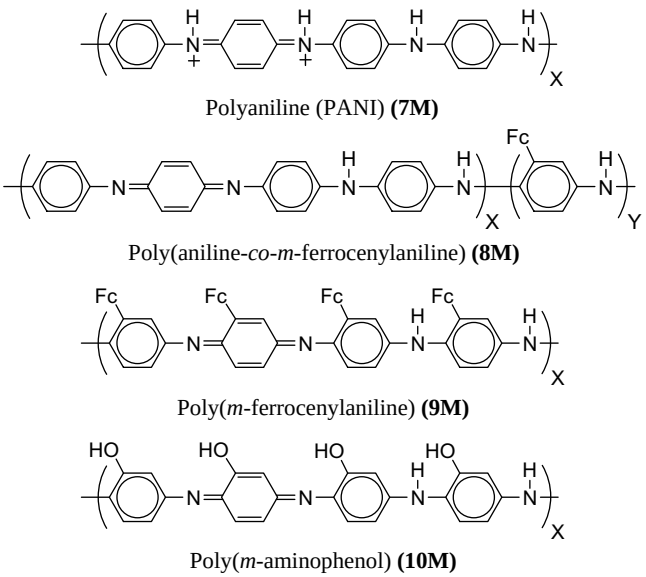

Polyaniline (PANI) **(7M)**

Poly(aniline-*co*-*m*-ferrocenylaniline) **(8M)**

Poly(*m*-ferrocenylaniline) **(9M)**

Poly(*m*-aminophenol) **(10M)**

Figure 4. Polyaniline (PANI) and its derivatives.

Table 4
Homocoupling reactions of **A** catalyzed by AuNPs stabilized by polyaniline and its derivatives (**7**–**10**)[a]

Entry	AuNPs:Polymer	Au(III) %	% Yield[b]		
			A	**C**	**D**
1	AuNPs:**7M**	4	90	7	3
2	AuNPs:**8M**	4	2	61	37
3	AuNPs:**9M**	4	—	60	40
4	AuNPs:**10M**	4	2	53	45
5	AuNPs:**7N**[c]	4	93	7	—
6	AuNPs:**8N**[c]	4	95	5	—
7	AuNPs:**9N**[c]	4	84	12	4
8	AuNPs:**10N**[c]	4	95	5	–

[a] Conditions: phenylboronic acid (0.82 mmol), Au(III) (0.03 mmol), polymer (12.34 mg), K_2CO_3 (2.5 mmol), 5 mL of H_2O, and 5 mL of THF, stirred for 24 h.
[b] Estimated from 1H NMR analysis.
[c] N = ferricinium-doped polymer (50 mol % of monomer).

were also used for the stabilization of AuNPs. The result of the reactions of **A** catalyzed by AuNPs:polymers (**7–10**) are shown in Table 4.

The ferricinium-doped polymers (Table 4, entries 5–8) gave very low conversions (5–16%). However, it was unexpected that the polyaniline (entry 1) would show a similar result. The form of polyaniline (**7M**) used in this experiment was as the emeraldine salt[26] with a positive charge on the backbone of the polymer. The lower positive charge density on the backbone of polymers (**8M–9M**) was evident from the smaller EPR intensities compared to polyaniline (**7M**). Hence, it is proposed here that cationic species destabilized the transition state during homocoupling of **A**. The electrostatic interactions[1,2] between ferricinium or cations and the peroxo species might inhibit the transmetalation of **A**.

In summary, we have demonstrated the catalytic activities of AuNPs stabilized by ligands containing ferrocene moieties in the homocoupling of **A** and demetalation of **B**.

General procedure for reactions of boronic acid: Arylboronic acid (1 equiv) and K_2CO_3 (3 equiv) were mixed in 5 mL of H_2O. Gold nanoparticles in 5 mL of THF were added, and the reaction mixture was stirred vigorously at room temperature under aerobic conditions for 24 h. The reaction was quenched with 1 M HCl solution and the products were extracted with EtOAc (20 mL × 3). The combined organic layer was dried over Na_2SO_4 and evaporated in vacuo. The resulting mixture was analyzed by ^{1}H NMR spectroscopy.

Acknowledgments

We acknowledge the support from the Thailand Research Fund, the Commission on Higher Education (RMU4980050), and Center of Excellence for Innovation in Chemistry (PERCH-CIC).

Supplementary data

Experimental methods, kinetic curves, and NMR spectra of **3** and dicyclopentadienone (***E***) are available. Supplementary data associated with this article can be found, in the online version, at doi:10.1016/j.tetlet.2008.10.040.

References and notes

1. Astruc, D.; Lu, F.; Aranzaes, J. R. *Angew. Chem., Int. Ed.* **2005**, *44*, 7852.
2. Daniel, M. C.; Astruc, D. *Chem. Rev.* **2004**, *104*, 293.
3. Gonzalez-Arellano, C.; Abad, A.; Corma, A.; Garcia, H.; Iglesias, M.; Sanchez, F. *Angew. Chem., Int. Ed.* **2007**, *46*, 1536.
4. Corma, A.; Gonzalez-Arellano, C.; Iglesias, M.; Sanchez, F. *Angew. Chem., Int. Ed.* **2007**, *46*, 7820.
5. Manea, F.; Houillon, F. B.; Pasquato, L.; Scrimin, P. *Angew. Chem., Int. Ed.* **2004**, *43*, 6165.
6. Carrettin, S.; Guzman, J.; Corma, A. *Angew. Chem., Int. Ed.* **2005**, *44*, 2242.

7. Tsunoyama, H.; Sakurai, H.; Ichikuni, N.; Negishi, Y.; Tsukuda, T. *Langmuir* **2004**, *20*, 11293.
8. Gonzalez-Arellano, C.; Corma, A.; Iglesias, M.; Sanchez, F. *Chem. Commun.* **2005**, 1990.
9. Deng, J. P.; Shih, W. C.; Mou, C. Y. *J. Phys. Chem. C* **2007**, *111*, 9723.
10. Togni, A.; Hayashi, T. *Ferrocene*; VCH: Weinheim, 1995.
11. Gual, A.; Axet, M. R.; Philippot, K.; Chaudret, B.; Denicourt-Nowicki, A.; Roucoux, A.; Castillon, S.; Claver, C. *Chem. Commun.* **2008**, 2759.
12. Guin, D.; Baruwati, B.; Manorama, S. V. *Org. Lett.* **2007**, *9*, 1419.
13. Baruwati, B.; Guin, D.; Manorama, S. V. *Org. Lett.* **2007**, *9*, 5377.
14. Choudary, B. M.; Kantam, M. L.; Ranganath, K. V. S.; Mahendar, K.; Sreedhar, B. *J. Am. Chem. Soc.* **2004**, *126*, 3396.
15. Choudary, B. M.; Ranganath, K. V. S.; Pal, U.; Kantam, M. L.; Sreedhar, B. *J. Am. Chem. Soc.* **2005**, *127*, 13167.
16. Perry, R. J.; Wilson, B. D. *Organometallics* **1994**, *13*, 3346.
17. Feng, K.; Wu, L. Z.; Zhang, L. P.; Tung, C. H. *Dalton Trans.* **2007**, 3991.
18. Savage, D.; Malone, G.; Alley, S. R.; Gallagher, J. F.; Goel, A.; Kelly, P. N.; Mueller-Bunz, H.; Kenny, P. T. M. *J. Organomet. Chem.* **2006**, *691*, 463.
19. Savage, D.; Alley, S. R.; Gallagher, J. F.; Goel, A.; Kelly, P. N.; Kenny, P. T. M. *Inorg. Chem. Commun.* **2006**, *9*, 152.
20. Savage, D.; Alley, S. R.; Goel, A.; Hogan, T.; Ida, Y.; Kelly, P. N.; Lehmann, L.; Kenny, P. T. M. *Inorg. Chem. Commun.* **2006**, *9*, 1267.
21. Stephen, A.; Hashmi, K. *Chem. Rev.* **2007**, *107*, 3180.
22. Toda, F.; Tanaka, K.; Marks, D.; Goldberg, I. *J. Org. Chem.* **1991**, *56*, 7332.
23. Harmata, M.; Barnes, C. L.; Brackley, J.; Bohnert, G.; Kirchhoefer, P.; Kurti, L.; Rashatasakhon, P. *J. Org. Chem.* **2001**, *66*, 5232.
24. Zotti, G.; Schiavon, G.; Zecchin, S.; Favretto, D. *J. Electroanal. Chem.* **1998**, *456*, 217.
25. Li, W. G.; Jia, Q. X.; Wang, H. L. *Polymer* **2006**, *47*, 23.
26. Sherman, B. C.; Euler, W. B.; Force, R. R. *J. Chem. Educ.* **1994**, *71*, A94.

Carbohydrate Polymers 75 (2009) 694–704

Contents lists available at ScienceDirect

Carbohydrate Polymers

journal homepage: www.elsevier.com/locate/carbpol

Starch vermicelli template-assisted synthesis of size/shape-controlled nanoparticles

Sanoe Chairam [a], Channarong Poolperm [b], Ekasith Somsook [b,*]

[a] Institute for Innovation and Development of Learning Process, Mahidol University, 272 Rama VI Road, Rachathewi, Bangkok 10400, Thailand
[b] NANOCAST Laboratory and Center for Alternative Energy, Department of Chemistry and Center of Excellence for Innovation in Chemistry, Faculty of Science, Mahidol University, 272 Rama VI Road, Rachathewi, Bangkok 10400, Thailand

ARTICLE INFO

Article history:
Received 6 August 2007
Received in revised form 12 August 2008
Accepted 12 September 2008
Available online 30 September 2008

Keywords:
Silver nanoparticles
Gold nanoparticles
Silver chloride nanoparticles
Starch
Green chemistry
Starch vermicelli

ABSTRACT

Size- and shape-controlled syntheses of silver and gold nanoparticles have been successfully developed using partially hydrolyzed starch vermicelli templates as green nanoreactors for the growth of nanoparticles. Mung bean vermicelli is of interest due to the higher amylose content and its transparency, allowing the formation of coloured particles on the vermicelli to be observed. The as-prepared silver and gold nanoparticles were characterized by UV–Visible spectroscopy, transmission electron microscopy (TEM), and X-ray diffraction (XRD). The carbonization of as-prepared vermicelli at 200 °C, 300 °C, and 500 °C was carried out to investigate nanoparticles embedded in the starch vermicelli templates. TEM of carbonized samples revealed the interesting patterns of gold nanorods and silver nanowire-liked assemblies along with carbon nanotubes. The carbonization of silver nanoparticles at 500 °C resulted to the loss of starch vermicelli capping nanoparticles and this led to the higher diffusion rate of nanoparticles to generate silver nanodendrites on TEM images. XRD data of carbonized yellow and purple silver nanoparticles revealed the presence of silver nanoparticles and a mixture of silver and silver chloride nanoparticles, respectively. This approach offers a great potential to design new fine structures of vermicelli and utilize its structure as a template for the large-scale synthesis of size- and shape-controlled silver and gold nanoparticles for chemical and biological applications.

1. Introduction

Inorganic nanoparticles have been attracting considerable interests due to their novel properties which are strongly influenced by size, shape, surface composition, spatial ordering, and interactions with surrounding environments (Cushing, Kolesnichenko & O'Connor, 2004; Daniel & Astruc, 2004; He, Kunitake, & Nakao, 2003; Panigrahi et al., 2006; Qu, Dai, & Osawa, 2006; Sun & Xia, 2002). The development has been focused on the inorganic nanostructures attached on the surface and embedded in the biomolecular structures such as DNA (Dean, Haynes, & Schmaljohn, 2005; Hill, Lyon, Allen, Stevenson, & Shear, 2005; Stoeva, Lee, Thaxton, & Mirkin, 2006; Xu, Hua Zeng, Lu, & Bing Yu, 2006), polypeptides (Chumbimuni-Torres et al., 2006; Xu et al., 2006), and virus (Deniger, Kolokoltsov, Moore, Albrecht, & Davey, 2006) for many applications in nanoelectronics, drug delivery, and catalysis. Among several biomolecules, starch is one of the most abundant materials on earth. The knowledge on the structure of starch has been recently advanced (Gidley, 2001). The description of starch is well-known as polymer structures containing mostly linear amylose and branched amylopectin. The spectroscopic and microscopic methods are now well advanced for probing the branching pattern and the branch length of starch polymers (Baker, Miles, & Helbert, 2001; Gallant, Bouchet, & Baldwin, 1997; Gidley, 1985; Jodelet, Rigby, & Colquhoun, 1998). The structure of starch is packed in semicrystalline granules containing concentric growth rings. Amylose and amylopectin are arranged radically and aligned perpendicularly to the growth rings and to the granule surface. Starch granules can be transformed into other forms such as starch paste, starch gel, and retrograded starch depending on the cooking conditions (Buléon, Colonna, Planchot, & Ball, 1998; Jenkins & Donald, 1995; Moorthy, Andersson, Eliasson, Santacruz, & Ruales, 2006; Rindlav-Westling, Stading, & Gatenholm, 2002; Tester, Karkalas, & Qi, 2004). The starch transformation provides diverse structures and properties for numerous applications. For example, starch gels can be produced from high amylose mung bean starch which is a major material for producing transparent starch vermicelli (Oates, 1990; Tan, Gu, Zhou, Wu, & Xie, 2006).

Though it is cheap and widely-used, less attention has been paid to the construction of nanoarchitectures on the surface and embedded in the structure of starch. Several environmental friendly approaches have been shown by using starch and polysaccharides as templates for nanoparticles synthesis (Huang & Yang, 2004; Lu, Gao, & Komarneni, 2005; Raveendran, Fu, & Wallen, 2003; Raveendran, Fu, & Wallen, 2006; Sarma & Chattopadhyay, 2004). The concept of green chemistry used in the synthesis of nanoparticles was first reported by Wallen and co-workers in

* Corresponding author. Tel.: +662 201 5123; fax: +662 354 7151.
E-mail address: scess@mahidol.ac.th (E. Somsook).

0144-8617/$ - see front matter © 2008 Elsevier Ltd. All rights reserved.
doi:10.1016/j.carbpol.2008.09.022

which the synthesis of silver nanoparticles was carried out and stabilized by soluble starch and using β-D-glucose as a nontoxic reducing agent (Raveendran et al., 2003; 2006). In the past decade, starch has been shown as a good host for many guests of inorganic nanoparticles, such as gold (Daniel & Astruc, 2004), silver (Raveendran et al., 2003) and iron oxides (Chairam & Somsook, 2008; Somsook et al., 2005) to form inclusion complexes. In this study mung bean vermicelli is of interest due to the higher amylose content and its transparency, allowing the formation of coloured particles on the vermicelli to be observed. Furthermore, it would be interesting if amylose or amylopectin containing glucose units could be utilized as a template for the fabrication of nanoparticles for potential applications in chemistry and biology. Here we demonstrated a simple fabrication of size- and shape-controlled silver and gold nanoparticles on the surface and embedded in the mung bean starch vermicelli.

2. Experimental

2.1. Materials and equipments

All materials in our experiments are biocompatible and environmental-friendly. Silver nitrate ($AgNO_3$) and hydrogen tetrachloroaurate(III) trihydrate ($HAuCl_4{\cdot}3H_2O$, ⩾99.9+%) were purchased from VWR international Ltd. and Sigma–Aldrich, respectively. β-D-glucose was purchased from Ajax Finechem. Hydrochloric acid (HCl), 98% AR grade, was purchased from Merck. Mung bean starch vermicelli, "Kaset" and "Dragon" brands (Bangkok, Thailand), was purchased from local supermarkets. All glassware used in this experiment was cleaned with an aqueous 10% nitric acid solution, washed with de-ionized water obtained from a Nanopure® Analytical Deionization system with an electric resistance 18.2 MΩ-cm purified with a Barnstead Nanopure Ultrapure Water system, and dried before use. A microwave machine used was M181 GN Samsung household microwave with an operating power output from 100–850 W, 7 power levels, and 35 min dual-speed timer.

2.2. Conventional heating

In a typical condition, 5 mL of 0.1 M solution of $AgNO_3$ or 0.1% of $HAuCl_4{\cdot}3H_2O$ was added to 300 mL of distilled water with 0.51 g of mung bean starch vermicelli under argon gas. The pH of the reaction was adjusted to a pH of 4 by diluted HCl in order to partially hydrolyze the surface of mung bean starch vermicelli. The reaction mixture was stirred for 1 h under argon gas, then 7.5 mL of 0.1 M of β-D-glucose was added and the reaction was continually stirred for 20 h. Mung bean starch vermicelli pieces were then collected from the reaction, dried in an oven at 60 °C prior to further analysis.

2.3. Microwave heating

A typical synthesis of nanoparticles with microwave heating was carried out as follows. First, 0.50 g of mung bean starch vermicelli was added to a 50 mL of deionized water and then heated in a microwave oven for 1 min to soak starch vermicelli in water. Then 150 μL of metal salt solution and 300 μL of 0.1 M of β-D-glucose were added to the reaction and heated in a microwave for a given period. The lowest power of the microwave oven at 100 W was chosen. Mung bean starch vermicelli pieces were then collected from the reaction, dried in an oven at 60 °C prior to further analysis.

2.4. Carbonization of vermicelli

Vermicelli with nanoparticles was heated in a crucible in a furnace at 200 °C, 300 °C and 500 °C in an ambient atmosphere for 48 h, respectively. A black precipitate was then obtained and dispersed in water by sonication in an ultrasonic bath for a given period.

2.5. The origin colours of purple and yellow silver nanoparticles

To further investigate the origin of two colours of vermicelli, two separated experiments were carried out and then followed by the carbonization.

2.5.1. Synthesis of yellow vermicelli

About 50 mL of deionized water was added into 0.5 g of mung bean starch vermicelli in a 250 mL beaker. Then, 5 mL of 0.1 M of $AgNO_3$ was added into the beaker. The reaction solution was heated by a microwave oven at 100 W in the presence of air for 5 min. After that, the mixture was transferred into a 100 mL Schlenk flask. A 7.5 mL of 0.1 M of β-D-glucose was added into the reaction flask. The reaction was heated at 60 °C and stirred under argon gas for 6 h. The colour of vermicelli was observed with a yellow colour. The mixture solution was cooled to room temperature. Mung bean starch vermicelli pieces were then collected from the reaction, dried in an oven at 60 °C prior to further analysis.

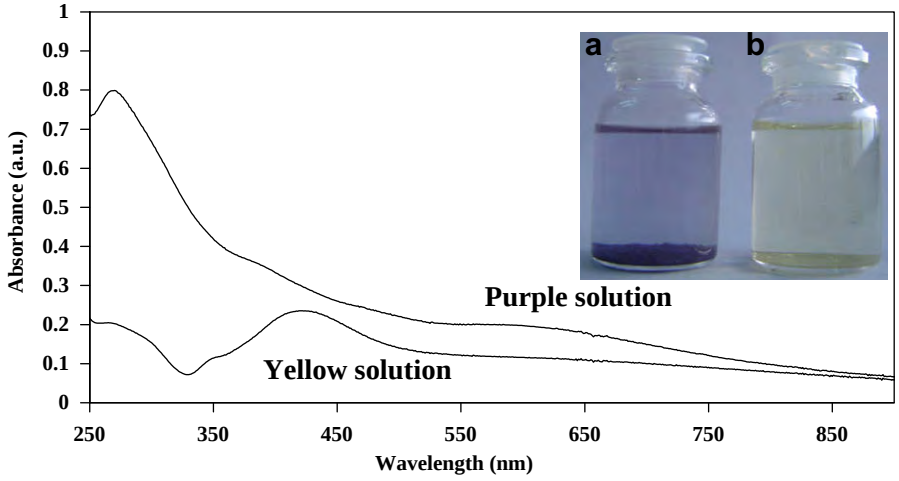

Fig. 1. UV–Visible spectra of purple and yellow colloidal solutions. The inset picture is purple (a) and yellow solutions (b) after removing vermicelli and centrifugation, respectively.

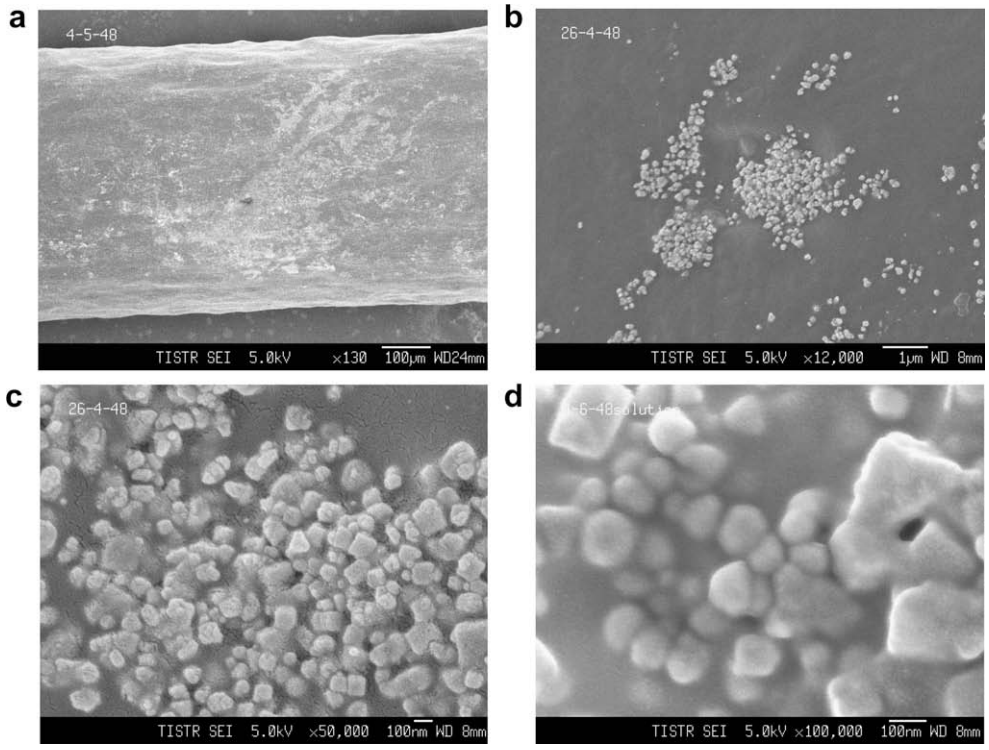

Fig. 2. FESEM of silver nanoparticles on the surface of mung bean starch vermicelli in different views and magnification powers. The bars for (a–d) are 100 μm, 1 μm, 100 nm, and 100 nm, respectively.

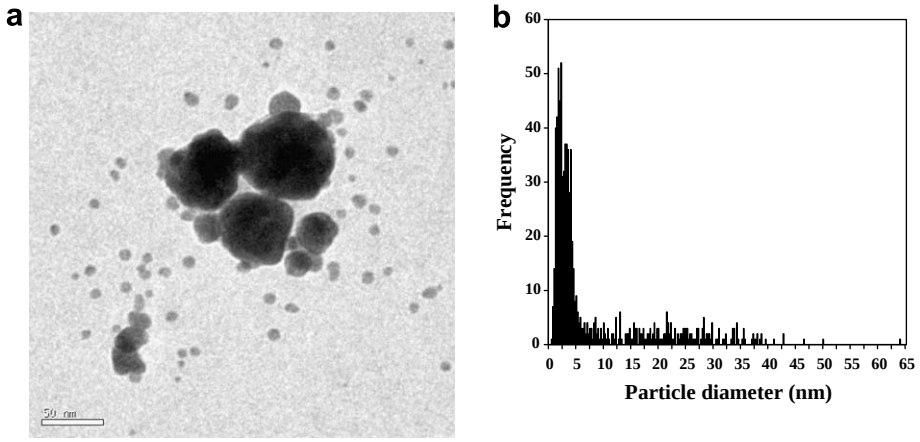

Fig. 3. (a) TEM image of starch silver nanoparticles in colloidal solution. The bar is 50 nm. (b) Histogram showing the size distribution of purple silver nanoparticles on the surface of vermicelli and in colloidal solution. The total number of counted nanoparticles is 806.

Fig. 4. Photographs of vials containing: (a) only starch vermicelli without the reduction of gold nanoparticles (left) and starch vermicelli capped gold nanoparticles (right): (b) and (c) starch vermicelli capped gold nanoparticles after the period time of three days and three months of storage at room temperature, respectively.

2.5.2. Synthesis of purple vermicelli

About 50 mL of deionized water was added into 0.5 g of mung bean starch vermicelli in a 250 mL beaker. After that, 5 mL of 0.1 M of $AgNO_3$ was added into the beaker. The reaction solution was heated by a microwave oven at 100 W in the presence of air for 5 min. The vermicelli was then washed with a dilute solution of NaCl. The mixture was transferred into a 100 mL Schlenk flask. 7.5 mL of 0.1 M of β-D-glucose was added into the reaction flask. The reaction was heated at 60 °C and stirred under argon gas for 6 h. The colour of vermicelli was observed with a purple colour. Then, the mixture solution was cooled to room temperature. Mung bean starch vermicelli pieces were then collected from the reaction, dried in an oven at 60 °C prior to further analysis.

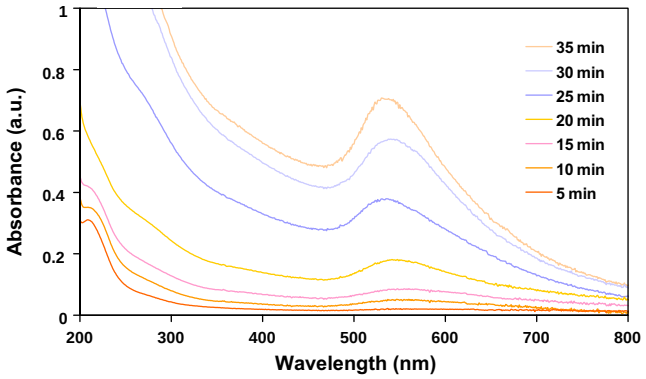

Fig. 5. UV–Visible absorption spectra showing the time evolution of the growth of gold nanoparticles at the different reaction time from 5 to 35 min.

2.5.3. Carbonization of vermicelli

As-prepared vermicelli with silver nanoparticles was heated in an alumina cup in a furnace at 200 °C and 300 °C in the ambient atmosphere for 24 h. Samples were placed in an alumina cup and heated at a heating rate of 5 °C min^{-1}. A black precipitate was obtained and characterized by XRD.

2.6. Characterization

The morphologies of nanostructures were recorded using a JEOL JSM-6340 F field emission scanning electron microscope (FESEM) with energy dispersive X-ray analysis (EDX). The XRD was carried out on a D8 Advance Bruker analytical X-ray system operating at the CuK_α wavelength of 1.5650 nm, 40 mA, and 40 kV. The diffraction patterns over the range of 30–70 ° of 2θ were recorded at a scan rate of 5 s/step and step size 0.020 2θ/s. The TEM micrographs of the as-synthesized samples were performed with a Philip Tecnia-G2 Sphera Transmission Electron Microscope by accelerating voltage at 80 kV. The UV absorption spectra of colloidal metal nanoparticles were performed by using a HP8453 HEWLETT PACKARD UV–Visible spectrophotometer with the path length of the quartz cell at 10 mm, over the wavelength ranging from 250 to 900 nm.

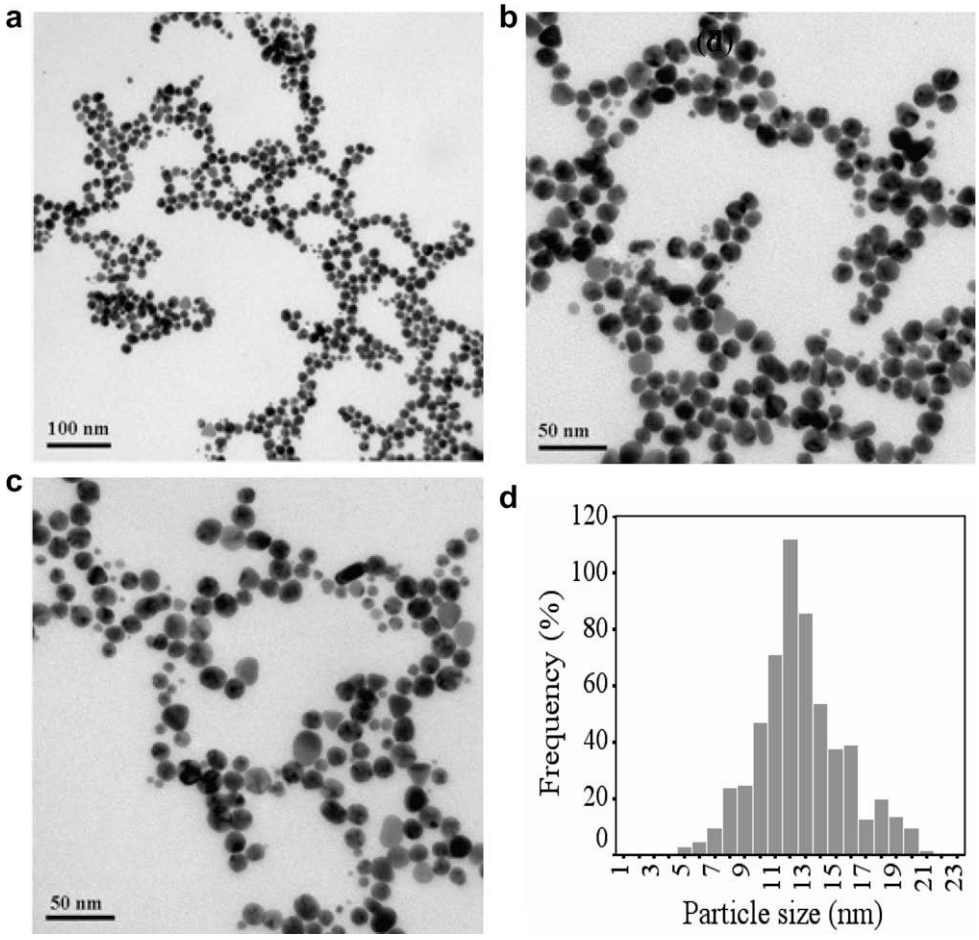

Fig. 6. TEM images of as-synthesized gold nanoparticles corresponding to a histogram of the size distribution from TEM micrographs (average particle size = 12.7 ± 2.8 nm). The bars of (a–c) are 100, 50 and 50 nm, respectively. The total number of single particles counted for a histogram is 573.

3. Results and discussion

3.1. Synthesis of silver nanoparticles

Following conventional heating of the reaction mixture for 2–3 h, a purple colour was observed for the mung bean starch vermicelli and the solution also adopted a purple colour which increased in intensity with time. Fragments of starch were detached from the vermicelli to generate a colourful purple solution. After the purple colloidal solution was centrifuged, the colour of the colloidal solution turned to yellow. The particle growth was monitored using UV–Visible absorption spectroscopy in which the strong, medium and weak absorption bands were observed at 270, 390 and 600 nm, respectively. The UV–Visible spectra of purple and yellow solutions are shown in Fig. 1. The yellow solution exhibited the UV–Visible spectrum with λ_{max} at 420 nm which was similar to recently reported silver nanoparticles (Raveendran et al., 2003; 2006).

The typical FESEM images of silver nanoparticles attached to mung bean starch vermicelli are shown in Fig. 2. The average particle diameter of silver nanoparticles on the surface of mung bean starch vermicelli was approximately 20 nm. The biggest particle diameter on the surface was observed up to 65 nm. The TEM images of the purple suspension are also shown in Fig. 3a. It was unexpected that 40 nm range nanoparticles were found with 3 nm nanoparticles on the TEM images. The histogram of the size distribution of starch silver nanoparticles on the surface of vermicelli including those in colloidal solution displayed two different sizes of nanoparticles (1–5 nm and 10–65 nm) showing the broad particle size distribution (Fig. 3b). The smaller particles (Fig. 3b) were approximately the same particle size as Wallen's starch silver nanoparticles but the size distribution was narrower. The EDXspectrum confirmed the presence of silver, carbon, and oxygen as major elements suggesting that the interactions between silver and starch in the samples and silver nanoparticles must be stabilized by starch.

3.2. Synthesis of gold nanoparticles

Microwave heating speeds up the synthesis of nanoparticles. The colour of mung bean starch vermicelli turned to pale red after microwave irradiation for a couple of minutes (Fig. 4 and 5). Interestingly, starch vermicelli capped gold nanoparticles were stable in the vermicelli templates over the period time of three months of storage at room temperature, while there was no sign of aggregation of gold nanoparticles. This indicated that the mung bean starch vermicelli template could be used to prevent the aggregation of nanoparticles in sterile condition. The UV–Visible absorption spectra of colloidal gold solutions were collected to investigate the growth of nanoparticles by microwave irradiation at different reaction times (5–35 min). It was found clearly that the intensity of the surface plasmon band of colloidal gold nanoparticles increased with the reaction time. It is well-known that the colloidal gold nanoparticles in an aqueous solution exhibit a broad absorption band in the visible region at wavelength from 517 nm to 575 nm due to the Mie theory (Daniel & Astruc, 2004). As can be shown in Fig. 5, the results showed clearly that the strong absorption peaks of as-prepared gold nanoparticles showed

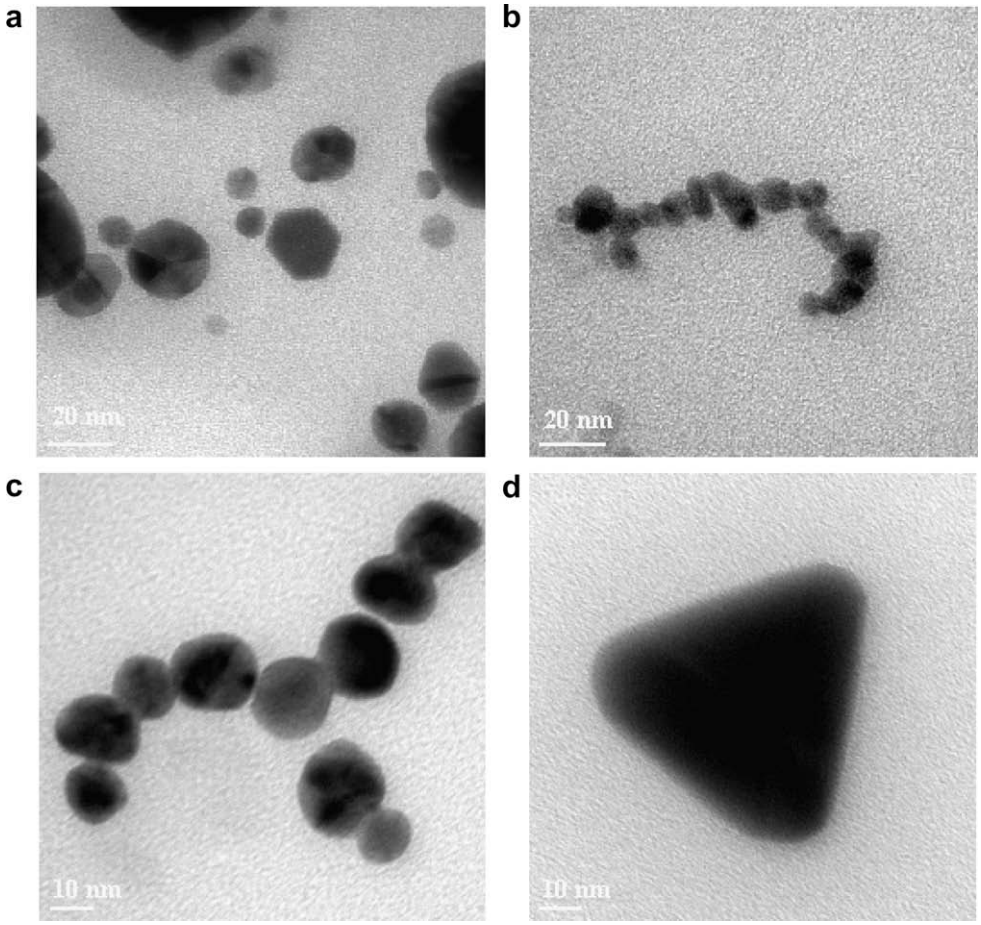

Fig. 7. HRTEM images of as-synthesized gold nanoparticles after microwave heating for 5 min. The bars of (a–d) correspond to 20, 20, 10, 10 nm, respectively.

a match with the reported results (Daniel & Astruc, 2004). These absorption values may not include the protecting agent of starch vermicelli templates, because the Mie scattering responds only to the nanoscale gold particles (Su et al., 2003; Templeton, Pietron, Murray, & Mulvaney, 2000). Also, the surface plasmon band was symmetric indicating that the colloidal solutions had no aggregation of particles. The strong intensity of an absorption peak became increasing indicating that the reduction reaction of gold nanoparticles had greatly proceeded. In addition, the tendency of the absorption peak also slightly shifted to blue, implying a decrease in the particle size for the formation of gold nanoparticles.

The morphologies and sizes of as-prepared gold nanoparticles were examined by TEM. As can be observed in Fig. 6, TEM images showed clearly well-dispersed gold nanoparticles synthesized at the different TEM magnifications corresponding to a histogram of the size distribution from TEM micrographs. The resulting product

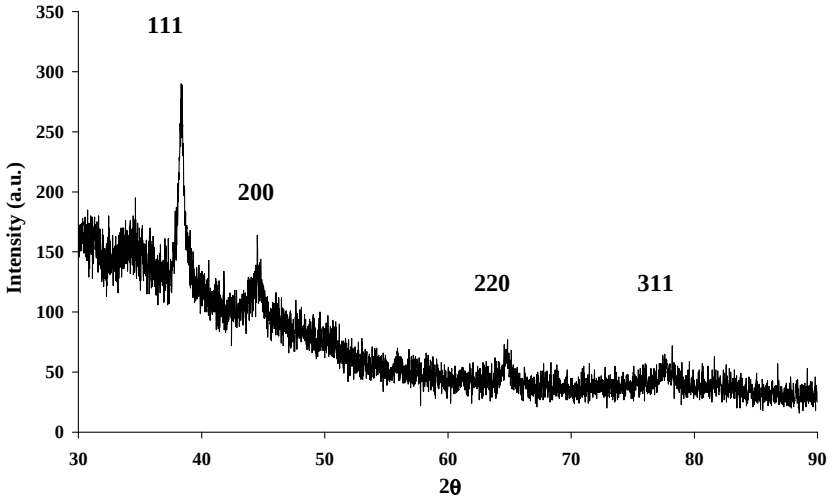

Fig. 8. The XRD pattern of the as-prepared gold nanoparticles.

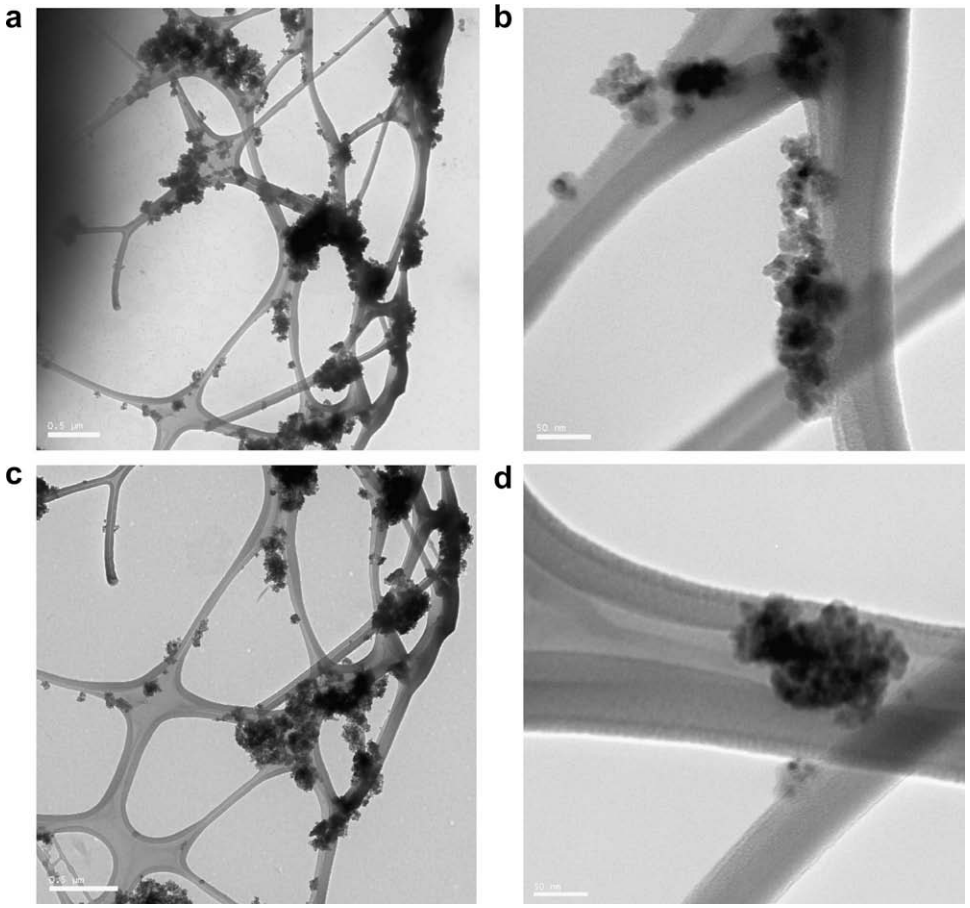

Fig. 9. TEM images of carbonization products at 200 °C with the sonication time of 30 min showing silver (a and b) and gold nanoparticles (c and d) attached to the surface of carbon nanotubes. The bars are 0.5 μm, 50 nm, 0.5 μm and 50 nm, respectively.

mainly consisted of an extremely uniform size of spherical gold nanostructures. The average particle size of the as-prepared gold nanoparticles with diameters was 12.7 nm with a standard deviation of 2.8 nm ($n = 573$), with a maximum of 21 nm in size distribution.

Interestingly, a few of different morphologies of the as-prepared gold nanoparticles were also found in the same sample. To obtain a clear picture, the regular structure of these particles was further examined using high-resolution TEM (HRTEM) observation. As shown in Fig. 7, a representative sample of the resulting product of various shapes (e.g., polygonal, hexagonal and triangular shape) of gold nanoparticles was obtained when increasing of the reaction time for the microwave heating process. As shown in Fig. 7b and c, gold nanowires with the approximate distance of 100 nm were observed in the same sample. It is suggested that the formation of nanowires jointed by gold nanoparticles was facilitated by the helical molecular structure of starch acting as nanoreactors.

In order to understand the crystalline structure of the gold nanoparticle formation, X-ray diffraction was carried out to investigate the atomic structure of small nanoparticles. It has been used as a common tool to examine the crystallinity of samples. After drying in an oven at 60 °C for 24 h, the dried powder product was ground and further characterized by XRD. The XRD pattern of the as-prepared gold nanoparticles is shown in Fig. 8. There were four diffraction peaks with the 2θ of 38.4, 44.5, 64.7 and 77.6 corresponding to the (111), (200), (220) and (311) planes, respectively, of the face-centered cubic (fcc) metallic gold (JCPDS file no.04-0784). These positions of the diffraction peaks of the as-prepared gold nanoparticles showed a match with the reported results (Lu et al., 2005). Since gold nanoparticles were embedded within mung bean starch vermicelli acting as stabilizing templates, the broad diffractions were observed over a 2θ range due to the low crystallinity of starch vermicelli.

3.3. Carbonization of nanoparticles embedded in vermicelli

The carbonization allows us to investigate the patterns of nanoparticles embedded in the starch vermicelli. First, vermicelli prepared by the microwave technique was carbonized in a crucible in an oven at 200 °C, 300 °C and 500 °C. After the carbonization, black vermicelli was obtained and then ground and dispersed in water by ultrasonic sonication. The 30 min duration time for the sonication was first chosen. TEM images of as-prepared samples are shown in Fig. 9. The aggregated nanoparticles were attached to carbon nanotubes which were confirmed by EDX spectra showing that the major elements of the carbon nanotubes were carbon and oxygen only. This is an alternative way to synthesize carbon nanotubes from saccharides.

Longer period of the sonication time led to the aggregation of the nanoparticles. Therefore, shorter period of the sonication time was carried out to disperse nanoparticles in water. TEM images of nanowire-like assemblies of silver nanoparticles and gold nanorods are shown in Fig. 10. The pattern of silver nanoparticles looks like to a wire in an electronic circuit even though nanoparticles were not totally next to each other. A histogram analysis showed that the mean particle diameter was observed at 8.24 nm with a standard deviation of 2.20 nm. This unique morphology is probably a result of the inclusion of silver nanoparticles in the amylose

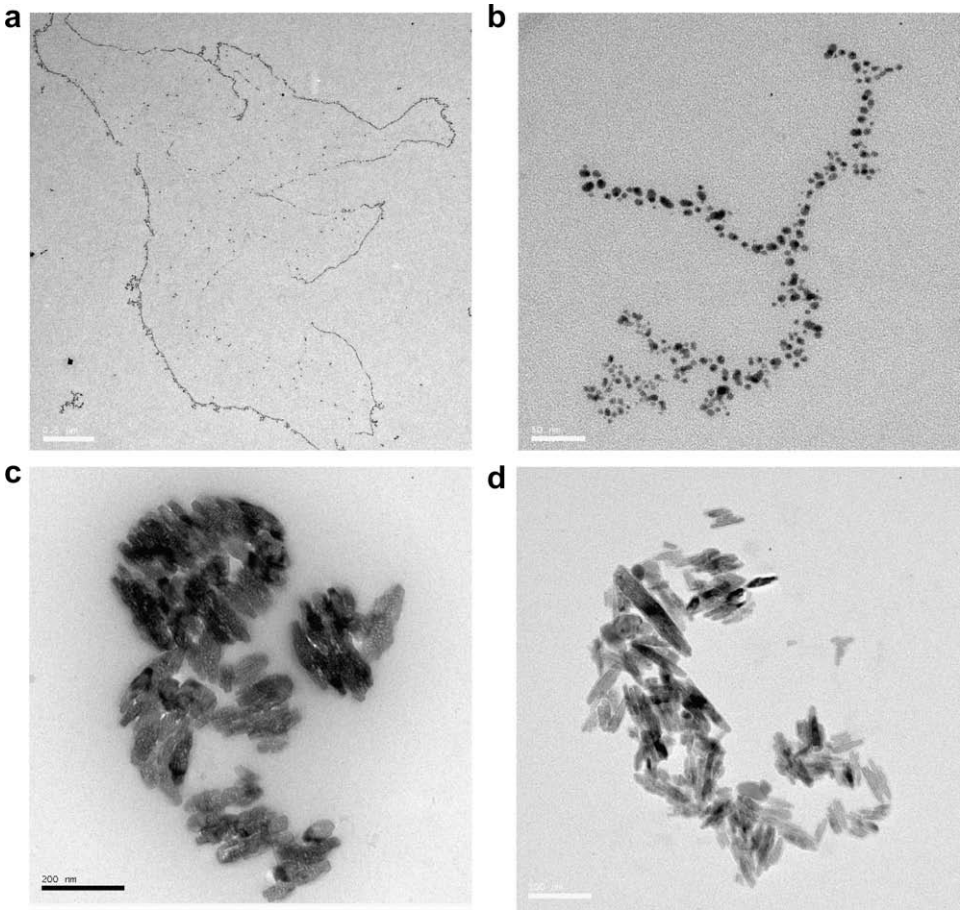

Fig. 10. TEM images of carbonization products at 200 °C (a–c) and 300 °C (d) with the sonication time of 10 min showing the self-assembly of silver nanowires (a and b) and gold nanorods (c and d). The bars are 0.5 μm, 50 nm, 200 nm, and 100 nm, respectively.

helical structure. Moreover, the particle size distribution of nanoparticles embedded in vermicelli was narrower than one in the colloidal solution. TEM images with low magnification clearly show lengthy gold nanorods with the lengths are up to 100 nm and the width is approximately 10–20 nm in which is about the same size of carbon nanotubes obtaining from the carbonization.

TEM images in Fig. 11 showed the growth of silver nanodendrites on a copper grid. This is well explained that the carbonization at higher temperature resulted the lower number of molecules of starch vermicelli capping nanopaticles. This led to the increasing diffuson rate resulting in the growth of nanodendrite of silver nanoparticles on copper grids. The average diameter of particles was 29.0 nm with a standard deviation of 10.54 nm. The growth mechanism of our nanodendrites is well described on the basis of a diffusion-limited aggregation (DLA) model (Kaniyankandy, Nuwad, Thinaharan, Dey, & Pillai, 2007) where the individual atoms are bond to the growing surface during the process.

3.4. Two colours of silver nanoparticles

To further investigate the origin of different colours of the as-prepared silver nanoparticles, two separate experiments were carried out by first incorporating Ag(I) ions into the inside of vermicelli by microwave radiation, then reducing Ag(I) ions to Ag(0) nanoparticles by β-D-glucose under an inert atmosphere with a conventional heating. The two experiments were different only in that the vermicelli for one experiment was washed with a solution of NaCl before heating with β-D-glucose. Two colours of silver nanoparticles were successfully synthesized (Fig. 12). Although the results from FESEM and TEM images demonstrated clearly that silver nanoparticles were produced on the surface of mung bean starch vermicelli and in the colloidal solution, the phase of silver nanoparticles was further examined by the carbonization of nanoparticles embedded in vermicelli at 200 °C and 300 °C and then characterized by XRD. After the carbonization of yellow (Fig. 12a) and purple (Fig. 12b) silver nanoparticles stabilized by

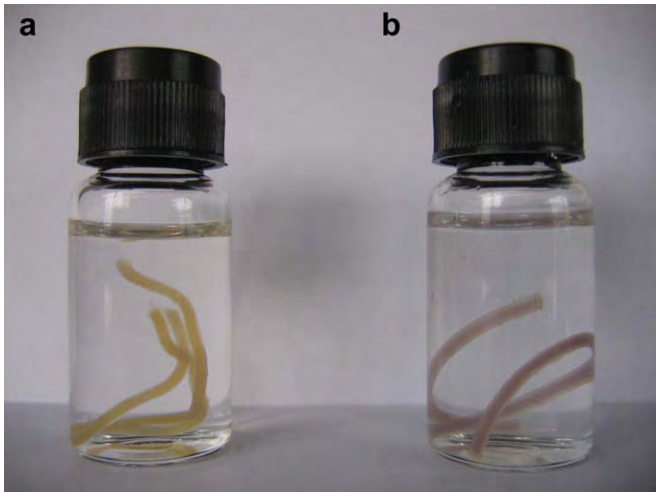

Fig. 12. Pictures of (a) yellow and (b) purple vermicelli fabricated with silver nanoparticles.

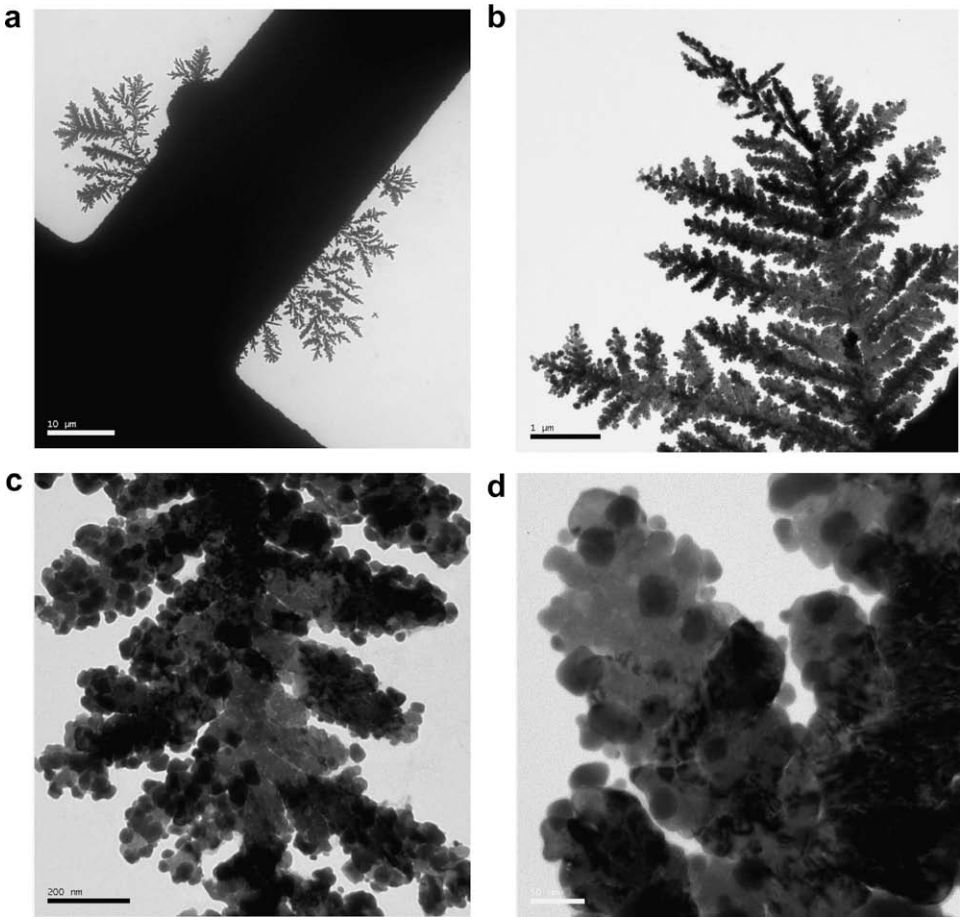

Fig. 11. (a–d) TEM micrographs of silver dendrites obtained from carbonization at 500 °C for 24 h. The bars are 10 μm, 1 μm, 200 nm and 50 nm, respectively.

vermicelli templates in a furnace at 200 °C and 300 °C for 24 h, a black precipitate powder was also obtained in a crucible cup. The XRD was used to examine the phase of the obtaining products. The diffraction patterns of two colours of yellow and purple vermicelli demonstrated different patterns (Fig. 13). From all diffraction patterns, the presence of metal oxides (e.g. silver oxide) was also not detected.

For the yellow mung bean starch vermicelli, the diffraction patterns (Fig. 6a and c) showed strong diffraction peaks assigned 2θ around 38.2°, 44.4° and 64.5°, which can be indexed to the (111), (200), and (220) planes of the face-centered cubic silver (JCPDS Card File, No. 04-0783). However, the diffraction pattern of yellow silver nanoparticles showed broad peaks on the diffractogram. This is possibly due to the inclusion of silver nanoparticles in the starch vermicelli templates. According to the molecular structure reported by Gidley (Gidley, 2001), it is now accepted that there is a continuum of starch polymer structures from linear amylose to branched amylopectin. This is suggested that the linear amylose- or branched amylopectin-nanoparticle complexes are formed to be non-crystalline in the native granule starch, indicating that the appearance of broad diffraction lines is present in a poor crystallinity for XRD patterns. The results obtained here were found to be similar to Sarma and Chattopadhyay (Sarma & Chattopadhyay, 2004) and Chairam and Somsook (Chairam & Somsook, 2008) who reported that a poor crystallinity was observed over a range of 2θ positions for starch-mediated synthesis of metal and metal-oxide nanoparticles, respectively. Therefore, some diffraction peaks were not observed from the XRD observation. After carbonization, it was noted that the absence of any different peaks was hidden most likely due to black carbon precipitate powder. The results from diffractogram indicated clearly that the origin of yellow vermicelli was demonstrated from the presence of silver nanoparticles.

Several 2θ positions of the diffraction pattern were observed for the sample obtaining from the carbonized purple vermicelli powder (Fig. 13b and d). In addition to the XRD pattern of Ag nanoparticles (peaks at 38.2°, 44.4°,and 64.6°), 5 other peaks are 32.3°, 46.4°, 54.9°, 57.6°, and 67.7° corresponding to the (200), (220), (311), (222), and (400) planes of the face-centered cubic AgCl (JCPDS Card File, No. 06-0480). The XRD indicated clearly the presence of silver chloride in the powder after the carbonization of purple vermicelli at 200 °C and 300 °C. AgCl nanoparticles have been reported as nanocomposites with other materials such as silk fibers (Potiyaraj, Kumlangdudsana, & Dubas, 2007) and polyaniline (Feng, Liu, Lu, Hou, & Zhu, 2006). Recently, Li and Zhu investigated the formation of Ag nanoparticles toward HCl. A white precipitate product was formed immediately when the HCl solution was added into a Ag colloidal solution (Li & Zhu, 2006). Li and Zhu also indicated that chloride ions could react with colloidal Ag nanoparticles; however, the purple silver nanoparticles were not reported. Interestingly, the purple silver nanoparticles were produced in our experiment. The vermicelli before and after washing with a diluted NaCl solution was still transparent. A white precipitate of silver chloride was not observed. After the reaction of silver ions with β-D-glucose using as a reducing agent, the colour of transparent vermicelli turned to purple. It might be possible that during the nanoparticles formation process some silver nanoparticles may react with chloride ions to form silver chloride. It is noted that all 2θ positions obtained from purple vermicelli were the combination of the diffraction patterns of silver chloride and silver nanoparticles. The nanoparticles in the range 10–65 nm in Fig. 3 are possibly silver chloride nanoparticles which could be separated out by centrifugation.

3.5. Utilization of the starch structure in the synthesis of nanoparticles

Starch has been used for the synthesis and stabilization of nanoparticles, such as gold and silver (Raveendran et al., 2003; 2006; Sarma & Chattopadhyay, 2004) due to its inexpensive and renewable with numerous applications. Starch is a polyhydroxylated macromolecules consisting of glucose units connected by an oxygen linkage to form amylose and amylopectin chains. It presents an interesting dynamic supramolecular associations facilitated by inter- and intra-molecular hydrogen bonding resulting helical structure, which can act as nanoreactors for the growth of nanoparticles (Imberty, Chanzy, Perez, Buleon, & Tran, 1988). During the microwave heating process, metal-aqua complexes were introduced into the starch vermicelli template. The hydroxyl groups of starch possibly facilitated metal ions by electrostatic binding in the helical structure of polysaccharide. Aldehyde terminals from the partial hydrolysis of starch reduced metal ions to metallic nanoparticles while mung bean starch vermicelli itself was used as templates to stabilize as-prepared nanoparticles (as shown in Scheme 1). It has been proposed that the nanoparticle size and polydispersity are controlled by the fine structure of protecting biomolecules including reducing reagents and thermodynamic conditions (Raveendran et al., 2003). Based on the model of starch structure (Buléon et al., 1998; Gallant et al., 1997; Jenkins & Donald, 1995; Tester et al., 2004), the formation of the 38 nm range silver nanoparticles was controlled by the size of helical amylose.

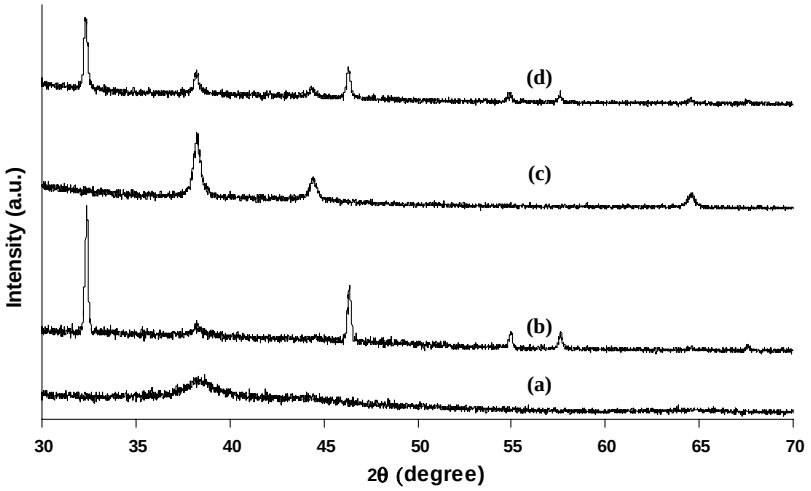

Fig. 13. XRD diffraction pattern of yellow vermicelli (a and c) and purple vermicelli (b and d) at 200 °C and 300 °C, respectively.

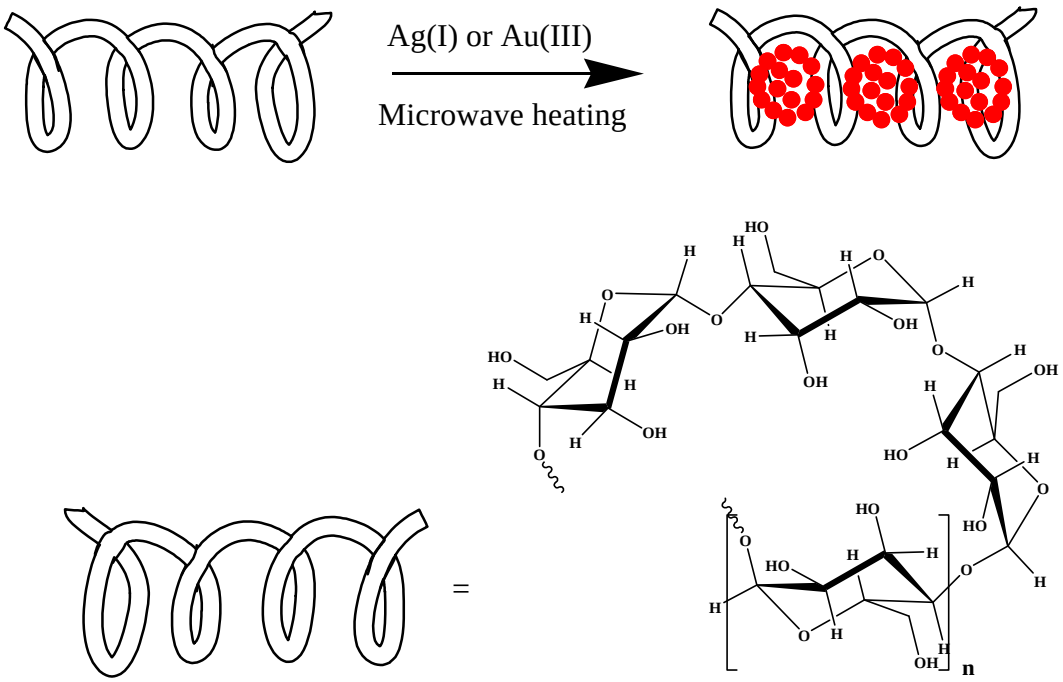

Scheme 1. Illustration of the helical structure of starch template-assisted synthesis of size-controlled nanoparticles.

4. Conclusion

In summary, we have successfully developed a green route to synthesize size- and shaped-controlled silver and gold nanoparticles using mung bean starch vermicelli acting as a stabilizing template. This approach to synthesize size- and shaped-controlled silver and gold nanoparticles is very simple, safe and easily accessible and offers an opportunity to design new fine structures and utilize mung bean starch vermicelli serving as raw materials for the large-scale synthesis of size- and shaped-controlled silver and gold nanoparticles for chemical and biological applications.

Acknowledgements

This research was supported by the Center for Innovation in Chemistry (PERCH-CIC), the Thailand Research Fund, The Commission on Higher Education (RMU4980050) and Faculty of Science, Mahidol University. We thank the Thailand Institute of Scientific and Technological Research (TISTR) for FESEM measurements.

References

Baker, A. A., Miles, M. J., & Helbert, W. (2001). Internal structure of the starch granule revealed by AFM. *Carbohydrate Research, 330*(2), 249–256.

Buléon, A., Colonna, P., Planchot, V., & Ball, S. (1998). Starch granules: structure and biosynthesis. *International Journal of Biological Macromolecules, 23*(2), 85–112.

Chairam, S., & Somsook, E. (2008). Starch vermicelli template for synthesis of magnetic iron oxide nanoclusters. *Journal of Magnetism and Magnetic Materials, 320*(15), 2039–2043.

Chumbimuni-Torres, K. Y., Dai, Z., Rubinova, N., Xiang, Y., Pretsch, E., Wang, J., & Bakker, E. (2006). Potentiometric biosensing of proteins with ultrasensitive ion-selective microelectrodes and nanoparticle labels. *Journal of the American Chemical Society, 128*(42), 13676–13677.

Cushing, B. L., Kolesnichenko, V. L., & O'Connor, C. J. (2004). Recent advances in the liquid-phase syntheses of inorganic nanoparticles. *Chemical Review, 104*(9), 3893–3946.

Daniel, M. C., & Astruc, D. (2004). Gold nanoparticles: assembly, supramolecular chemistry, quantum-size-related properties, and applications toward biology, catalysis, and nanotechnology. *Chemical Review, 104*(1), 293–346.

Dean, H. J., Haynes, J., & Schmaljohn, C. (2005). The role of particle-mediated DNA vaccines in biodefense preparedness. *Advanced Drug Delivery Reviews, 57*(9), 1315–1342.

Deniger, D. C., Kolokoltsov, A. A., Moore, A. C., Albrecht, T. B., & Davey, R. A. (2006). Targeting and penetration of virus receptor bearing cells by nanoparticles coated with envelope proteins of Moloney murine leukemia virus. *Nano Letters, 6*(11), 2414–2421.

Feng, X. O., Liu, Y. G., Lu, C. L., Hou, W. H., & Zhu, J. J. (2006). One-step synthesis of AgCl/polyaniline core-shell composites with enhanced electroactivity. *Nanotechnology, 17*(14), 3578–3583.

Gallant, D. J., Bouchet, B., & Baldwin, P. M. (1997). Microscopy of starch: evidence of a new level of granule organization. *Carbohydrate Polymers, 32*(3–4), 177–191.

Gidley, M. J. (1985). Quantification of the structural features of starch polysaccharides by NMR spectroscopy.. *Carbohydrate Research, 139*, 85–93.

Gidley, M. J. (2001). Starch structure/function relationships: achievements and challenges. In T. L. Barsby, A. M. Donald, & P. J. Frazier (Eds.), *Starch: advances in structure and function* (pp. 1–7). Cambridge, UK: The Royal Society of Chemistry.

He, J., Kunitake, T., & Nakao, A. (2003). Facile in-situ synthesis of noble metal nanoparticles in porous cellulose fibers. *Chemistry of Materials, 15*(23), 4401–4406.

Hill, R. T., Lyon, J. L., Allen, R., Stevenson, K. J., & Shear, J. B. (2005). Microfabrication of three-dimensional bioelectronic architectures. *Journal of the American Chemical Society, 127*(30), 10707–10711.

Huang, H., & Yang, X. (2004). Synthesis of polysaccharide-stabilized gold and silver nanoparticles: a green method. *Carbohydrate Research, 339*(15), 2627–2631.

Imberty, A., Chanzy, H., Perez, S., Buleon, A., & Tran, V. (1988). The double-helical nature of the crystalline part of A-starch. *Journal of Molecular Biology, 201*(2), 365–378.

Jenkins, P. J., & Donald, A. M. (1995). The influence of amylose on starch granule structure. *International Journal of Biological Macromolecules, 17*, 315–321.

Jodelet, A., Rigby, N. M., & Colquhoun, I. J. (1998). Separation and NMR structural characterisation of singly branched [α]-dextrins which differ in the location of the branch point. *Carbohydrate Research, 312*(3), 139–151.

Kaniyankandy, S., Nuwad, J., Thinaharan, C., Dey, G. K., & Pillai, C. G. S. (2007). Electrodeposition of silver nanodendrites. *Nanotechnology, 18*(12).

Li, L., & Zhu, Y.-J. (2006). High chemical reactivity of silver nanoparticles toward hydrochloric acid. *Journal of Colloid and Interface Science, 303*(2), 415–418.

Lu, L., Randjelovic, I., Capek, R., Gaponik, N., Yang, J., Zhang, H., & Eychmuller, A. (2005). Controlled fabrication of gold-coated 3D ordered colloidal crystal films and their application in surface-enhanced Raman spectroscopy. *Chemistry of Materials, 17*(23), 5731–5736.

Lu, Q., Gao, F., & Komarneni, S. (2005). A green chemical approach to the synthesis of Tellurium nanowires. *Langmuir, 21*(13), 6002–6005.

Moorthy, S. N., Andersson, L., Eliasson, A.-C., Santacruz, S., & Ruales, J. (2006). Determination of amylose content in different starches using modulated differential scanning calorimetry. *Starch - Stärke, 58*, 209–214.

Oates, C. G. (1990). Fine structure of mung bean starch: an improved method of fractionation. *Starch - Stärke, 42*, 464–467.

Panigrahi, S., Praharaj, S., Basu, S., Ghosh, S. K., Jana, S., Pande, S., Vo-Dinh, T., Jiang, H., & Pal, T. (2006). Self-assembly of silver nanoparticles: synthesis, stabilization, optical properties, and application in surface-enhanced Raman scattering. *Journal of Physical Chemistry B, 110*(27), 13436–13444.

Potiyaraj, P., Kumlangdudsana, P., & Dubas, S. T. (2007). Synthesis of silver chloride nanocrystal on silk fibers. *Materials Letters, 61*(11–12), 2464–2466.

Qu, L., Dai, L., & Osawa, E. (2006). Shape/size-controlled syntheses of metal nanoparticles for site-selective modification of carbon nanotubes. *Journal of the American Chemical Society, 128*(16), 5523–5532.

Raveendran, P., Fu, J., & Wallen, S. L. (2003). Completely "green" synthesis and stabilization of metal nanoparticles. *Journal of the American Chemical Society, 125*(46), 13940–13941.

Raveendran, P., Fu, J., & Wallen, S. L. (2006). A simple and green method for the synthesis of Au, Ag, and Au–Ag alloy nanoparticles. *Green Chemistry, 8*, 34–38.

Rindlav-Westling, A., Stading, M., & Gatenholm, P. (2002). Crystallinity and morphology in films of starch, amylose and amylopectin blends. *Biomacromolecules, 3*(1), 84–91.

Sarma, T. K., & Chattopadhyay, A. (2004). Starch-mediated shape-selective synthesis of Au nanoparticles with tunable longitudinal plasmon resonance. *Langmuir, 20*(9), 3520–3524.

Somsook, E., Hinsin, D., Buakhrong, P., Teanchai, R., Mophan, N., Pohmakotr, M., & Shiowatana, J. (2005). Interactions between iron(III) and sucrose, dextran, or starch in complexes. *Carbohydrate Polymers, 61*(3), 281–287.

Stoeva, S. I., Lee, J.-S., Thaxton, C. S., & Mirkin, C. A. (2006). Multiplexed DNA detection with biobarcoded nanoparticle probes. *Angewandte Chemie International Edition, 45*(20), 3303–3306.

Su, K. H., Wei, Q. H., Zhang, X., Mock, J. J., Smith, D. R., & Schultz, S. (2003). Interparticle coupling effects on plasmon resonances of nanogold particles. *Nano Letters, 3*(8), 1087–1090.

Sun, Y., & Xia, Y. (2002). *Shape-controlled synthesis of gold and silver nanoparticles Science, 298*, 2176–2179.

Tan, H. Z., Gu, W. Y., Zhou, J. P., Wu, W. G., & Xie, Y. L. (2006). Comparative study on the starch noodle structure of sweet potato and mung bean. *Journal of Food Science, 71*(8), C447–C455.

Templeton, A. C., Pietron, J. J., Murray, R. W., & Mulvaney, P. (2000). Solvent refractive index and core charge influences on the surface plasmon absorbance of alkanethiolate monolayer-protected gold clusters. *Journal of Physical Chemistry B, 104*(3), 564–570.

Tester, R. F., Karkalas, J., & Qi, X. (2004). Starch-composition, fine structure and architecture. *Journal of Cereal Science, 39*(2), 151–165.

Xu, Z. P., Hua Zeng, Q., Lu, G. Q., & Bing Yu, A. (2006). Inorganic nanoparticles as carriers for efficient cellular delivery. *Chemical Engineering Science, 61*(3), 1027–1040.

International Journal of Environmental & Science Education
Vol. 4, No. 2, April 2009, 147-168

Understanding Mental Models of Dilution in Thai Students

Ninna Jansoon
Mahidol University, Thailand

Richard K. Coll
University of Waikato, New Zealand

Ekasith Somsook
Mahidol University, Thailand

Received 21 June 2008; Accepted 12 February 2009

The purpose of this study was to investigate Thai students' understanding of dilution and related concepts. The literature suggests that a complete understanding of chemistry concepts such as dilution entails understanding of and the ability to integrate mental models across three levels of representation: the macroscopic, sub-microscopic and symbolic. In this work students' understanding was probed using the interview about events (IAE) approach employing open-ended questions, and also by analysis of student descriptions, and drawings. The research findings suggest that all students were able to answer open-ended questions related to dilution and related concepts. Less able students presented representations at the symbolic level and subsequently described events at the sub-microscopic and macroscopic levels. However, these latter representations typically were unrelated to the representations presented at the symbolic level. In contrast, more able students were able to present consistent representations of dilution at each level of representation.

Key Words: dilution, mental model, macroscopic level, sub-microscopic level, symbolic level

Introduction

Mental Models

Mental models represent ideas in an individual's mind that they use to describe and explain phenomena. According to Van Der Veer and Del Carmen Puerta Melguizo (2003), mental models are constructed from perception, imagination, or from the comprehension of discourse. When studying science, students gain knowledge of scientific mental models as a result of exposure to the teaching of such models (Harrison & Treagust, 2000). That is, students create their own mental models when they learn and try to understand scientific knowledge during the learning process (Chittleborough, Treagust, Mamiala, & Mocerino, 2005).

ISSN 1306-3065

http://www.ijese.com/

In science "mental models are used to describe a system and its component parts as well as its states, to explain its behavior when changing from a state to another and to predict future states of the system" (Franco & Colinvaux, 2000, p. 105). According to Coll (1999), mental models are used to produce simpler forms of concepts, to provide stimulation and support for the visualization, and to provide explanations for scientific phenomena (Coll, 1999). The literature suggest that mental models play a central role in science (Gilbert, Boulter, & Rutherford, 2000; Gobert & Buckley, 2000) and in the communication of scientific knowledge (Dagher, 1994; Treagust, 1993). In science teaching, teachers use mental models in two distinct ways. First, they try to communicate the models of science (e.g., atomic structure) to their students. Second, they use certain types of models – particularly analogy, to explain scientific ideas to students (Duit, 1991). Students likewise construct their own individual mental models, and also to try use them to understand scientific phenomena that they encounter during instruction or in everyday life (Duit, 1991; Pittman, 1999; Venville, Bryer, & Treagust, 1994). However, the literature suggests that student understanding of science models, including mental models, and some of their own constructed mental models are often at variance with scientific models (Greca & Moreira, 2000; Norman, 1983).

Mental Models and Explanations of Experts and Novices

A science expert is a person who is recognized as a reliable source of knowledge, technique, or skill with significant experience gained through practice and education in a particular scientific field. In contrast, a novice is a person who is newly introduced to any science or another field of study and undergoing training in order to meet normal requirements of being regarded a mature and equal participant in a community of practice (e.g., science). Experts and novices are different in terms of four basic processes: knowledge, representation, problem-solving, and understanding (Heyworth, 1999; Savelsbergh, De Jong, & Ferguson-Hessler, 2002). Savelsbergh et al. (2002) investigated the differences between experts and novices in gaining knowledge: content, structure, and sources. It seems that the experts are able to modify and to construct representations, and also are highly capable at problem-solving due to a high qualitative content knowledge in their fields. In contrast, novices lack this qualitative content knowledge, and typically seek to solve problems by use of quantitative representations, and rote use of formulae. Kozma and Russell (1997) observe that experts use underlying principles to categorize their representations and transformed representations. In order to shift from novice to expert capability, it is necessary to enhance problem-solving capability. To do this we need to develop their declarative knowledge to help them to learn how to synthesize knowledge, to create the mental models, and to recognize similarities across many problems (Foshay & Kirkley, 2003).

Farnham-Diggory (1994) identified five types of knowledges: *declarative*, *procedural*, *conceptual*, *analogical* and *logical*. Declarative knowledge is things that we know; it consists of the facts, concepts and principles for a knowledge domain. Farnham-Diggory claim that knowledge is stored in an individual's cognitive structures, and that a person constructs associations, lists, scripts, plans, schemata and mental models. Of these associations, mental models are deemed the most powerful cognitive structures, and work to relate procedural and declarative knowledge. Anderson (1995) describes mental models as the synthesis of declarative knowledge to solve problems. Jonassen and Tessmer (1996), however, believe that the mental models are distinct from declarative and procedural knowledge.

Grosslight, Unger, Jay, and Smith.(1991) report that mental models help experts to understand and think about phenomena and are used to formulate and test real ideas. They go on to note that a person's understanding of mental models can be categorized into three levels. At

level 1, models are seen as a 'toy' or a 'copy' of reality. At level 2, models serve a specific and explicit purpose. At level 3, models are constructed to develop and test an idea, and can be manipulated and subjected to test. Unal, Çalık, Ayas, and Coll (2006) similarly classify the level of student's understanding into three categories: reasoning ability, hierarchy of qualitatively different understandings, and structural characteristics.

Mental Models and Levels of Representation

Chemistry is composed of many abstracts concept and topics (Gabel, 1999; Johnstone, 1993). When describing chemistry phenomena, chemists generally present concepts at three levels of knowledge representation: the macroscopic, sub-microscopic, and symbolic levels (Johnstone, 1991).

- *The macroscopic level*, is a concrete level corresponding to observable objects. At this level, students observe the chemical phenomena in their experiments or experiment (Johnstone, 1991; Treagust, Chittleborough, & Mamiala, 2003);
- *The sub-microscopic level*, is an abstract level, but corresponding to observable phenomena at the macroscopic level. This level is characterized by concepts, theories and principles used to explain what is observed at the macroscopic level, using things such as the movement of electrons, molecules, or atoms (Johnstone, 1991);
- *The symbolic level*, is used to represent chemical and macroscopic phenomena by the use of chemical equations, mathematical equations, graphs, reaction mechanisms, analogies and model kits (Johnstone, 1991).

Gabel (1999) says that chemical phenomena, which we observe or study at the macroscopic level, can also be described and explained at the sub-microscopic level. But are generally described at the sub-microscopic and symbolic levels in order to solve they complicated problems. Students are apparently able to understand complex ideas better when asked to express the relationships between macroscopic and sub-microscopic levels using chemical symbols, chemical equations and mathematical equations.

Johnstone (1993) says that in order to understand scientific knowledge, students must understand the knowledge at three levels of representations: macrochemistry, submicrochemistry and representational chemistry. In order to integrate the three levels of representation, students need to confront a variety of problems: fragmented topics that do not fit well rather than be presented with simple problems that have one, rather obvious answer (Gabel, 1999). Second, they need to learn how to connect abstract representations (Wu, Krajcik, & Soloway, 2001), and third they need to be exposed to abstract phenomena that are difficult to interpret or visualize at the sub-microscopic and symbolic levels (Johnstone, 1991).

Johnstone (1991) and Treagust et al. (2003) argue that the three levels of representation are interconnected in a triangle analogy as shown in Figure 1. The macroscopic level is the basis of chemistry, and teachers usually explain what happens at this level by using symbolic and sub-microscopic levels (Johnstone, 1991; Treagust et al., 2003).

Devetak (2005) developed the Interdependence of Three Levels of Science Concepts (ITLS) model in order to explain the connection between concrete and abstract levels as shown in Figure 2. In order to induct knowledge into their long-term memory, students should be encouraged to use mental models in order to see how to connect all three levels (Devetak, Vogrinc, & Glažar, in press).

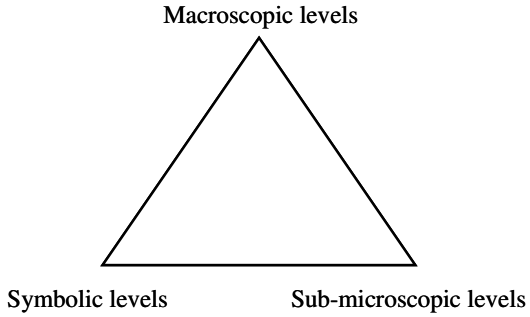

Figure 1. Three levels of representation used in chemistry (based on Johnstone, 1991 and Treagust et al., 2003).

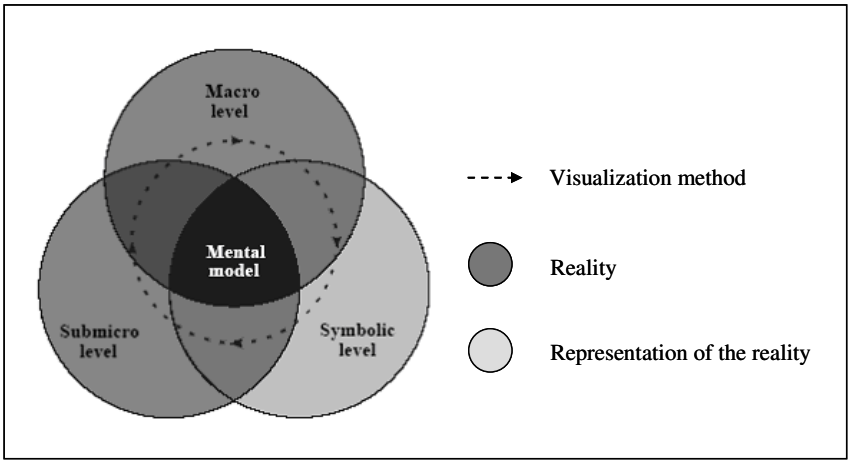

Figure 2. The interdependence of the three levels of science concepts model (after Devetak, 2005).

If students understand the role of each level of chemical representation, they can often then see how transfer knowledge from one level to another - meaning they are able to generate understandable explanations, thus reducing alternative conceptions (Russell et al., 1997; Treagust et al., 2003). Gabel (1999) states that if students see how the three levels are interconnected then students are able to generate relational understanding - reducing alternative conceptions (Mulford & Robinson, 2002; Russell et al., 1997; Treagust et al., 2003).

Making transitions between the three levels of representations is apparently difficult for students. Hinton and Nakhleh (1999) report that chemical phenomena are generally understandable at the macroscopic level, and able to be interpreted at the symbolic level by undergraduate students. However, it seems students are often unable to connect either of these levels to the sub-microscopic level. Nurrenbem and Pickering (1987) likewise report that students do not understand the nature of matter, and they are unable to imagine the nature of particles. This means students also struggle to connect the symbolic level with the submicroscopic level. Dori and Hameiri (2003) support this saying that students can see, touch, or

smell things when doing experiments at the macroscopic level, but find it difficult to explain the nature of matter at the symbolic level.

Gabel (1993) states that students should be encouraged to understand the cross relationships in daily life. A variety of instructional approaches have been used to help students understand chemistry at the three levels of representation (Wu et al., 2001): instructional technology (Ardac & Akaygun, 2004; Russell et al., 1997; Tasker & Dalton, 2006), laboratory activities (Chandrasegaran, Treagust, & Mocerino, 2008; Gabel, 1999), mental models (Chittleborough & Treagust, 2007) and concrete models (Copolo & Hounshell, 1995). In addition, numerous researchers have used the three levels of representation in order to probe students' deep understanding (Bowen, 1998; Raviolo, 2001). Interestingly, it seems that secondary school students who learn the chemical concepts at the three levels of representation are able to solve problems better than first year students (Devetak, Urbančič, Wissiak Grm, Krnel, & Glažar, 2004).

A particular issue arises when trying to teach students chemistry concepts involving representation at all three levels. Chemistry teachers often provide students with algorithms or formulas for solving chemical problems. It seems this mostly occurs because of pressure to 'perform' in external summative examination which reward correct numerical answers (Dahsah & Coll, 2008). However, it seems students often use mathematical equations without understanding them in terms of the underlying chemistry or science concepts. In order to acquire the 'right' answers, they usually memorize the mathematical equations and plug in numbers, rather than attempt to solve problems using the basic concepts (Beall & Prescott, 1994; Bunce, Gabel, & Samuel, 1991; Lythcott, 1990; Robinson, 2003). Interestingly, Bunce et al. (1991) report that students are often able to 'solve' chemistry problems numerically. But this does not mean they actually understand the related chemistry. Dahsah and Coll (2008) say students are better able to solve new problems if they understand the basic chemistry concepts first.

Mental Models for Dilution

An understanding of dilution methods is an important part of much introductory chemistry, particularly in the laboratory. For example, most chemistry experiments require students to know how to prepare solutions of known concentrations (e.g., standard solutions) or to dilute solutions of known concentration (Dunnivant, Simon, & Willson, 2002; McElroy, 1996; Wang, 2000). Dahsah and Coll (2007) point out that when students cannot solve problems it is often because they misunderstand the related underlying concepts (e.g., solvent, solute, solution, concentration, solubility, and the mole). Additionally, there are other topics such as volume and molecules which are embedded in the above concepts, and which are needed to solve numerical problems. Dilution and related concepts are abstract and difficult leading to many student alternative conceptions such as the relationship between amount of solute and volume of solution (Dahsah & Coll, 2008; Devetak et al., in press) a diluted solution (Çalik, 2005), the relationship between solvent and solute (Çalik & Ayas, 2005; Devetak et al., in press) the solution concentration at particulate level (Devetak et al., in press) , and the meaning of homogenous solutions (Çalik & Ayas, 2005).

Hence, in summary, students' understanding of dilution and related concepts is typically evaluated by consideration of their ability to solve numerical problems (Dahsah & Coll, 2007; Staver & Lumpe, 1995) but this does not necessarily mean they understand related chemistry concepts (Çalik, 2005; Case & Fraser, 1999; Dahsah & Coll, 2007; Pinarbasi & Canpolat, 2003; Schmidt & Jignéus, 2003).

Research Purpose

The purpose of this study was to investigate and evaluate Thai undergraduate students' understanding of dilution and related concept by accessing their mental models. We also were interested to see how they were able to make connections between the macroscopic and submicroscopic levels (Coll & Treagust, 2003a, 2003b). The research aims for this study were:

- To identify how students tried to explain dilution topics at the macroscopic, submicroscopic, and symbolic levels; and
- To evaluate student understanding for dilution and related concepts.

Theoretical Basis to the Study

We suggest here that in order to answer the research aims, what we need to do is access the mental models students possess for dilution concepts. Harrison and Treagust (2000) say all representations of chemistry concepts are in fact expressions of students' mental models. Hence, here we draw upon literatures about mental models to underpin the study. The theoretical basis of this study was based thus on Norman's (1983) typology of mental models. According to Norman mental models can be classified into four types: the *target system*, the *conceptual model* of that target system, the *user's mental model* of the target system, and the *scientist's conceptualization* of the target system (Norman, 1983). Coll and Treagust (2003b) comment that the target model is the model we are striving to teach. Thus to link this to scientist's conceptualization of the target system, necessitates a synthesis of mental models for the target system, situated into the particular context in which the teaching and learning occurs (i.e., in this case Thailand). This was achieved from a synthesis of curriculum materials; namely, textbook descriptions of concepts, analysis of lecture notes and lesson plans. During teaching students try to understand abstract concepts in chemistry and in the present work we tried to access the students' metal model (i.e., the users' mental model to employ Norman's term) for the target system. In doing so (see below for the specific approach used) we requested participants to depict their models at three levels of chemical representations: macroscopic, sub-microscopic, and symbolic, and got them to try to relate each level (Russell et al., 1997; Treagust et al., 2003).

Methodology

Sample

The sample used in this study consisted on an entire intact class of 414 first-year undergraduate students (aged 18-19 years) who were enrolled in the SCCH 108 chemistry laboratory I in the at Mahidol University. The students consisted of male (39.10%) and female (60.90%). Mahidol University is at autonomous university that is one of the most prestigious universities in Thailand. It is located at Bangkok, Thailand.

Procedures

The first year class was divided into 23 groups, with each group supervised by a teaching assistant. Each group was then divided into 4-5 subgroups; and the sub-groups performed experiments about dilution and related concepts. The students were assigned to do hands-on activi-

ties to evaluate their understanding of dilution and related concepts. They performed experiments and write-up a laboratory report in group. The purpose of this was to evaluate the students' academic ability before the data collection phase (see below).

Data Collection

The researcher first analyzed scores from student laboratory reports. The results suggested that the students could be classified into two groups (A and B) based on an evaluation of their laboratory reports - as high or low ability.

- Group A: High ability students (students A1, A2, A3, A4, and A5)
  These students' scored more than 70%.
- Group B: Low ability students (students B1, B2, B3, B4, and B5)
  These students' scored less than 70%.

Ten students volunteered to be interviewed by IAE technique and were subsequently interviewed using the interview-about-events technique (IAE) championed by Gilbert, Watts, and Osborne (2005) to probe the students' mental models. Three approaches were used to investigate the students' mental models at the same time - as is normal in the IAE technique: open-ended questions, drawing with description, and interview data. Students' mental model was elicited their understandings at three levels of representation: macroscopic, sub-microscopic and symbolic. The interview protocol was developed from a pilot study in a similar manner to that reported in Coll and Treagust (2003a, 2003b). The IAE focus cards were developed based on the eight-step algorithm reported by Gilbert et al. (2005). In the interviews, the students were encouraged to speak freely, the cards were designed to connect the events to possible students' life experiences (Ünal, Çalık, Ayas, & Coll, 2006).

There were three IAE focus cards employed and these were labeled DA 01, DA 02, and DA 03: DA 03 (see appendix). The interviewer used these IAE focus cards to conduct a 60-minute interview with four students for each of the achievement levels described above, and followed the protocol detailed below (i.e., open-ended questions, drawing with description, and interview questions to clarify meaning of drawings or responses).

Task 1 IAE Focus Card DA01

- Students were asked to explain what they understood about a 1 M solution of sodium chloride by giving an explanation in terms of solvent, solute, and homogeneity of solution.
- Students were also asked to depict a 1000 mL of 1 M NaCl at the macroscopic, sub-microscopic, and symbolic levels.

Task 2 IAE Focus Card DA02

- The interviewer showed participants a can of Coke with a label showing that it was a 10 %w/v sugar solution. Then students were asked to describe what they understood by this term.
- The interviewer showed participants IAE focus card DA02 and asked 'Which figure shows the most diluted Coke beverage?' Participants were asked to depict what they understood at the macroscopic, sub-microscopic, and symbolic level.
- Participants were asked to link IAE focus card DA02 with a solution and a diluted solution.

- Participants were asked to describe the differences between a solution and a diluted solution at the macroscopic, sub-microscopic, and symbolic levels.

Task 3 IAE Focus Card DA03

- Participants were asked to calculate the percentage of sugar by w/v in a Coke solution with extra ice in a tumbler.
- Participants were asked to describe what they understood about the concentration of sugar in terms of the % w/v unit at the macroscopic, sub-microscopic, and symbolic levels.

Coll and Treagust (2003a, 2003b) say using cards like this rather than just asking students questions is less threatening and helps established a more relaxed environment because the students attention is focused on the card rather than on their ability to respond to challenging questions directly.

Data Analysis

The interview data and drawings produced by the IAE protocol detailed above were analyzed thematically looking for evidence in terms of students' understanding at the three levels of chemical representations, and their ability to relate each level to the others. Excerpts of interviews and some typical student drawings are provided below when we present the findings to show the nature of this analysis.

Research Findings and Discussion

The research findings suggest that the students' (or users') mental models of many aspects of dilution chemistry were generally in accord with the scientific conceptualization that is to say they did not show many alternative conceptions. However, their ability to represent the concepts at the three levels of representation varied as is detailed below.

At the macroscopic level, students were able to depict their mental models by observing the chemical phenomena in laboratory classes. At the sub-microscopic level, students were able to depict their mental models by imagination at the particulate level. At the symbolic level, students were able to depict their mental models by using of chemical symbols and mathematical formulae.

The interviewer showed the students IAE focus card: DA01. The students' understanding was first probed by asking "Can you explain what you understand about a 1M solution of sodium chloride?, and the following responses were typical of the responses obtained:

Student A1 : 1 liter of solution contains 1 mol of solute. This solution is a mixture of sodium chloride and water. The solute is sodium chloride.
Student A2 : 1000 mL of sodium chloride solution contains 1 mol of sodium chloride.
Student B2 : the volumetric flask contains 1 L of solution
: 1 mol NaCl.
Student B4 : 1 mol/L

These data suggests that these students were able to successfully describe the meaning of '1 M of sodium chloride'. The students next were asked to depict their understanding at the three levels of representation. Solvent, solute, and homogeneity of solution were linked in the concepts as shown in Figure 3.

Two students provided detail in the interviews and talked of ionization. Student B3 pointed that NaCl is ionized in water to give Na^+ and Cl^- ions while student A2 described NaCl in solution in the form of pairs of cations and anions, which conflicts with the scientific conceptualization (note: she also inadvertently wrote the symbol for calcium instead of sodium). This point to a molecular view of sodium chloride, which is an alternative conception.

Then interviewer next showed the students a label on a Coke bottle showing that the concentration was 10%w/v sugar, and students were asked to describe what they understood by this term. It seems that all of the students understood the meaning of a 10% w/v sugar solution.

The interviewer then showed the students IAE focus card DA02, and the students' understanding was probed by asking "Which figure shows the most diluted Coke beverage? ", and then asked "Why do you think that is the correct answer?". All students provided correct answers for Figure C. Students depicted their understanding at the three levels of representation as shown in Figure 4.

Level of representation		
Macroscopic	Sub-microscopic	Symbolic
A2's Drawing		
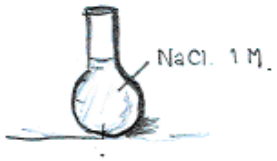	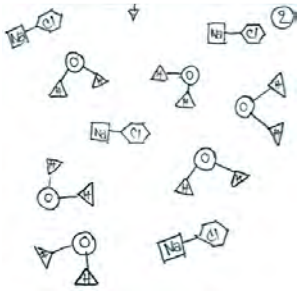	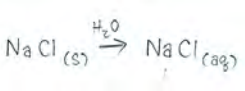
B3's Drawing		
	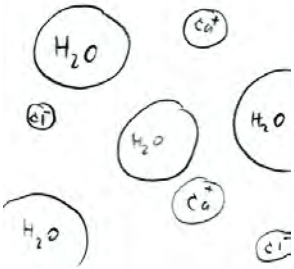	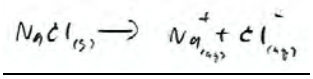

Figure 3. Sample students' depictions of a 1M solution of sodium chloride at three levels of representation.

Level of representation		
Macroscopic	Sub-microscopic	Symbolic
A2's Drawing 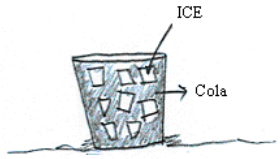 Ice melts into water, the cola is diluted.	 	
B2's Drawing 	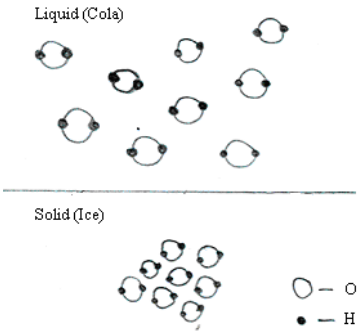 	

Note Student B2 meant $H_2O(s)$ is water in solid state; ice, and $H_2O(aq)$ is water in the liquid state.

Figure 4. Sample students' depictions of dilution of Coke and sugar solutions at three levels of representation

All students provided correct representations at the macroscopic level for the dilution of Coke solutions which in this case was related to their daily life (i.e., involving a familiar beverage 'Coke'). However some of the less able students were unable to depict the diluted Coke solution at the sub-microscopic level. To further probe students' understanding, the interviewer asked a more general question, "What is a solution?" and "What is a diluted solution?". The following responses are typical:

Student A1 : The solution is a homogeneous mixture of solvents and solutes in which the volume of solvent is greater than the volume of solute.
: A diluted solution is made by adding some solvent into the solution. The number of moles of the solute is unchanged but the solution volume of the solution is increased.

Student A3 : A solution composes of a solvent and a solute. Adding more solvent makes the solution less concentration.

Student B2 : The solution consists of a solvent and a solute.
: A diluted solution is made by adding water into the solution in order to decrease the concentration.
Student B4 : The solution is diluted because of the impurity of solution.
: The more diluted solution has a lower concentration.

Students then presented depictions of the differences between a solution and a diluted solution at the three levels of representation as shown in Figures 5 and 6, and described their mental models in the interview transcripts which follow.

Interviewer : How do you know it is a solution or a diluted solution?

Student A3 : Solution is a mixture of a solvent and a solute. The addition of solvent into a solution makes it a diluted solution.
Interviewer : So what is the difference between a solution and a diluted solution?
Student A3 : The amount of solvent is increased. Added n mL of solvent into the solution then the volume of solvent is y + n mL.
Interviewer : What else do you know about a diluted solution?
Student A3 : The amount of solvent is increased but the mole is constant.

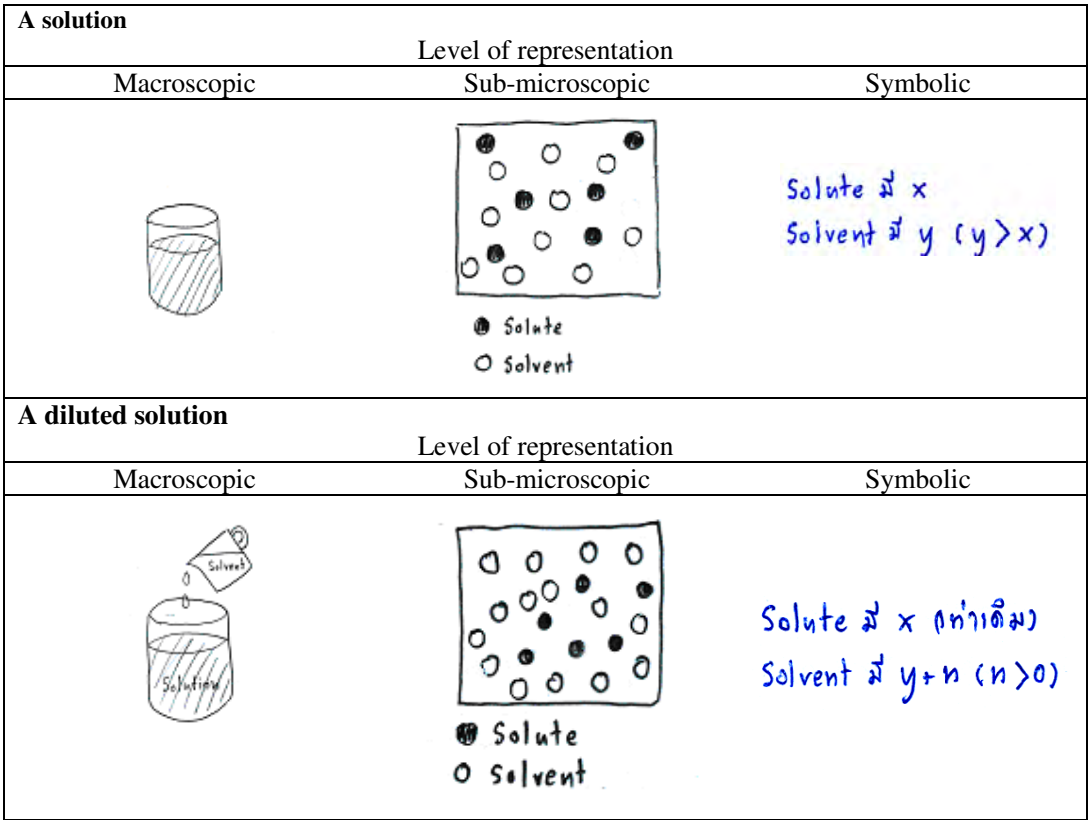

Figure 5. Sample of a more able student's depictions of the differences between a solution and diluted solution at three levels of representation

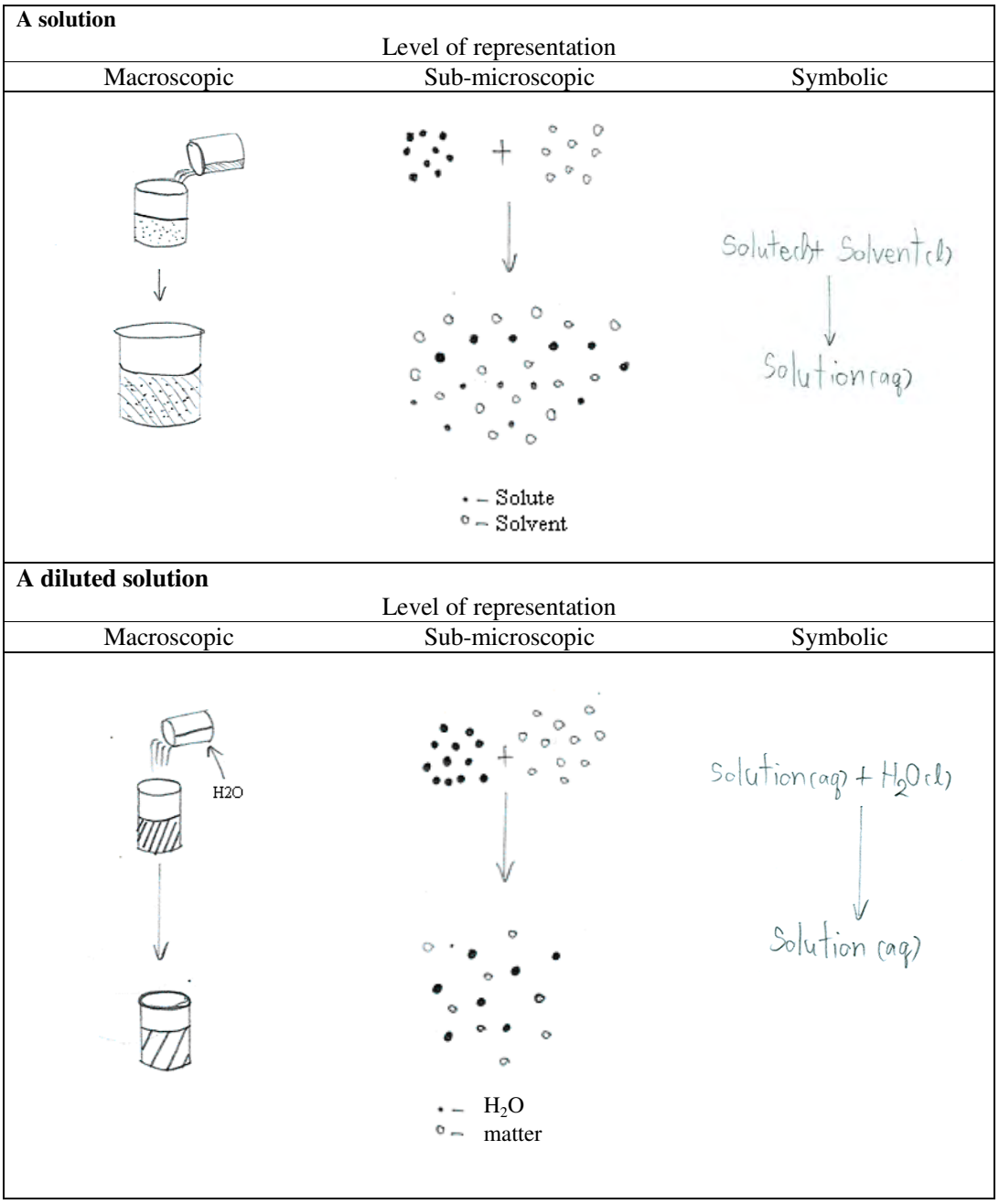

Figure 6. Sample of a less able student's depictions of the differences between a solution and diluted solution at three levels of representation

These data suggest that in this case, student A3 had a good understanding of the dilution concept. Additionally, this student was able to depict a solution and a diluted solution at each

level of representation, and identify the relationship between the levels. Hence, the more able students understood the dilution concept because they explained 'added solvent into solution' at the macroscopic level when they depicted by drawing of what they preformed in the laboratory classes, at the sub-microscopic level where in their drawings they depicted the numbers of solvent and solute particles, and at the symbolic level where they depicted mathematical equations:

> x symbol is solute.
> y symbol is solvent because of $y > x$.
> In addition, n symbol is solvent.
> That diluted solution, solute is constant and solvent is increase($y + n$).

Contrast this with a less able student, student B2, whose depiction of a solution and diluted solution are presented in Figure 6:

The interviewer asked student B2 the same questions as student A3. The less able student B2 successfully depicted the nature of a solution (top part of Figure 6), the number of solvent and solute particles seems to be much the same in the diluted and undiluted solutions (see bottom part of Figure 6), meaning the student's depiction of a diluted solution at the sub-microscopic level was not consistent with the scientific conceptualization. Likewise this student's depiction of dilution at the symbolic level in fact represents the solution process, rather than dilution (RHS of Figure 6). In summary, the less able students seem unsure about the dilution concept because they explained dilution as being 'adding water into solution' at the sub-microscopic level and by depicting the number of solvent and solute particles, but with the wrong ratio of particles. Likewise, at the symbolic level they presented dilution simply in terms of by increasing the amount of water.

Then the interviewer showed students IAE focus card DA03 and told a story about a boy who added ice to a tumbler of Coke and then drank it. Students were asked to describe what they understood based on IAE focus card DA03. The purpose of this phase of the data collection was to use an additional probe for dilution that was based on an activity very familiar to these Thai students' everyday lives (i.e., rather than just a substance that they were familiar with).

> Based on IAE focus card, The questions were classified into 4 steps.
>
> 1. Pour 100 mL of Coke beverage into a tumbler.
>   The Coke solutions contain 10 % w/v sugar. → 10 g/100 mL
> 2. Added 50 mL of ice into 100 mL of Coke beverage, so we can assume the ice melted, meaning the Coke beverages were diluted, and the concentration of sugar is 10 g/150 mL.
> 3. Assuming that students are drinking 50 mL of diluted Coke beverage in a tumbler. Then volume of solution is 100 mL. But the concentration is constant.
>   The concentration of sugar is 6.67 g/100 mL that it equals 10g/150 mL.
> 4. Added 100 mL of ice into 100 mL of Coke solution, so interviewer assumed ice melted. Then Coke solutions were diluted.
>   Then the percentage of sugar by w/v in a Coke solution is 3.33 g/100 mL

The students were then asked to draw a depiction of this event and also asked to calculate the concentration of sugar in units of % w/v. Sample responses are shown in Figure 7

As might be expected the more able students were able to calculate the concentration of sugar in a tumbler of Coke successfully and were able to integrate between the levels of repre-

sentation. At the sub-microscopic level, all students depicted things such as the amount, ratio and structure of particles in a solution. Sample depictions are shown in Figure 8.

In contrast the less able students were able to depict the concentration of sugar at the symbolic level but only 1 of the 5 less able students was able to depict the concentration of sugar at the sub-microscopic level.

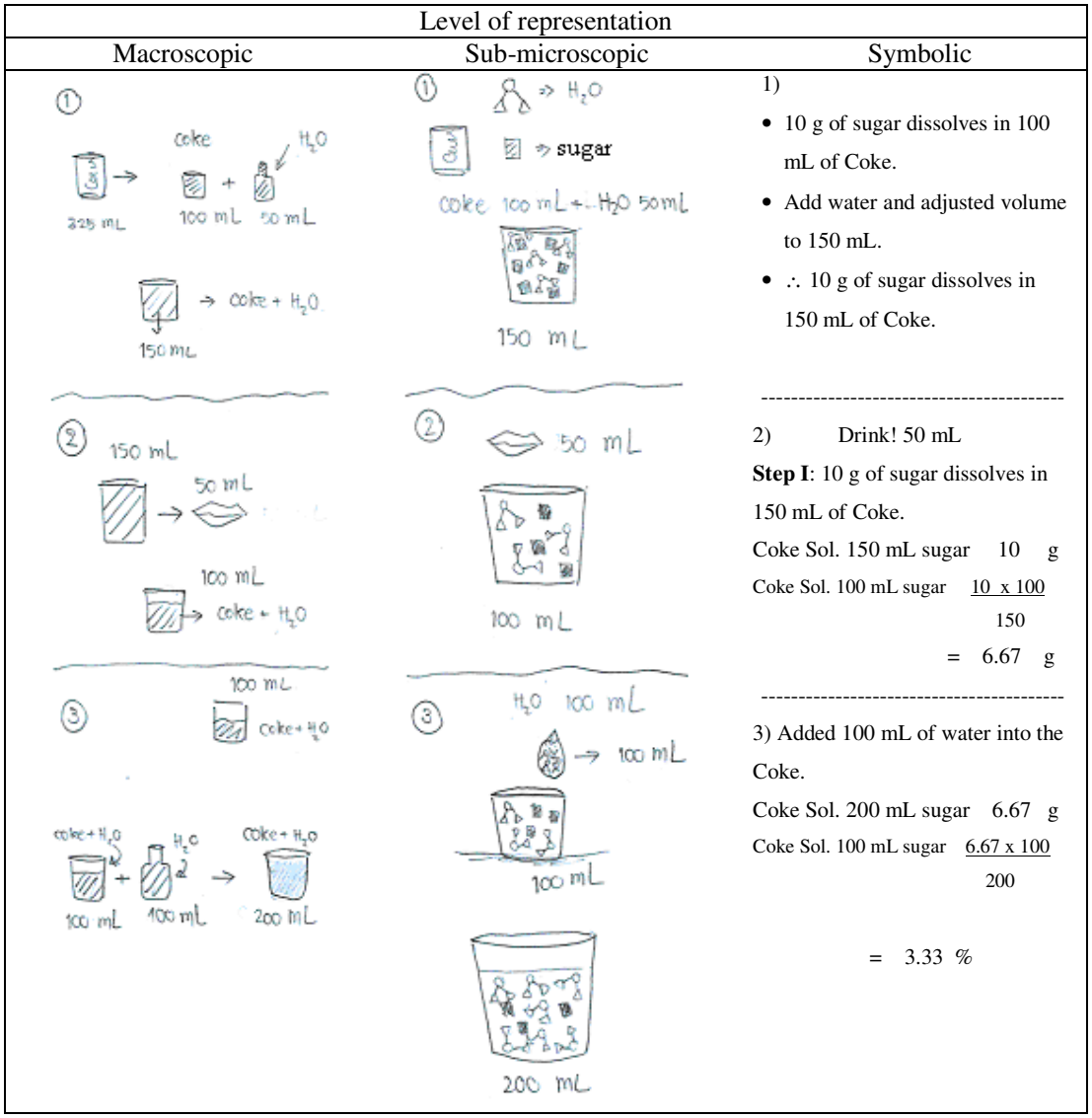

Figure 7. Sample of a student's depictions of the addition of ice to a tumbler of Coke at three levels of representation

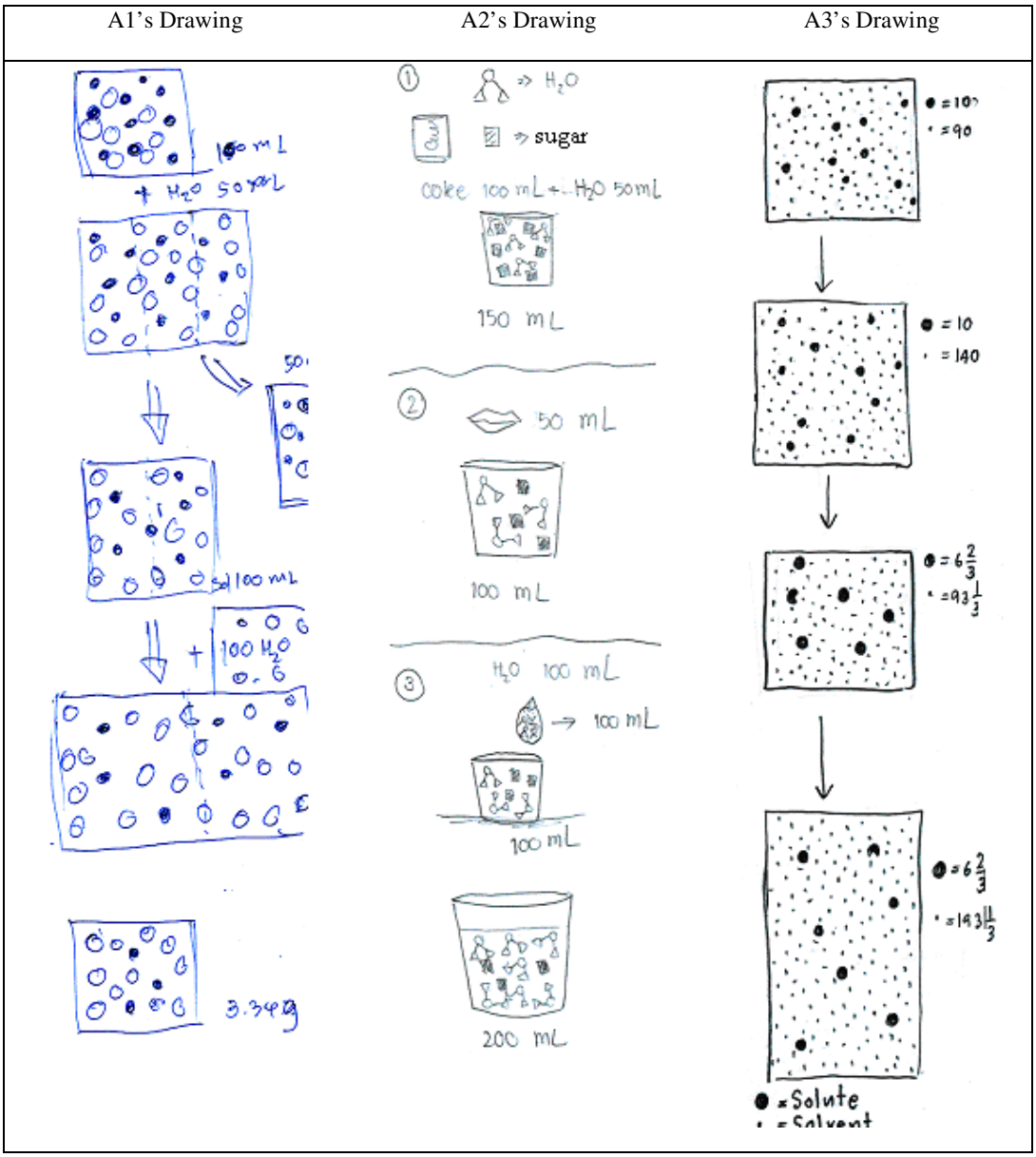

Figure 8. More able students' depictions of dissolution at the sub-microscopic level.

In addition, they were not able to relate the macroscopic level to the other levels. Sample drawings by less able students are shown in Figure 9.

The less able students tended to address this probe by firstly using an algorithm to do the calculation of the concentration of the solutions and then depicting the event at the sub-microscopic and macroscopic levels. Neither the sub-microscopic nor the macroscopic levels were then related to the symbolic level. As an interesting aside, dissolution of ice into water as occurs here also involves a phase change which would result in an increase in volume. This

was not noted or commented on by any of the students. We feel this is probably a consequence of the probes used, which tended to drive the students to focus on dissolution rather than changes of phase.

Discussion and Conclusions

In this work chemistry at the three levels of representations was taught to students with an intention to enhance their understanding of dilution. Their understanding of dilution was probed by several techniques: open-ended questions, drawing with description, and interviews. The findings do suggest that the interview about events approach is a useful technique to

Macroscopic Level	Sub-microscopic Level	Symbolic Level
		10% → 10 g/100 mL 10 g of sugar dissolves in 150 mL of water. ---------- 150 mL of solution → 10 g 100 mL of solution $\frac{100 \times 10}{150}$ = 6.66 g ---------- Add 100 mL of water into the solution ∴ 6.66 g of sugar dissolves in 200 mL of water. 200 mL of solution → 6.66 g 100 mL of solution $\frac{6.66 \times 100}{200}$ = 3.33 %

Figure 9. Less able students' depictions of dissolution at the sub-microscopic level

probe students' understanding especially when the IAE focus cards with events that connected to students' experience are used.

The more able students in the study seemed to understand the role and relationships of representations at all three levels using Johnstone's (1991) framework. In particular, they understood the role of macroscopic and sub-microscopic levels of representation and were able to integrate into the other level as noted by (Chittleborough & Treagust, 2007) and consistent with the recommendation of Gabel (1999) and Wu et al., (2001). In contrast less able students usually presented their work mostly at the symbolic level followed by the sub-microscopic and macroscopic levels which were typically not related to the symbolic level. Hence, as might be expected students' mental models for dilution vary, with more able students possessing more complete, relational mental models than their less able peers. This focus on the symbolic level may be related to the mode of science instruction in Thailand. Dahsah and Coll (2008) comment that in the case of stoichiometry, teachers teach using algorithms, something they argue results in superficial or shallow understanding.

Russell et al. (1997) and Treagust et al. (2003) argue that in order to understand chemistry concepts students need to be able to represent their mental models at all three of Johnstone's (1991) levels of representation, and furthermore be able to relate these levels to each other. It seems the present work points to a need to shift students from too heavy a focus on the symbolic level and drives them to consider how the three levels relate to each other. We suggest then that the use of IAE cards and activities that use local, familiar examples are one way teachers can seek to do this. Hence, we recommend a pedagogy that involves the combination of instruction, laboratory activities development of mental models and the use of concrete models as suggested by Wu et al. (2001). Our assessment regimes then also must be consistent with such an approach and reward more than a correct numerical answer that reinforces the use of an algorithm to solve chemical problems, and fails to genuinely probe student understanding.

Acknowledgments

This work is partly supported by Institute of Innovation and Development of Learning Process (IL), Center of Excellence for Innovation in Chemistry (PERCH-CIC), the Thailand Research Fund (TRF), Mahidol University Research Grant, and Department of Chemistry, Faculty of Science, Mahidol University.

References

Anderson, J. R. (1995). *Learning and memory: An integrated approach*. New york: Wiley.

Ardac, D., & Akaygun, S. (2004). Effectiveness of multimedia-based instruction that emphasizes molecular representations on students' understanding of chemical change. *Journal of Research in Science Teaching, 41*(4), 317-337.

Beall, H., & Prescott, S. (1994). Concepts and calculations in chemistry teaching and learning. *Journal of Chemical Education, 71*(2), 111-112.

Bowen, C. W. (1998). Item design considerations for computer-based testing of student learning in chemistry. *Journal of Chemical Education, 75*(9), 1172-1174.

Bunce, D. M., Gabel, D. L., & Samuel, K. B. (1991). Enhancing chemistry problem-solving achievement using problem categorization. *Journal of Research in Science Teaching, 28*(6), 505-521.

Çalik, M. (2005). A cross-age study of different perspectives in solution chemistry from junior to senior high school. *International Journal of Science and Mathematics Education, 3*(4), 671–696.

Çalik, M., & Ayas, A. (2005). A cross-age study on the understanding of chemical solution and their components. *International Education Journal, 6*(1), 30-41.

Case, J. M., & Fraser, D. M. (1999). An investigation into chemical engineering students' understanding of the mole and the use of concrete activities to promote conceptual change. *International Journal of Science Education, 21*(12), 1237-1249.

Chandrasegaran, A. L., Treagust, D. F., & Mocerino, M. (2008). An evaluation of a teaching intervention to promote students' ability to use multiple levels of representation when describing and explaining chemical reactions. *Research in Science Education, 38*(2), 237-248.

Chittleborough, G., & Treagust, D. F. (2007). The modelling ability of non-major chemistry students and their understanding of the sub-microscopic level. *Chemistry Education Research and Practice, 8*(3), 274-292.

Chittleborough, G. D., Treagust, D. F., Mamiala, T. L., & Mocerino, M. (2005). Students' perceptions of the role of models in the process of science and in the process of learning. *Research in Science and Technological Education, 23*(2), 195-212.

Coll, R. K. (1999). *Learners' mental models of chemical bonding.* Unpublished dissertation, Curtin University of Technology, Perth, Australia.

Coll, R. K., & Treagust, D. F. (2003a). Investigation of secondary school, undergraduate, and graduate learners' mental models of ionic bonding. *Journal of Research in Science Teaching, 40*(5), 464-486.

Coll, R. K., & Treagust, D. F. (2003b). Learners' mental models of metallic bonding: A cross-age study. *Science Education, 87*(5), 685-707.

Copolo, C. E., & Hounshell, P. B. (1995). Using three-dimensional models to teach molecular structures in high school chemistry. *Journal of Science Education and Technology, 4*(4), 295-305.

Dagher, Z. R. (1994). Does the use of analogies contribute to conceptual change? *Science Education, 78*(6), 601-614.

Dahsah, C., & Coll, R. K. (2007). Thai Grade 10 and 11 students' conceptual understanding and ability to solve stoichiometry problems. *Research in Science and Technological Education, 25*(2), 227-241.

Dahsah, C., & Coll, R. K. (2008). Thai Grade 10 and 11 students' understanding of stoichiometry and related concepts. *International Journal of Science and Mathematics Education, 6*(3), 573-600.

Devetak, I. (2005). *Explaining the latent structure of understanding submicropresentations in science.* Unpublished dissertation, University of Ljubljana, Slovenia.

Devetak, I., Urbančič, M., Wissiak Grm, K. S., Krnel, D., & Glažar, S. A. (2004). Submicroscopic representations as a tool for evaluating students' chemical conceptions. *Acta Chimica Slovenica, 51*, 799-814.

Devetak, I., Vogrinc, J., & Glažar, S. A. (in press). Assessing 16-Year-Old students' understanding of aqueous solution at submicroscopic level. *Research in Science Education*.

Dori, Y. J., & Hameiri, M. (2003). Multidimensional analysis system for quantitative chemistry problems: Symbol, macro, micro, and process aspects. *Journal of Research in Science Teaching, 40*(3), 278-302.

Duit, R. (1991). On the role of analogies and metaphors in learning science. *Science Education, 75*(6), 649-672.

Dunnivant, F. M., Simon, D. M., & Willson, S. (2002). The making of a solution: A simple but poorly understood concept in general chemistry. The Chemical Educator, 7(4), 207-210.

Farnham-Diggory, S. (1994). Paradigms of knowledge and instruction. *Review of Educational Research*. 64(3), 463-477.

Foshay, R., & Kirkley, J. (2003). *Principles for Teaching Problem Solving. Technical Paper* (No. PLATO-TP-4). U.S. Minnesota

Franco, C., & Colinvaux, D. (2000). Grasping mental models. In J. K. Gilbert & C. J. Boulter (Eds.), *Developing models in science education* (pp. 93-118). Dordrecht: Kluwer

Gabel, D. L. (1993). Use of the particle nature of matter in developing conceptual understanding. *Journal of Chemical Education, 70*(3), 193-194.

Gabel, D. L. (1999). Improving teaching and learning through chemistry education research: A look to the future. *Journal of Chemical Education, 76*(4), 548-554.

Gilbert, J. K., Boulter, C. J., & Rutherford, M. (2000). Explanations with models in science education. In J. K. Gilbert & C. J. Boulter (Eds.), *Developing models in science education* (pp. 193-208). Dordrecht: Kluwer.

Gilbert, J. K., Watts, D. M., & Osborne, R. J. (2005). Eliciting student views using an interview-about-instances technique. In J. K. Gilbert (Ed.), *Constructing worlds through science education: The selected works of John K. Gilbert*. London: Routledge.

Gobert, J. D., & Buckley, B. C. (2000). Introduction to model-based teaching and learning in science education. *International Journal of Science Education, 22*(9), 891-894.

Greca, I. M., & Moreira, M. A. (2000). Mental models, conceptual models, and modelling. *International Journal of Science Education, 22*(1), 1-11.

Grosslight, L., Unger, C., Jay, E., & Smith, C. (1991). Understanding models and their use in science: Conceptions of middle and high school students and experts. *Journal of Research in Science Teaching, 28*(9), 799-822.

Harrison, A. G., & Treagust, D. F. (2000). Learning about atoms, molecules, and chemical bonds: A case study of multiple-model use in grade 11 chemistry. *Science Education, 84*(3), 352-381.

Heyworth, R. M. (1999). Procedural and conceptual knowledge of expert and novice students for the solving of a basic problem in chemistry. *International Journal of Science Education, 21*(2), 195-121.

Hinton, M. E., & Nakhleh, M. B. (1999). Students' microscopic, macroscopic, and symbolic representations of chemical reactions. *The Chemical Educator, 4*(4), 1-29.

Johnstone, A. H. (1991). Why is science difficult to learn? Things are seldom what they seem. *Journal of Computer Assisted Learning, 7*, 75-83.

Johnstone, A. H. (1993). The development of chemistry teaching: A changing response to changing demand. *Journal of Chemical Education, 70*(9), 701-705.

Jonassen, D., & Tessmer, M. (1996). An outcome-based taxonomy for instructional systems design, evaluation and research. *Training Research Journal, 2*, 11-46.

Kozma, R. B., & Russell, J. (1997). Multimedia and understanding: Expert and novice responses to different representations of chemical phenomena. *Journal of Research in Science Teaching, 34*(9), 949-968.

Lythcott, J. (1990). Problem solving and requisite knowledge of chemistry. *Journal of Chemical Education, 67*(3), 248-252.

McElroy, L. J. (1996). Teaching dilutions. *Journal of Chemical Education, 73*(8), 765-766.

Mulford, D. R., & Robinson, W. R. (2002). An inventory for alternate conceptions among first-semester general chemistry students. *Journal of Chemical Education, 79*(6), 739-744.

Norman, D. A. (1983). Some observations on mental models. In D. A. Gentner & A. L. Stevens (Eds.), *Mental models* (pp. 7-14). Hillsdale, NJ: Lawrence Erlbaum Associates.

Nurrenbem, S. C., & Pickering, M. (1987). Concept learning versus problem solving: Is there a difference? *Journal of Chemical Education, 64*(6), 508-510.

Pinarbasi, T., & Canpolat, N. (2003). Students' understanding of solution chemistry concepts. *Journal of Chemical Education, 80*(11), 1328-1332.

Pittman, K. M. (1999). Student-generated analogies: Another way of knowing? *Journal of Research in Science Teaching, 36*(1), 1-22.

Raviolo, A. (2001). Assessing students' conceptual understanding of solubility equilibrium. *Journal of Chemical Education, 78*(5), 629-631.

Robinson, W. R. (2003). Chemistry problem-solving: Symbol, macro, micro, and process aspects. *Journal of Chemical Education, 80*(9), 978-982.

Russell, J. W., Kozma, R. B., Jones, T., Wykoff, J., Marx, N., & Davis, J. (1997). Use of simultaneous-synchronized macroscopic, microscopic, and symbolic representations to enhance the teaching and learning of chemical concepts. *Journal of Chemical Education, 74*(3), 330-334.

Savelsbergh, E. R., De Jong, T., & Ferguson-Hessler, M. G. M. (2002). Situational knowledge in physics: The case of electrodynamics. *Journal of Research in Science Teaching, 39*(10), 928-951.

Schmidt, H. J., & Jignéus, C. (2003). Students´ strategies in solving algorithmic stoichiometry problems. *Chemistry Education: Research and Practice, 4*(3), 305-317.

Staver, J. R., & Lumpe, A. T. (1995). Two investigations of students' understanding of the mole concept and its use in problem solving. *Journal of Research in Science Teaching, 32*(2), 177-193.

Tasker, R., & Dalton, R. (2006). Research into practice: Visualisation of the molecular world using animations. *Chemistry Education Research and Practice, 7*(2), 141-159.

Treagust, D. F. (1993). The evolution of an approach for using analogies in teaching and learning science. *Research in Science Education, 23*, 293-301.

Treagust, D. F., Chittleborough, G., & Mamiala, T. L. (2003). The role of submicroscopic and symbolic representations in chemical explanations. *International Journal of Science Education 25*(11), 1353-1368.

Ünal, S., Çalık, M., Ayas, A., & Coll, R. K. (2006). A review of chemical bonding studies: Needs, aims, methods of exploring students' conceptions, general knowledge claims and students' alternative conceptions. *Research in Science and Technological Education, 24*(2), 141-172.

Van Der Veer, C. G., & Del Carmen Puerta Melguizo, M. (2003). Mental models. In J. A. Jacko & A. Sears (Eds.), *The human-computer interaction handbook: Fundamentals, evolving technologies, and emerging applications* (pp. 52-80). Uitgever: Lawrence Erlbaum & Associates.

Venville, G., Bryer, L., & Treagust, D. F. (1994). Training students in the use of analogies to enhance understanding in science. *Australian Science Teachers Journal, 40*(60-68).

Wang, M. R. (2000). An introductory laboratory exercise on solution preparation: A rewarding experience. *Journal of Chemical Education, 77*(2), 249-250.

Wu, H.-K., Krajcik, J. S., & Soloway, E. (2001). Promoting understanding of chemical representations: Students' use of a visualization tool in the classroom. *Journal of Research in Science Teaching, 38*(7), 821-842.

Authors

Ninna Jansoon is a PhD student at Institute for Innovation and Development of Learning Process, Mahidol University, Thailand. She holds a MSc in analytical chemistry from Prince of Songkla University, Thailand. Her research interests include the design and implementation of intervention strategies in chemistry education, especially experimental design for undergraduate students. She is also interested in using a mental model and analogy to develop students' understanding.

Richard K. Coll is associate professor of science education at the University of Waikato, New Zealand. Richard holds a PhD in chemistry from Canterbury University and an EdD in science education from Curtin University of Technology. He worked as a lecturer in chemistry in the Pacific and Caribbean before taking up his appointment at Waikato. Richard is deputy dean of the School of Science & Engineering, Associate Dean (International), and Director of Cooperative Education. Richard is Chief Editor of the Journal of Cooperative Education & Internships and serves or has served on the editorial board of numerous science education periodical including the *International Journal of Science Education*, and the *Journal of Research in Science Teaching*. Richard is guest editor for a special issue of the *International Journal of*

Environmental & Science Education dedicated to scientific literacy, and he has published over 200 peer-reviewed papers and numerous edited books.

Ekasith Somsook is assistant professor of chemistry at Department of Chemistry, Faculty of Science, Mahidol University, Thailand. Ekasith holds a PhD in chemistry from University of Wisconsin-Madison, USA. He is now head of NANOCAST laboratory. His ongoing research projects include the synthesis of new ligands for nanotechnology and catalysis, the determination of NMR-based solution structure of biomolecules, the utilization of biomass for sufficiency economy, and the development of new learning process for science students. **Correspondence:** NANOCAST Laboratory and Center for Alternative Energy, Department of Chemistry and Center of Excellence for Innovation in Chemistry, Faculty of Science, Mahidol University, 272 Rama VI Rd., Rachathewi, Bangkok 10400, Thailand. E-mail: scess@mahidol.ac.th.

Appendix

DA03

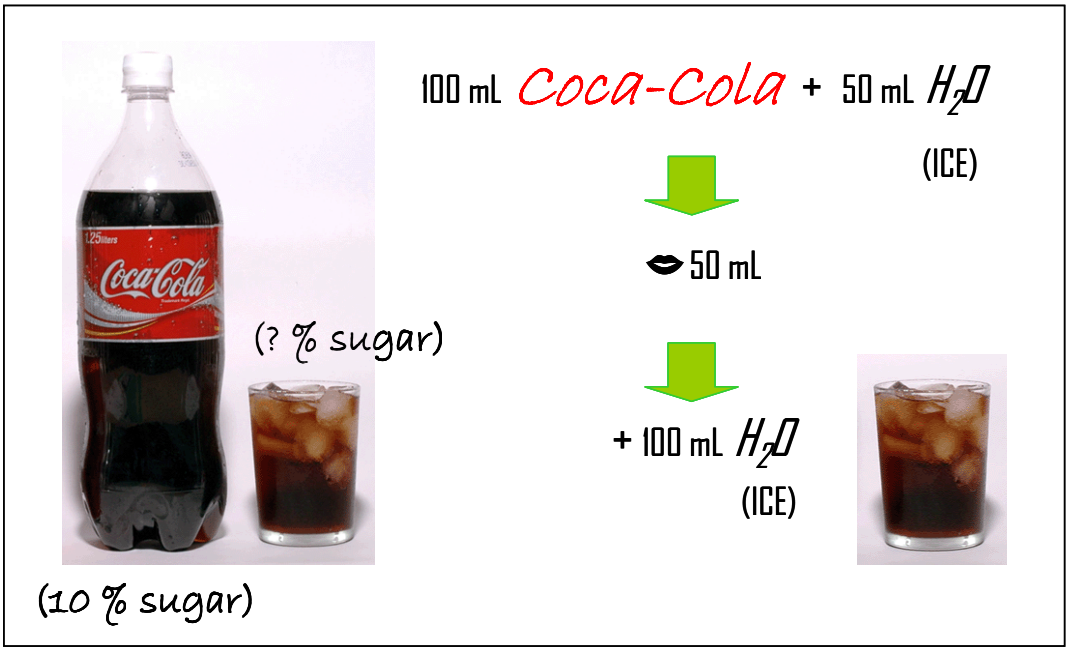

Effect of Ferrocene Moieties on the Copper-Based Atom Transfer Radical Polymerization of Methyl Methacrylate

Atchariya Sunsin, Nuttaporn Wisutsri, Sarisa Suriyarak, Rattapon Teanchai, Sudarat Jindabot, Laksamee Chaicharoenwimolkul, Ekasith Somsook

Nanocast Laboratory and Center for Alternative Energy, Department of Chemistry and Center of Excellence for Innovation in Chemistry, Faculty of Science, Mahidol University, 272 Rama VI Road, Rachathewi, Bangkok 10400, Thailand

Received 8 May 2008; accepted 24 February 2009
DOI 10.1002/app.30354
Published online 14 May 2009 in Wiley InterScience (www.interscience.wiley.com).

ABSTRACT: The atom transfer radical polymerization (ATRP) of methyl methacrylate catalyzed by copper–tripodal complexes with ferrocene moieties (Cu*X*/TRENFcImine, where *X* is Br or Cl, and TRENFcImine is tris-[2-(ferrocenylmethyleneimino)ethyl]amine) was investigated to understand the effect of redox active moieties on the performance of ATRP catalysts. The CuBr/TRENFcImine system was highly active, with 82% conversion in 2 h. However, the polymerization became slower at higher molar ratios of monomer to catalyst. The polydispersity index was broad, and the initiation efficiency was relatively low. On the basis of the conformational analysis, the highly active and less controlled polymerization was probably caused by the electronic effect rather than the steric effect on the ferrocene moieties, which led to the higher and lower values in the activation and deactivation steps, respectively. The polydispersity index was improved by the addition of $CuBr_2$, but this led to slower rates of polymerization. The effect of halide groups on ATRP caused a faster rate in the CuBr/TRENFcImine polymerization system than in the CuCl/TRENFcImine system. The higher molar ratio of monomer to catalyst had no significant effect on the CuCl/TRENFcImine system. Nonetheless, the trace of water in the $CuCl_2{\cdot}2H_2O$ system accelerated the rate of propagation, which led to a higher molecular weight. © 2009 Wiley Periodicals, Inc. J Appl Polym Sci 113: 3766–3773, 2009

Key words: atom transfer radical polymerization (ATRP); catalysts; conformational analysis

INTRODUCTION

Atom transfer radical polymerization (ATRP)[1,2] is one of the controlled/living radical polymerization processes that has grown rapidly in the past decade because of its successful polymerization with controlled molecular weight, well-defined compositions, architectures, and functionalities of polymers.[3–10] In the general process of ATRP (Scheme 1), a radical (R·) and a metal complex at the higher oxidation state ($X{-}M_t^{n+1}$) were generated by the transfer of halogen (X) from an alkyl halide initiator (R—X) to the lower oxidation state of the metal complex (M_t^n). Then, the radical is propagated with the consumption of monomers [with the rate constant of propagation (k_p)], and it is somehow deactivated by reacting with the oxidized complex, transforming into the original active catalyst and an oligomeric alkyl halide. This process repeats itself [with the rate constants of activation (k_{act}) and deactivation (k_{deact})], and the molecular weights of the polymers are controlled in this process to obtain high molecular weights and narrow molecular weight distributions. The ATRP process is involved in the chemical exchange between the metal catalyst active species and the oxidized metal complex deactivated species; therefore, the catalyst (transition metals and ligands) in ATRP plays a crucial role in the catalytic pathway. A successful ATRP requires a fast activation/deactivation equilibrium with a small k_{act} and large k_{deact} to control the polymerization process. A wide variety of transition metal complexes used in ATRP systems, such as copper,[11] iron,[12] nickel,[13] ruthenium,[14] rhenium,[15] molybdenum,[16] and osmium,[17] with suitable ligands, such as multidentate amines, has been reported.

Ligands play a major role in ATRP by tuning the activity of the metal center and solubilizing the metal salts. Examples of highly active ATRP catalysts are a copper(I) bromide system with tetradentate ligands, such as CuBr/*tris*-[2-(*N*,*N*-dimethylamino)ethyl]amine (Me_6TREN)[18] and CuBr/*tris*-(2-pyridylmethyl)amine,[19] which are much more active than the original CuBr/bipyridine system. The ligand structure greatly influences the effectiveness of the catalyst. A linear correlation between the

Correspondence to: E. Somsook (scess@mahidol.ac.th).
Contract grant sponsor: Center of Excellence for Innovation in Chemistry (through the Postgraduate Education and Research Program in Chemistry).
Contract grant sponsor: Thailand Research Fund; contract grant number: TRF-RMU4980050.
Contract grant sponsor: Faculty of Science of Mahidol University.

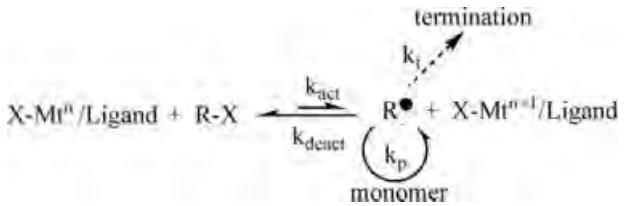

Scheme 1 Transition-metal-catalyzed ATRP.

redox potential of copper complexes and the logarithm of the apparent rate constant of propagation has been reported for ATRP in aqueous media.[20] The performance of more active and stable ATRP catalysts is based on the electron transfer processes.[21] Nevertheless, the redox potential of the metal complex is an important parameter to be considered in the design of new catalysts.

The objective of this study was to modulate the redox potential of the metal center of the ATRP catalyst on the basis of the redox properties of ferrocene moieties to obtain a high reactivity and dynamics for the atom transfer process due to the fast electron transfer process. Tripodals with ferrocene moieties were well characterized in the study of electron communication among ferrocene centers.[22,23] In this study, we studied the effect of the ferrocene moieties on the reactivities of ATRP catalyzed by copper–tripodal complexes.

EXPERIMENTAL

Materials and equipment

Methyl methacrylate (MMA; 99%, Fluka, Steinheim, Germany) was vacuum-distilled before use. (1-Bromoethyl)benzene (97%, Acros, Geel, Belgium), (1-chloroethyl)benzene (97%, Acros, Geel, Belgium), CuBr (97%, Riedel-de Haën, Seelz, Germany), $CuBr_2$ (99%, J. T. Baker Chemical Co., Phillipsburg, NJ), CuCl (98%, Merck, Hohenbrunn, Germany), $CuCl_2{\cdot}2H_2O$ (97%, Fluka), acetonitrile (ACN; analytical-reagent-grade, Lab Scan, Bangkok, Thailand), tetrahydrofuran (THF; analytical-reagent-grade, Lab Scan, Bangkok, Thailand), and diethyl ether (analytical-reagent-grade, Lab Scan, Bangkok, Thailand) were used without purification. The starting materials for the tripodal ligand were as follows: ferrocenecarboxaldehyde (98%, Aldrich, Steinheim, Germany) and *tris*-(2-aminoethyl)-amine (TREN; 98%, Fluka). ^{1}HNMR spectra were collected on a 300-MHz Bruker Avance spectrometer (Rheinstetten, Germany). Electrospray ionization mass spectra were recorded on a Bruker Daltonics Data Analysis 3.3 Esquire-LC mass spectrometer, which was equipped with an electrospray source.

Synthesis of tris-(2-(ferrocenyl methylene amino)ethyl)amine (TRENFcImine)

TRENFcImine was prepared as shown in Scheme 2 with a moderate yield. The synthesis was performed under ambient conditions at room temperature.

The synthetic method was modified from the literature.[22,23] A mixture of TREN (1.00 g, 6.86 mmol) and ferrocenecarboxaldehyde (4.07 g, 19.01 mmol) with a small amount of ACN was mixed and stirred overnight at room temperature. The obtained orange precipitate was filtered, then washed with ACN and then diethyl ether several times to remove impurities, and dried under reduced pressure to yield the tripodal *tris*-imine ligand (3.93 g, 5.35 mmol, 78%).

^{1}HNMR (300 MHz, CD_3OD, δ, ppm): 8.02 [*s*, 3(*H*C=N), 3H], 4.54 [*m*, 3(C_5H_4), 6H], 4.36 [*m*, 3(C_5H_4), 6H], 4.09 [*s*, 3(C_5H_5), 15H], 3.49 [*t*, 3(N—$CH_2C\mathit{H}_2$—), 6H], 2.78 [*t*, 3(N—$C\mathit{H}_2CH_2$—), 6H]. Electrospray ionization mass spectrometry (m/z): 735.3 $[M+H]^+$ (calcd for $C_{39}H_{42}N_4Fe_3$: 734.1).

Polymerization

The polymerization of MMA was carried out under dry argon in a dried Schlenk flask equipped with a magnetic stirring bar. The Schlenk flask was charged with the required amount of ligand and metal halide catalyst, sealed with a rubber septum, and then evacuated and backfilled with argon gas three times. After the MMA monomer was added via a syringe, three freeze–pump–thaw cycles were performed to

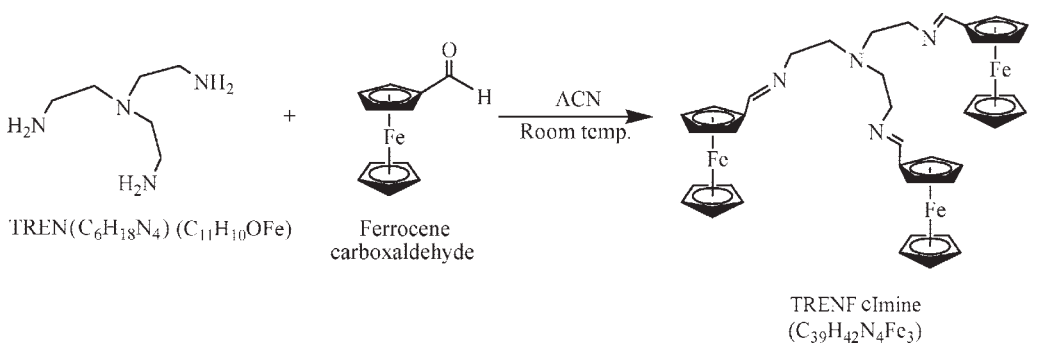

Scheme 2 Synthesis of the tripodal ligand with ferrocene moieties (TRENFcImine).

remove oxygen, and then, degassed solvents were added with an argon-purged syringe. The solution mixture was stirred for 10–15 min at room temperature before we continued to preheat the mixture at the desired temperature with an oil bath and continually stirred it for 10 min; then, an initiator was added to initiate polymerization. After a given time, the reaction was quenched with THF and cooled to room temperature. The obtained polymer solution was passed over an alumina column to remove the remaining catalysts. The polymer product and remaining ligands with THF were removed by evaporation and then washed with an excess amount of methanol. Finally, the final polymer product was dried *in vacuo* and further used for the kinetic studies.

Polymer characterization

We determined the yield percentage of the polymerization gravimetrically by weighing the dried polymer products. The molecular weight and polydispersity index (PDI) values of the polymer products (relative to polystyrene standard calibration) were measured with a Waters 150-CV gel permeation chromatograph (Milford, MA) equipped with PLgel 10-μm mixed B2 columns (molecular weight resolving range = 500–10,000,000) and a refractive-index detector with THF as an eluent at 30°C with a flow rate of 1.0 mL/min.

Conformer search

The model structures of Cu(I)–TRENFc(*cis*-Imine) and Cu(I)–TRENFc(*trans*-Imine) were generated by the Conformer Search Module of CERIUS^2 (version 4.9, Accelrys, San Diego, CA) with the universal force field.[24] The starting structure of each model was randomly generated and minimized by CERIUS^2. The free-rotation torsion angles of each model were randomly varied over 360° in the conformer searching. A total of 200 minimized conformers for each model were obtained and then overlaid on the minimized conformers by CERIUS^2.

RESULTS AND DISCUSSION

Polymerizations of MMA with the tripodal ligand/CuBr catalyst

Multidentate nitrogen-based ligands are the most effective ligands in copper-based ATRP, and Me_6TREN is the best active ATRP ligand among the tripodal ligand architecture.[25] A sterically hindered ligand usually promotes a much slower and less controlled polymerization.[18] Although a ferrocene moiety is bulkier than a methyl group, the redox active properties of ferrocene moieties are expected to facilitate the electron transfer process in ATRP and also to enhance the catalytic activities. The polymerization of MMA catalyzed by CuBr/Me_6TREN in toluene was not very successful with less than 10% initiation,[25] even though controlled polymerization was achieved in a highly polar solvent.[26] In this study, the CuBr/TRENFcImine system was tested in toluene, a common nonpolar solvent for polymerization, for the ATRP of MMA with 1-bromoethyl benzene (PEBr) as an initiator at 90°C (Table I, entries 1–5). No significant amount of polymer was obtained after polymerization with the ligand or CuBr/TRENFcImine system for 35 min at 90°C. Figure 1 shows a kinetic plot of the percentage conversion versus time. The monomer conversion increased with time, and the rate of the reaction was relatively fast (82% conversion within 2 h); this indicated that this catalytic system was highly active. The slower rate of polymerization due to the sterically hindered ligand could be overcome with the facilitation of electron transfer from ferrocene moieties. Figure 2 shows a plot of $\ln([M]_0/[M]_t)$ (where $[M]_0$ is the initial monomer concentration and $[M]_t$ is the monomer concentration at time t) versus time for the homogeneous ATRP of MMA in 60% (v/v) toluene. The linearity of $\ln([M]_0/[M]_t)$ versus time was observed with an observed rate constant (k_{obs}) value of 2.3×10^{-4} s^{-1} [Fig. 2(A)]; this suggested that the polymerization was first-order with respect to the monomer, and the concentration of growing radicals remained constant throughout the reaction.[27] The number-average molecular weight (M_n) from gel permeation chromatography was not observed with a linear increase in M_n versus monomer conversion (as required for living polymerization). This was possibly due to an inefficiency of the initiation step, which was influenced by several factors, including the bond dissociation ability of the R—X initiator, the bond formation ability between the metal catalyst and halide group from the initiator, the bond dissociation ability of the M—X of Cu(II)X/ligand complex, and the solubility of the metal catalyst in the reaction solvent, which leads to the production of active radicals for the growing chains of polymers. The rate of initiation and rate of propagation are usually dependent on the bond dissociation energy of R—X and P_n—X, respectively. If the structures of the initiator and monomer are not similar, a rate of propagation higher than that of initiation might be observed. Therefore, the initiation efficiency might be improved with the use of an initiator with a structure similar to the growing chain of the polymer. All of the M_n results in Table I (entries 1–5) show that M_n increased with monomer conversion and reaction time. A broad molecular weight distribution [weight-average molecular weight/number-average molecular weight (M_w/M_n) = 1.63–2.11] was obtained in the polymerizations of MMA with the condition of [Monomer]/[Initiator]/[Metal catalyst]/[Ligand] = 100 : 1 : 1 : 1 at 90°C.

TABLE I
ATRP of MMA Catalyzed by CuBr/TRENFcImine

Entry	Time (h)	Yield (%)	M_w/M_n	M_n (theo)[d]	M_n (exp)	Initiation efficiency[e]
1[a]	0.33	30.4	2.11	3,231	10,575	0.3
2[a]	1	72.2	1.86	7,418	9,721	0.8
3[a]	2	81.7	1.71	8,369	11,877	0.7
4[a]	3	89.4	1.63	9,138	15,129	0.6
5[a]	4	96.1	2.11	9,804	12,203	0.8
6[b]	1	44.0	1.58	4,589	11,527	0.4
7[b]	2	61.3	1.49	6,326	13,559	0.5
8[b]	3	72.2	1.53	7,417	16,278	0.5
9[b]	4	77.4	1.59	7,937	17,302	0.5
10[b]	5	83.0	1.67	8,496	16,456	0.5
11[c]	1	18.7	1.32	2,056	7,312	0.3
12[c]	2	60.7	1.45	6,264	13,862	0.5
13[c]	3	73.2	1.41	7,515	14,382	0.5
14[c]	4	78.1	1.52	8,005	18,609	0.4
15[c]	8	99.0	1.50	10,095	17,209	0.6

The conditions were as follows: temperature = 90°C; toluene concentration = 60% (v/v); [Monomer]/[Initiator]/[CuBr]/[Ligand] = 100 : 1 : 1 : 1; and $[MMA]_0 = 3.8M$.
[a] No addition of $CuBr_2$.
[b] Addition of 20 mol% $CuBr_2$ with respect to CuBr.
[c] Addition of 40 mol% $CuBr_2$ with respect to CuBr.
[d] M_n (theo) = $[([Monomer]_0/[Initiator]_0) \times \text{Conversion} \times MW_{monomer}] + MW_{initiator}$, where $MW_{monomer}$ is the monomer molecular weight and $MW_{initiator}$ is the initiator molecular weight.
[e] Initiation efficiency = M_n (theo)/M_n (exp).

This was probably due to the faster and slower rates in the activation and deactivation steps, respectively, with the high concentration of active radicals in the system. Therefore, $CuBr_2$ was added as an additive to increase the rate of the deactivation step. In the results shown in Table I (entries 6–10), it is apparent that the addition of $CuBr_2$ led to an improvement in PDI (lower M_w/M_n) with decreasing rate of polymerization. The addition of $CuBr_2$ increased the concentration of Cu(II) species, and then, the concentration of dormant species (R—X) was increased. Therefore, the radical coupling termination was suppressed, and this resulted in lower M_w/M_n values in the range 1.49–1.67 [eqs. (1) and (2)[4] with $K_{eq} = k_{act}/k_{deact}$; cf. Scheme 1 for an explanation of all symbols] and a slower rate of polymerization [$k_{obs} = 1.1 \times 10^{-4}$ s^{-1}; Fig. 2(B)].[18,28] Moreover, this system also performed effectively at the higher concentration of 40 mol % $CuBr_2$ with respect to CuBr (Table I, entries 11–15), which led to the lower M_w/M_n (in the range 1.32–1.52). The comparable rate of polymerization [$k_{obs} = 1.1 \times 10^{-4}$ s^{-1}; Fig. 2(C)] to the 20 mol % system indicated that the rate of propagation in this system was relatively faster than the rate of initiation. However, the addition of $CuBr_2$ did not improve the initiation efficiency because the production of the Cu(II) complex decreased the concentration of the Cu(I) complex for the production of the active radicals in the initial step. The narrow PDI, due to the $CuBr_2$ addition, showed that the TRENFcImine system was an efficient catalytic system for copper-based ATRP, although the initiation efficiency was relatively low:

$$R_p = k_p K_{eq}[M][R—X]([Cu^I]/[X—Cu^{II}]) \quad (1)$$

$$M_w/M_n = 1 + (k_p[R—X]/k_{deact}[X—Cu^{II}])(2/p - 1) \quad (2)$$

where R_p is the rate of polymerization, [M] is the monomer concentration, and p is the monomer conversion.

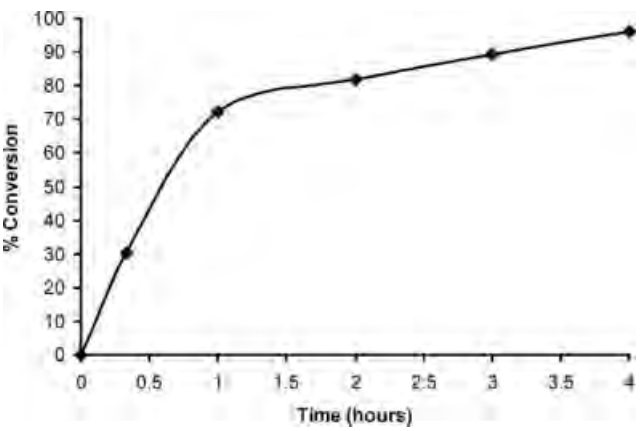

Figure 1 Solution polymerization of MMA catalyzed by CuBr/TRENFcImine with PEBr as the initiator in toluene (60% v/v) at 90°C ([Monomer]/[Initiator]/[CuBr]/[Ligand] = 100 : 1 : 1 : 1).

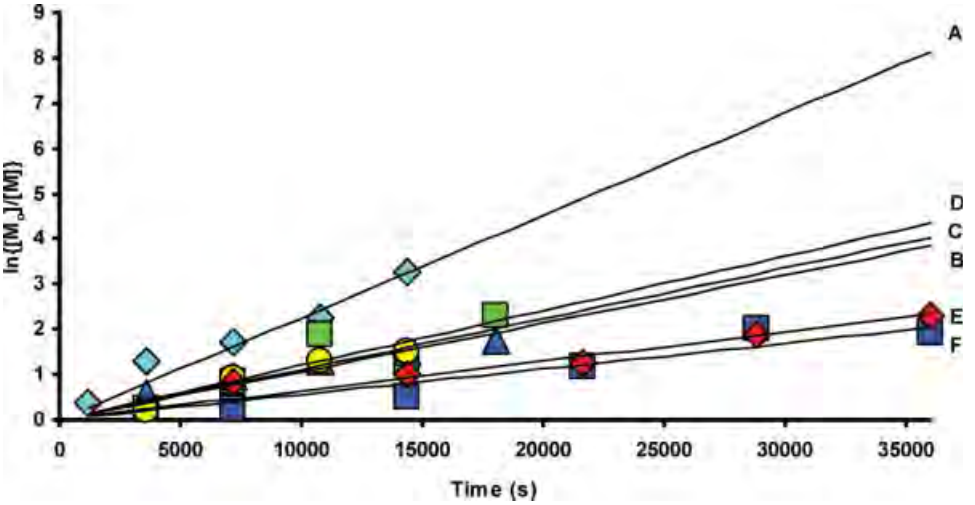

Figure 2 Kinetic plots of $\ln([M]_0/[M]_t)$ versus time for the solution polymerization of MMA catalyzed by CuX/TRENFcImine with PEX as the initiator in toluene (60% v/v) at 90°C with the following monomer/initiator/CuX/ligand molar ratios: (A) 100 : 1 : 1 : 1 ($k_{obs} = 2.3 \times 10^{-4}$ s^{-1}; blue diamonds), (B) 100 : 1 : 1 : 1 with 20% $CuBr_2$ ($k_{obs} = 1.1 \times 10^{-4}$ s^{-1}; blue triangles), (C) 100 : 1 : 1 : 1 with 40% $CuBr_2$ ($k_{obs} = 1.1 \times 10^{-4}$ s^{-1}; yellow circles), and (D) 250 : 1 : 1 : 1 ($k_{obs} = 1.2 \times 10^{-4}$ s^{-1}; green squares) for the CuBr systems and (E) 100 : 1 : 1 : 1 ($k_{obs} = 6.5 \times 10^{-5}$ s^{-1}; blue squares) and (F) 250 : 1 : 1 : 1 ($k_{obs} = 5.7 \times 10^{-5}$ s^{-1}; red diamonds) for the CuCl systems. [Color figure can be viewed in the online issue, which is available at www.interscience.wiley.com.]

Polymerizations of MMA with the tripodal ligand/CuCl catalyst

The effect of halides on the ATRP of MMA was investigated in this study (Table II, entries 1–5). The catalytic activity of CuCl/TRENFcImine was tested for the ATRP of MMA with 1-chloroethyl benzene (PECl) as an initiator at 90°C in toluene. PDI of the CuCl system (Table II, entries 1–5) was slightly similar to that of the CuBr system (Table I, entries 1–5), whereas M_n(exp) of the CuCl system was slightly higher than that of the CuBr system. The lower initiation efficiency was due to the stronger bond of

TABLE II
ATRP of MMA Catalyzed by CuCl/TRENFcImine

Entry	Time (h)	Yield (%)	M_w/M_n	M_n (theo)[d]	M_n (exp)	Initiation efficiency[e]
1[a]	2	23.5	1.88	2,497	13,215	0.2
2[a]	4	39.3	1.68	4,079	14,732	0.3
3[a]	6	69.5	1.74	7,102	15,877	0.4
4[a]	8	86.4	2.26	8,793	21,730	0.4
5[a]	10	85.2	1.85	8,667	39,752	0.2
6[b]	2	27.6	1.65	2,899	20,380	0.1
7[b]	4	35.0	1.56	3,641	22,705	0.2
8[b]	6	85.8	2.20	8,727	20,241	0.4
9[b]	8	75.9	2.26	7,739	39,397	0.2
10[b]	10	80.5	1.95	8,199	24,203	0.3
11[c]	1	35.3	1.92	3,676	46,321	0.1
12[c]	2	44.3	1.95	4,577	47,814	0.1
13[c]	3	59.7	2.00	6,113	32,302	0.2
14[c]	4	84.8	2.03	8,633	62,112	0.1

The conditions were as follows: temperature = 90°C; toluene concentration = 50% (v/v); [Monomer]/[Initiator]/[Metal catalyst]/[Ligand] = 100 : 1 : 1 : 1; and $[MMA]_0$ = 4.7*M*.

[a] No addition of $CuCl_2 \cdot 2H_2O$.

[b] Addition of 2 mol % $CuCl_2 \cdot 2H_2O$ with respect to CuCl.

[c] Addition of 2 mol % $CaCl_2 \cdot 2H_2O$ with respect to CuCl.

[d] M_n (theo) = $[([\text{Monomer}]_0/[\text{Initiator}]_0) \times \text{Conversion} \times MW_{monomer}] + MW_{initiator}$, where $MW_{monomer}$ is the monomer molecular weight and $MW_{initiator}$ is the initiator molecular weight.

[e] Initiation efficiency = M_n (theo)/M_n (exp).

TABLE III
ATRP of MMA Catalyzed by CuBr/TRENFcImine and CuCl/TRENFcImine

Entry	[Monomer] : [Initiator] : [Cu*X*]	Time (h)	Yield (%)	M_w/M_n	M_n (theo)[c]	M_n (exp)	Initiation efficiency[d]
1[a]	100 : 1 : 0.5	0.5	52.8	1.80	5,475	9,317	0.6
2[a]	100 : 1 : 0.5	1	57.2	1.60	5,911	13,045	0.5
3[a]	100 : 1 : 0.5	1.5	60.9	1.94	6,281	8,140	0.8
4[a]	100 : 1 : 0.5	2	78.8	1.74	8,071	15,389	0.5
5[a]	250 : 1 : 0.5	1	46.2	1.55	11,761	33,966	0.3
6[a]	250 : 1 : 0.5	2	53.7	1.58	13,639	20,841	0.7
7[a]	250 : 1 : 0.5	4	65.8	1.56	16,645	30,937	0.5
8[a]	250 : 1 : 0.5	6	67.9	1.39	17,170	29,934	0.6
9[a]	250 : 1 : 0.5	8	50.2	1.56	12,755	24,380	0.5
10[a]	250 : 1 : 0.5	12	47.5	1.62	12,064	23,468	0.5
11[a]	250 : 1 : 1	1	20.7	1.52	5,374	16,745	0.3
12[a]	250 : 1 : 1	2	56.2	1.56	14,242	25,049	0.6
13[a]	250 : 1 : 1	3	84.5	1.60	21,347	28,625	0.7
14[a]	250 : 1 : 1	4	71.1	1.72	17,976	27,434	0.7
15[a]	250 : 1 : 1	5	89.9	1.65	22,690	41,908	0.5
16[b]	250 : 1 : 1	2	57.1	2.11	14,440	36,257	0.4
17[b]	250 : 1 : 1	4	63.9	2.22	16,145	21,809	0.7
18[b]	250 : 1 : 1	6	70.9	2.03	17,894	23,284	0.8
19[b]	250 : 1 : 1	8	84.5	2.15	21,298	26,480	0.8
20[b]	250 : 1 : 1	10	90.1	2.28	22,690	25,533	0.9

[a] The conditions were as follows: temperature = 90°C; toluene concentration = 60% (v/v); initiator = PEBr; [CuBr]/[Ligand] = 1 : 1; and $[MMA]_0 = 3.8M$.
[b] The conditions were as follows: temperature = 90°C; toluene concentration = 50% (v/v); initiator = PECl; [CuCl]/[Ligand] = 1 : 1; and $[MMA]_0 = 4.7M$.
[c] M_n (theo) = $[([Monomer]_0/[Initiator]_0) \times \text{Conversion} \times MW_{monomer}] + MW_{initiator}$, where $MW_{monomer}$ is the monomer molecular weight and $MW_{initiator}$ is the initiator molecular weight.
[d] Initiation efficiency = M_n (theo)/M_n (exp).

the C—Cl of the chloride system compared to the C—Br of the bromide system. The addition of 2 mol % $CuCl_2{\cdot}2H_2O$ with respect to CuCl (Table II, entries 6–10) showed that PDI was not significantly different from that of the CuCl system (Table II, entries 1–5), but the rate of propagation was faster (Table II). This was possibly due to the trace of water from $CuCl_2{\cdot}2H_2O$ to accelerate the rate of propagation, in which the halogen transfer equilibrium was shifted from the dormant to the active species.[27,29] The addition of a salt with hydrated water, such as in $CaCl_2{\cdot}2H_2O$ (Table II, entries 11–14), also accelerated the rate of propagation with a k_{obs} of 1.0×10^{-4} s^{-1}, which led to higher molecular weight polymers to support the acceleration rate by a trace of water.

Effects of the monomer-to-catalyst ratio on ATRP

The comparison of the ATRPs of MMA at molar ratios of monomer to catalyst of 100 : 1, 100 : 0.5, 250 : 1, and 250 : 0.5 was studied, and the results are shown in Table III. These led us to determine the catalyst position in the atom transfer equilibrium and the dynamics of exchange between the dormant and active species in the ATRP process.[27] Also, the catalytic activity at the higher ratio of monomer to catalyst indicated the efficiency of the catalytic system. One of the disadvantages of ATRP is the large amount of catalyst that is commonly required to achieve polymerization control. This causes additional cost for the amount of metal catalysts that are used in the polymerization. Moreover, the metal residues in the final products can be a limitation for industrial applications. Table III shows the solution polymerization under the conditions of the CuBr and CuCl systems with different molar ratios of monomer to catalyst. The CuBr systems (Table III, entries 1–15) showed that the optimum conditions with a 250 : 1 : 0.5 molar ratio of monomer to initiator to catalyst were good controlled polymerization conditions. The 250 : 1 molar ratio of monomer to catalyst indicated that the rate of polymerization [$k_{obs} = 1.2 \times 10^{-4}$ s^{-1}, Fig. 2(D)] slowed and the PDI was narrower. This was probably because the rate of ATRP, M_n, and PDI were dependent on the concentration of the Cu(I) complex catalyst, as shown in eqs. (1) and (3).[30] Increasing the molar ratio of monomer to catalyst led to a lower concentration of catalysts and a slower rate of polymerization. The CuCl systems (Table III, entries 16–20) with a 250 : 1 molar ratio of monomer to catalyst showed slightly broader PDIs with higher efficiencies in the

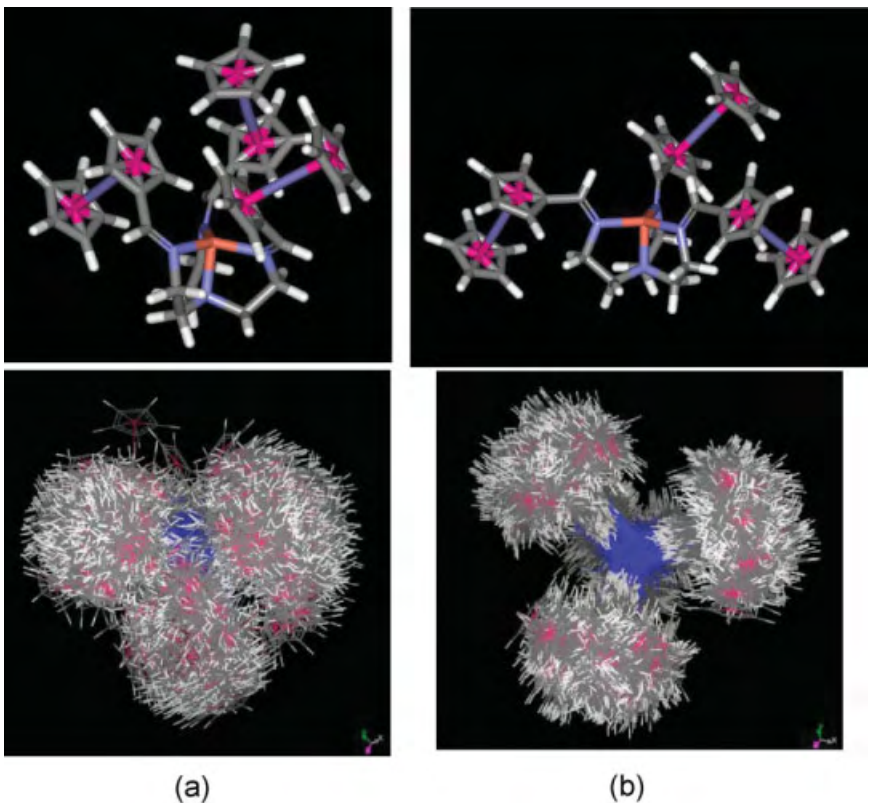

Figure 3 Model structures and overlay minimized conformers generated with the conformer search module in Cerius[2]: (a) Cu(I)–TREN(*cis*-FcImine) and (b) Cu(I)–TREN(*trans*-FcImine). The cis and trans configurations were assigned with respect to the copper center. [Color figure can be viewed in the online issue, which is available at www.interscience.wiley.com.]

initiation step than the CuBr systems (Table III, entries 11–15):

$$M_w/M_n = 1 + (2/k_{act}[Cu^I]t) \quad (3)$$

Conformer search studies of the copper–tripodal complexes

The conformational search was carried out by CERIUS[2] with a universal force field to study the steric effect of the Cu(I)–tripodal complexes: Cu(I)–TREN (*cis*-FcImine) and Cu(I)–TREN(*trans*-FcImine). The cis and trans configurations were assigned relatively to the copper center. The structures and the overlay minimized structures of the two models are shown in Figure 3. According to the universal force field on CERIUS[2], the trans model had a lower energy than the cis model. Therefore, the TRENFcImine ligand must have adopted a trans configuration with distortion from tetrahedral geometry. Moreover, it was obvious from the overlay structures that the *trans*-FcImine model had a pore structure for the incoming ligand to enter the copper center with less steric interactions on the ferrocene moieties than in the *cis*-FcImine model. The restricted rotation of the C=N imine functional groups relieved the steric interactions from the bulky ferrocene moieties for the incoming ligand. Here, we propose that the less controlled polymerization catalyzed by Cu(I)–TRENFcImine may not have been governed by the steric effect on the ferrocene moieties. In contrast, the electronic effect resulting from the redox active on the ferrocene moieties in the induction of the copper center to bind halides tightly might have been more pronounced in the explanation of the slower rate of the deactivation step. An investigation of the electronic effect of the ferrocene moieties on the ATRP is in progress.

CONCLUSIONS

Copper–tripodal complexes with ferrocene moieties (Cu*X*/TRENFcImine, where *X* is Br or Cl) were used in the ATRP of MMA. The high activity of the catalysts was probably due to the facilitation of the electron transfer process of the ferrocene moieties. However, this led to a broader PDI, which was improved effectively with the addition of $CuBr_2$ to the bromide system. The CuBr/TRENFcImine

system was more active than the CuCl/TRENFcImine system. Slight changes in the rate of polymerization and PDI of the CuCl/TRENFcImine were observed with increasing molar ratio of monomer to catalyst and with the addition of $CuCl_2 \cdot 2H_2O$. The trace of water in $CuCl_2 \cdot 2H_2O$ accelerated the rate of propagation, which led to a higher molecular weight.

References

1. Wang, J. S.; Matyjaszewski, K. J Am Chem Soc 1995, 117, 5614.
2. Kato, M.; Kamigaito, M.; Sawamoto, M.; Higashimura, T. Macromolecules 1995, 28, 1721.
3. Pintauer, T.; Matyjaszewski, K. Coord Chem Rev 2005, 249, 1155.
4. Tang, H. D.; Arulsamy, N.; Radosz, M.; Shen, Y. Q.; Tsarevsky, N. V.; Braunecker, W. A.; Tang, W.; Matyjaszewski, K. J Am Chem Soc 2006, 128, 16277.
5. Tsarevsky, N. V.; Matyjaszewski, K. Chem Rev 2007, 107, 2270.
6. Matyjaszewski, K.; Xia, J. Chem Rev 2001, 101, 2921.
7. Patten, T. E.; Matyjaszewski, K. Acc Chem Res 1999, 32, 895.
8. Braunecker, W. A.; Matyjaszewski, K. Prog Polym Sci 2007, 32, 93.
9. Braunecker, W. A.; Pintauer, T.; Tsarevsky, N. V.; Kickelbick, G.; Matyjaszewski, K. J Organomet Chem 2005, 690, 916.
10. Braunecker, W. A.; Brown, W. C.; Morelli, B. C.; Tang, W.; Poli, R.; Matyjaszewski, K. Macromolecules 2007, 40, 8576.
11. Goodwin, J. M.; Olmstead, M. M.; Patten, T. E. J Am Chem Soc 2004, 126, 14352.
12. O'Reilly, R. K.; Gibson, V. C.; White, A. J. P.; Williams, D. J. J Am Chem Soc 2003, 125, 8450.
13. Shao, Q.; Sun, H.; Pang, X.; Shen, Q. Eur Polym J 2004, 40, 97.
14. Kamigaito, M.; Watanabe, Y.; Ando, T.; Sawamoto, M. J Am Chem Soc 2002, 124, 9994.
15. Kotani, Y.; Kamigaito, M.; Sawamoto, M. Macromolecules 1999, 32, 2420.
16. Maria, S.; Stoffelbach, F.; Mata, J.; Daran, J. C.; Richard, P.; Poli, R. J Am Chem Soc 2005, 127, 5946.
17. Braunecker, W. A.; Itami, Y.; Matyjaszewski, K. Macromolecules 2005, 38, 9402.
18. Inoue, Y.; Matyjaszewski, K. Macromolecules 2004, 37, 4014.
19. Xia, J. H.; Matyjaszewski, K. Macromolecules 1999, 32, 2434.
20. Coullerez, G.; Carlmark, A.; Malmstrom, E.; Jonsson, M. J Phys Chem A 2004, 108, 7129.
21. Tsarevsky, N. V.; Braunecker, W. A.; Matyjaszewski, K. J Organomet Chem 2007, 692, 3212.
22. Bullita, E.; Casellato, U.; Ossola, F.; Tomasin, P.; Vigato, P. A.; Russo, U. Inorg Chim Acta 1999, 287, 117.
23. Heitzmann, M.; Moutet, J. C.; Pecaut, J.; Reynes, O.; Royal, G.; Saint-Aman, E.; Serratrice, G. Eur J Inorg Chem 2003, 20, 3767.
24. Rappe, A. K.; Casewit, C. J.; Colwell, K. S.; Goddard, W. A.; Skiff, W. M. J Am Chem Soc 1992, 114, 10024.
25. Queffelec, J.; Gaynor, S. G.; Matyjaszewski, K. Macromolecules 2000, 33, 8629.
26. Miura, Y.; Satoh, T.; Narumi, A.; Nichizawa, O.; Okamoto, Y.; Kakuchi, T. Macromolecules 2005, 38, 1041.
27. Ibrahim, K.; Yliheikkila, K.; Abu-Surrah, A.; Lofgren, B.; Lappalainen, K.; Leskela, M.; Repo, T.; Seppala, J. Eur Polym J 2004, 40, 1095.
28. Matyjaszewski, K.; Davis, T. P. Handbook of Radical Polymerization; Wiley: Hoboken, NJ, 2002.
29. Chatterjee, U.; Jewrajka, S. K.; Mandal, B. M. Polymer 2005, 46, 1575.
30. Nanda, A. K.; Matyjaszewski, K. Macromolecules 2003, 36, 599.

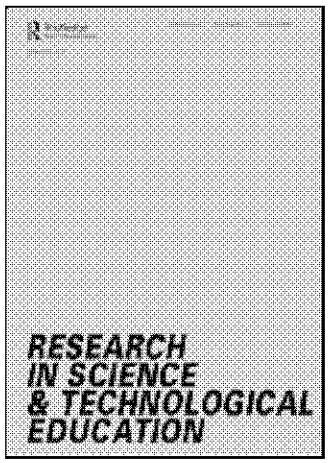

Research in Science & Technological Education
Publication details, including instructions for authors and subscription information:
http://www.informaworld.com/smpp/title~content=t713444901

Enhancing Thai students' learning of chemical kinetics

Sanoe Chairam [a]; Ekasith Somsook [b]; Richard K. Coll [c]
[a] Institute for Innovation and Development of Learning Process, Mahidol University, Bangkok, Thailand [b] Department of Chemistry, Faculty of Science, Mahidol University, Bangkok, Thailand [c] Centre for Science and Technology Education Research, University of Waikato, Hamilton, New Zealand

Online Publication Date: 01 April 2009

To cite this Article Chairam, Sanoe, Somsook, Ekasith and Coll, Richard K.(2009)'Enhancing Thai students' learning of chemical kinetics',Research in Science & Technological Education,27:1,95 — 115
To link to this Article: DOI: 10.1080/02635140802658933
URL: http://dx.doi.org/10.1080/02635140802658933

Research in Science & Technological Education
Vol. 27, No. 1, April 2009, 95 115

Routledge
Taylor & Francis Group

Enhancing Thai students' learning of chemical kinetics

Sanoe Chairam[a], Ekasith Somsook[b] and Richard K. Coll[c]*

[a]*Institute for Innovation and Development of Learning Process, Mahidol University, Rachathewi, Bangkok, Thailand;* [b]*Department of Chemistry, Faculty of Science, Mahidol University, Rachathewi, Bangkok, Thailand;* [c]*Centre for Science and Technology Education Research, University of Waikato, Hamilton, New Zealand*

Chemical kinetics is an extremely important concept for introductory chemistry courses. The literature suggests that instruction in chemical kinetics is often teacher-dominated at both the secondary school and tertiary levels, and this is the case in Thailand – the educational context for this inquiry. The work reported here seeks to shift students from passive learning to more active, student-centred learning and involved some 413 first year undergraduate science students in Thailand. Drawing on inquiry-based learning, the participants were asked to design an experiment investigating the reaction of acids and bases. The research findings suggest that participants were able to explain the changes of the rate of a chemical reaction, and developed good conceptual understanding of chemical kinetics both qualitatively and quantitatively. It also showed this more active teaching approach, which is radically different from normal teaching in Thailand, was an enjoyable experience for the students.

Keywords: chemical kinetics; inquiry-based practical chemistry; tertiary level

Teaching and learning chemical kinetics

Chemical kinetics is an extremely important concept for introductory chemistry courses. However, rather surprisingly Justi and Gilbert (1999a) commented that there is a paucity of research about chemical kinetics teaching and learning at both the secondary and higher educational levels. Chemical kinetics essentially seeks to provide insights into questions such as: how fast do chemical reactions go and what factors influence the rate of a chemical reaction? The science education literature suggests the teaching and learning of much physical chemistry – including chemical kinetics – is teacher-dominated in approach at both the secondary school and tertiary levels (see Choi and Wong 2004; Justi 2003; Parkash and Kumar 1999). In general, the teaching of chemical kinetics at the secondary school level emphasizes qualitative aspects. So science teachers typically introduce students to an understanding of the rate of reaction for different examples, and discuss how to investigate the influence of variables such as temperature, concentration, and a catalyst on the rate of a reaction. At this level, the concepts of rate determining step, rate equation and order of reaction are first introduced. Parkash and Kumar (1999) reported on experiments about chemical kinetics involving gaseous carbon dioxide formed from the reaction between ethanoic acid and sodium hydrogen carbonate at different time intervals. Such

*Corresponding author. Email: r.coll@waikato.ac.nz

ISSN 0263-5143 print/ISSN 1470-1138 online

DOI: 10.1080/02635140802658933
http://www.informaworld.com

experiments are used to illustrate to students the dependence of the rate of a reaction on the concentration of the reactants, and how to determine the order of a reaction with respect to each reactant, the overall order of a reaction, the rate constant of a reaction, and the half-life. Recently, Choi and Wong (2004) investigated student understanding of experiments demonstrating first-order kinetics involving the application of a data-logger (a computer interfaced to one or more sensors). The major advantage of the use of a datalogger, they argued, is that students can in real time monitor a number of variables simultaneously (e.g. temperature, electric current, electric potential, pressure, and pH), helping them see how such variables influence the rate of a reaction, and leading to better understanding of qualitative aspects of kinetics. However, such experiments are expensive to set up, and so are not always suitable for educational contexts for which there is limited access to sophisticated electronic instruments.

At the university level, as might be expected, the kinetics concepts taught are more complex than at the secondary school level. Chemical kinetics is reported to be difficult for university students to comprehend; mostly because at this level it generally involves more complex mathematics as well as qualitative explanations for both rate equations and variables that affect the rate of a reaction (Justi 2003). Here, the researchers propose that knowledge active learning which involves students doing practical experiments in the laboratory, rather than relying purely on classroom teaching, may help them to understand complex chemistry concepts, including chemical kinetics.

The importance of practical work in learning chemistry

A review of educational research suggests that the laboratory has been given a central and distinctive role in science education, and many science educators claim rich learning benefits accrue when using laboratory activities as part of pedagogy. Laboratory activities can be seen as a means of allowing learners to pursue learning, having a variety of multisensory experiences (see Lazarowitz and Tamir 1994).

Practical work is nowadays an important part of the science curriculum in many countries, including the USA, and in Europe, particularly the UK, at both the secondary and tertiary levels (Hegarty-Hazel 1990; Wellington 1998; Woolnough 1991). Science education and the practical teaching of science within universities were argued for in the mid-nineteenth century. In the 1960s, the teaching in laboratory classes was much criticized, and eventually practical work began to be taught to students using scientific problems. This signalled the beginning of practical work in school science (Wellington 1998; Woolnough 1991).

A number of activities come under the umbrella term 'practical work' in science education. Woolnough (1991) referred to practical work as 'typical laboratory work' where students encounter ideas and principles at first hand, i.e. they engage in 'hands-on' science. Similarly, Hegarty-Hazel (1990) defined student laboratory work as a form of practical work taking place in a purposely assigned environment where students engage in planned learning experiences, and interact with materials to observe and understand the phenomena. However, based on these sorts of definitions, the typical school laboratory is not a laboratory at all, because according to Ogborn (1977), students may attend practical classes, but instead of actually being engaged in hands-on work, they may instead watch teacher demonstrations.

In summary, overall, in spite of some reservations, laboratory work is now accepted by many authors as a key part of science education, and the science laboratory is

thought to take a central role in the teaching and learning of science (Nakhleh, Polles, and Malina 2002). This enhancement of learning may be by way of encouragement of students' interest, engaging them with experiences of concepts and developing their practical science abilities (Hofstein and Lunetta 1982, 2004). However, Nakhleh, Polles, and Malina (2002) suggested that an enabling factor is for teachers and students to have a clear understanding of the aims and purposes of chemistry practical classes.

Aims and purposes of chemistry practical classes

Although laboratory classes are more popular with students than lectures at both school and university; probably because students are introduced to new apparatus and scientific equipment (Hofstein and Lunetta 1982, 2004; Hofstein, Shore, and Kipnis 2004; Wellington 1998; Woolnough 1991), the value of the laboratory classroom as a learning environment is heavily dependent on the purpose of the classes and the curriculum materials used (Hegarty-Hazel 1990).

Hart et al. (2000) suggested that there are clear differences between the terms 'purpose' and 'aim' with respect to laboratory work. In their view, the purpose refers to the teachers' pedagogical intentions, i.e. the teachers' reasons for using a particular laboratory activity when the teachers decide to use it, with a particular class, and at a particular time. In contrast, the aim refers to the specific science learning outcomes intended for the activity. For example, the aim might reasonably be something that determines what is done in the activity itself, but the purpose is about how this activity is intended to result in learning, and how and why the activity links with the whole science experience. Tamir (1991) said that there are five reasons used to rationalize using the laboratory in science teaching. First, science involves complex and abstract subject matters. As a consequence, many students may fail to understand the concepts without the assistance and opportunities for carrying out activities in the laboratory. Second, student perceptions of actual investigations are an essential component of learning science as inquiry. Practical work allows students opportunities to act like a real scientist, to develop scientific attitudes such as honesty and critical assessment of results. Third, practical work experiences are essential for the development of specific student skills and strategies. Fourth, practical work is important for the identification, diagnosis and remediation of student alternative conceptions. Finally, practical work helps students enjoy activities and become interested in science.

Chemistry practical classes in higher education

As might be expected, the literature suggests that science learning in the laboratory at the undergraduate level is more difficult than at secondary school. Practical classes seldom make much connection between the laboratory work and lecture (Laws 1996), with practical classes often being treated as a 'separate component' of the whole learning experince.

There are three main aims of laboratory classes in higher education. First, that students can learn the basic practical skills of laboratory work – either from teacher demonstrations or by engaging in practical experiments (Ogborn 1977). Second, the practical class is used as a way of demonstrating to students concepts dealt with in the lectures, and indeed according to some authors this is the most valuable benefit of practical work (see Millar 1998). Finally, arguably the most important rationale for

laboratory courses is that students are provided with opportunities to do science as scientists do (Wellington 1998; Woolnough 1991), helping them to develop into scientists as a result of their higher educational training.

Some authors suggest that students can learn much more than just practical science skills in the laboratory, and they come to understand science and how science works by being engaged in doing science themselves, in hypothesizing, planning, designing, carrying out and interpreting their own experiments in the laboratory (Wellington 1998; Woolnough 1991). However, Hegarty-Hazel (1990) argued that undergraduate laboratory classes sometimes provide good learning situations – but that all too often they do not. She speculated that much difficulty in learning from laboratory work is due to a lack of 'coping skills' on the part of the teacher. She suggested that the many hours science undergraduates spend in the laboratory could be differentiated into learning skills and science concepts. In order for students to learn practical skills, different experimental approaches are needed, practical activities that are authentic in nature (i.e. like real science), in which students do things in a way more like that of scientists. A key part of this is for the laboratory to be a place where students can develop problem-solving skills (Gabel and Bunce 1994).

The nature of chemistry practical classes

The literature suggests that many science practical classes, at the school and higher educational levels, follow a 'cookbook' style, in which students are presented with aims, hypotheses, and detailed steps for carrying out the experiment. In laboratory instruction manuals, the cookbook approach is one of using the laboratory simply, with students following a detailed, pre-set laboratory procedure when conducting experiments. Students may, or may not, learn something about the way scientists do things in such circumstances. It is argued that this approach is not only an ineffective means of developing student understanding of science concepts, but also presents a misleading way of how scientists develop scientific knowledge (Lazarowitz and Tamir 1994).

Inquiry-based approaches to chemistry learning

Many authors now believe that for practical work at school or in higher education to be of real value it needs to involve inquiry-based learning. The literature suggests that students are able to understand the nature of scientific inquiry well only by engaging in inquiry themselves (see, for example, Hegarty-Hazel 1990; Klopfer 1990). The *National science education standards* (National Research Council [NRC] 1996) suggest that students can develop their understanding of scientific knowledge when they learn about the nature of science via inquiry-based practical classes in the laboratory (McComas, Clough, and Almazroa 1998).

The standards produced by the NRC (1996) define inquiry as:

> A multifaceted activity that involves making observations, posing questions, examining books and other sources of information to see what is already known, planning investigations, reviewing what is already known in the light of experimental evidence, using tools to gather, analyze and interpret data, proposing answers, explanations and predictions, and communicating the results. Inquiry requires the identification of assumptions, use of critical and logical thinking, and consideration of alternative explanations. (p. 23)

Students' knowledge about scientific inquiry and the nature of science does not occur automatically once they are placed in a laboratory. Students do not develop an understanding simply through experiencing inquiry, so students need to learn from their experiences in the laboratory (Schwartz, Lederman, and Crawford 2004). Hofstein and Walberg (1995) argued that in inquiry-based practical classes, students should be involved in the process of scientific inquiry – seeking an understanding of science phenomena, and that this process should be integrated with other complementary activities, such as the development of scientific concepts, related scientific skills and experiences. Hofstein and Lunetta (2004) likewise suggested that laboratory activities offer important experiences in science teaching and learning; further commenting that teachers should provide students with experiences in methods of scientific inquiry and reasoning, and in the application of scientific knowledge related to everyday life. Nowadays, many authors in the science education field believe that inquiry lies at the heart of good science teaching. Inquiry is seen as the way that students can learn about their environment, since the world is constantly being influenced by scientific and technological advances (NRC 2000).

Theoretical basis for the inquiry: social constructivism

The purpose of this study was to find ways to shift students from passive learning to active learning, and to develop more student-centred pedagogies. Probably the most common current theoretical approach to student-centred learning is based on constructivist views of learning, and a constructivist perspective has some implications for teaching and learning in school science laboratories. The key idea of constructivism that sets it apart from other theories of cognition is that knowledge cannot be transmitted directly from one knower to another, but learners have to actively construct their own knowledge rather than receive preformed information transmitted by others (Driver et al. 1994). Hence, under constructivism, teaching becomes a matter of creating situations in which students can actively participate in activities that enable them to make their own individual constructions (Duit and Treagust 1995; Tobin and Tippins 1993). Teaching can stimulate learners to find explanations for events and give them an insight into the nature of scientific inquiry and their own investigative work. A further key element of constructivism is the importance of prior knowledge and experiences on students' construction of knowledge. Because of the influence of direct everyday experiences, learners may explain events in different ways in different situations (e.g. between school and 'real life') and social settings. Knowledge then is not only *personally constructed* for learners through their own experiences, but also *socially mediated* (Tobin and Tippins 1993). This is usually termed *social constructivism*, and holds that personal constructivism is limited since humans are social beings, and any knowledge creation is influenced by the prior experiences and the social environment of the learners (Duit and Treagust 1998). Tobin and Tippins (1993) commented that 'the individual and social components [are] parts of a dialectical relationship where knowing is always seen dualistically as both individual and social, never one alone, but always both' (p. 20). Social constructivists thus believe that an important part of construction is the social interaction through which learners come to a common understanding of knowledge, including scientific concepts (Hodson and Hodson 1998). Language is a key tool in learning and one that facilitates communication between learners in society. It is important in science education to appreciate that, in nature, scientific knowledge is both symbolic and also socially negotiated (see Vygotsky 1978).

Research objective and research questions for the inquiry

In this study, the researchers developed an inquiry-based experiment for chemical kinetics, that incorporated the use of the *prediction–observation–explanation* (POE) sequence. We sought first to investigate what actually happened on this chemistry laboratory course at one Thai university involving first year undergraduate chemistry students. The general purpose of the practical class reported in this work is to enhance student understanding of kinetics by means of inquiry-based practical classes.

The research questions for this inquiry were as follows:

(1) Can an inquiry-based chemistry practical class enhance Thai students' learning of chemical kinetics?
(2) If so, how does an inquiry-based approach to chemistry practical classes enhance Thai students' conceptual understanding of chemical kinetics?
(3) Do Thai students enjoy an inquiry-based practical class more than their normal practical classes?

Background of Thai education: moving towards learner-centred education

Education has always been regarded as an important means for national development in Thailand, and it has been controlled by the government through a number of planning instruments (Office of National Education 1997). In Thailand, the Ministry of Education (MOE) is responsible for the provision of basic education nationwide (Office of the Prime Minister 2000), and the importance of science and technology is widely accepted nationally. Based on the 1960 National Curricula in Thailand, emphasis is placed on programmes which facilitate further advancement in scientific and technological fields and encourage various socio-economic changes with the country's transition from an agricultural to an agricultural-industrialized nation state (Rivera 2003).

In past decades, a teacher-centred approach played an important role in the educational system in Thailand. Science teachers in Thai education often concentrated on teaching theories rather than developing practical skills. Similarly, most chemistry practical classes in Thai universities are traditional in teaching approach, meaning they are teacher-dominated and that practical classes follow a cookbook style. In an effort to change from a teacher-centred approach to learning, there is currently discussion in Thailand as how to change the teaching and learning approaches and strategies in order to facilitate the acquisition of the new types of knowledge. So, the national curriculum, which is now regarded as the educational standard, states that *at any level of education*, teaching–learning activities must emphasize 'learning to think, to do and to solve problems' (Pravalpruk 1999, 76). The Institute for the Promotion of Teaching Science and Technology (IPST) plays an important role in the teaching of science in Thailand. Nowadays, the IPST has incorporated the inquiry approach in science curricula, and emphasizes an inquiry-based teaching and learning process (MOE 1996).

Methods and design

Research design

The research reported here is a case study conducted within an interpretive paradigm as described by Merriam (1988). Consistent with a case study approach, the inquiry

employed a variety of data collection tools, including quantitative and qualitative instruments of inquiry as described below.

(1) Development of student-centred laboratory experiments based on the use of a framework presented by Hofstein and Walberg (1995).
(2) Investigation of the pedagogies employed in the laboratory class through observation of the experiment used in the teaching laboratory.
(3) Evaluation of student views about this new experiment through a purpose designed questionnaire, face-to-face interviews, and content analysis of relevant documentation.

Before describing the above instruments, we first outline the nature of the new practical classes developed in this inquiry.

Development of an inquiry-based, student-centred, chemistry practical class

A new experimental design was developed for this inquiry, and this sought to develop student-centred learning processes based on inquiry-based learning. A key feature was a need to move students from passive to active learning. White and Gunstone (1992) proposed that the POE technique is a strongly learner-centred strategy that arouses student curiosity, and this was adopted as part of this inquiry. The practical classes focused on the concept of chemical kinetics in practical chemistry classes using four POE tasks. In a whole-class setting, students were asked to *predict* the results of some events and justify the reasons used to support their prediction. Next, students were asked to describe what they *observed* when a reaction occurs while doing the experiment – students were asked to write down their observations. Lastly, they were required to *explain* any conflict between what they predicted and observed. Here we used the POE activities to develop and practice a student-centred approach in this laboratory class in combination with other techniques, such as small-group learning (Billson 1986; Brown 1989; Johnson and Johnson 2005; Webb 1982) and negotiation involving argumentation (Pinnell 1984) (see Figure 1).

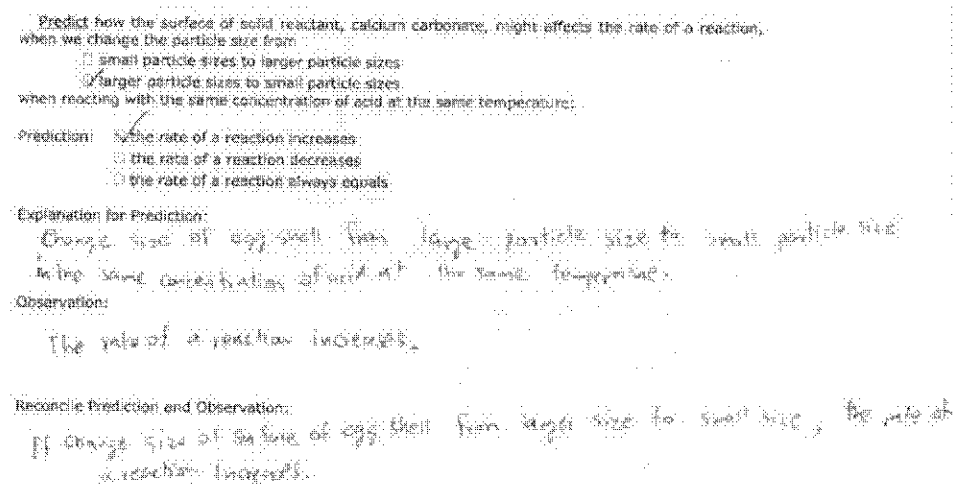

Figure 1. POE activity for chemical kinetics as used in the study.

This sort of experiment tends to be more 'open' in nature, and the intention was that the students would be doing things in a way more like scientists. That is, the students had to design the experimental procedure themselves, and this was intended to help them gain an understanding of the process of scientific inquiry.

In summary, in these practical chemistry classes the learning consisted of students developing the methodology to investigate the influence of some variables on rates of reaction, and specifically to use the POE strategy in small groups to predict and think about the expected results and write them down on answer sheets. Their ideas were discussed in small groups. During classes they completed four POE tasks in the form of paper-based drawings on sheets provided. Finally, students in each group reported their prediction, observations and explanations about the chemical kinetics in a whole-class setting.

Sample description

This study involved 413 first year undergraduate science students (age range 18–19 years) from the Faculty of Science, Mahidol University, Bangkok, Thailand. These students enrolled in a general chemistry laboratory course in the first semester. The course comprises 12 practical classes in which the chemical kinetics of acid–base reactions is one session. In general, the laboratory classes consist of practical experiments that complement the lecture material and the lectures are delivered before the related experiment. The practical classes overall try to teach basic practical chemistry techniques, including the use of pipette and burette, preparation of solutions, and redox chemistry. All of the students in classes here were familiar with cooperative group work and POE tasks, and completed the experiment in a three hour period. Here, for the student interactions small groups of four to five students were used, as recommended in the literature (Kaartinen and Kumpulainen 2002).

Data collection

The researchers began by collecting and conducting an in-depth analysis of materials produced in the laboratory when the students engaged in the POE inquiry-based learning practical classes mentioned above. Most of the groups of students completed their laboratory documentation in Thai, but some completed their documentation in English (many Thai students are bilingual in Thai and English). These reports, along with notes from observations of the practical classes, formed the data corpus used to judge students' conceptual understanding of chemical kinetics, and of inquiry. It is important to note that such teaching is radically different for undergraduate science students in Thailand. The students then completed a questionnaire that sought their views on their experiences of doing these new practical classes. Of the class of 413 students (age range 18–19 years), some 389 students, 129 male and 260 female, completed the questionnaire. Students' responses about their enjoyment of the experiment used a Likert scale (SD = strongly disagree, D = disagree, N = neutral, A = agree and SA = strongly agree) (Merriam 1988). A selection of students were interviewed in pairs in order to ascertain their views on the 'new' practical classes in more depth. Interviews were audiotaped and transcribed. Any translations were checked for veracity by independent bilingual advisors. Claims also supported the findings from interviews after completing the experiment.

Research findings

The students were required to conduct an experiment in which they tried to examine aspects of reaction kinetics for the reaction between eggshells (mostly calcium carbonate) and two acids (hydrochloric acid and vinegar). The research findings for this inquiry are summarized under themes that emerged from the data: student laboratory activities; student conceptual understanding of chemical kinetics; and the role of the teacher. These themes are now described in turn.

Student understanding of scientific inquiry

Scientists generally follow a number of logical steps when they attempt to solve problems such as that posed to the participants in this inquiry; in what is often termed 'the scientific method' (see Carin, Bass, and Contant 2005; Hassard 2004). The researchers here intended that the students be given an opportunity to think of steps or ways to approach the problems presented to them. That is, here we had an expectation that they should approach the experiment in a logical and systematic manner, like scientists. The data presented here thus provide insights into student understanding of scientific inquiry.

The findings suggest that the students in these groups adhered to a fairly traditional 'scientific method' approach that involved 'fair testing' (Hume and Coll 2008). Their approach resulted in them forming hypotheses to be tested by collecting data, and conducting 'scientific' experiments, in which they controlled all but one variable. However, a key difference here was the use of the POE activities, in which these students also sought to predict the outcome of their results in advance, and explain the expected results.

Many students provided logical steps in their experimental design in order to test their hypotheses. The experimental procedure was clear and simple and the students identified three groups of variables (i.e. independent variable, dependent variable and controlled variable) for investigation in the experiment, as seen in the following excerpt from one group report of the practical class.

> Problem – Influence of surface of eggshells on the rate of a reaction
>
> Hypothesis – The different surface of eggshells gives a different rate of reaction
>
> Independent variable – Influence of surface of eggshells
>
> Dependent variable – The rate of reaction
>
> Controlled variable – Size of Erlenmeyer flask, type of acid used, concentration of acid, reaction temperature, source of eggshells, laboratory environment

In this study, the experiment was different to what they usually encountered, mostly in that students were expected to design their own experimental procedure after they identified the variables and the problem (as above). The students reported their experimental procedure in their laboratory documentation, as seen in the following excerpt from one group report of the practical class:

> Weigh eggshells 0.1 g and then pour them into the flask. … Pour HCl (aq) 4.0 ml into the vial and then place it into the Erlenmeyer flask (be careful not to mix HCl with

> egg-shells) … fill the water into the 25.0 ml burette. … Connect the burette and the flask with the U-tube and the rubber stopper. … Shake gently the flask, mixing HCl and eggshells together. … Observe the volume of CO_2 in the burette and record the results over time. … Change the type of acid used from HCl to vinegar and then repeat the experimental procedure.

Next, the students had to conduct the experiment. The starting point here was sample preparation. The sample preparation in this experiment involved eggshells and solutions of acids. In this experiment, there is no single method of sample preparation for the solid reactant (i.e. the eggshells), meaning students had to decide how to prepare the solid sample themselves. The eggshells were collected and their surfaces mechanically cleaned. From analysis of students' laboratory documents it seems they felt the particle size of eggshells should be consistent, and thus they ground the shells to obtain a fine powder with a uniform, homogeneous, particle size (Figure 2). It seems that many students had learned how to conduct some aspects of this experiment when they engaged in previous practical classes at school. For example, many students readily understood the preparation of the solid sample and the acids before doing the experiment and they thus provided detailed instructions of how this should be done, as seen in the excerpt below.

> Sample preparation of eggshells – In this part, the particle sizes of the solid reactant should be made at least into three sizes: big, medium and small (like sand) size. The white layer which covers the eggshells should be removed before grinding.
>
> Preparation of the concentration of acid – The concentration of acid used in this experiment is 0.5, 1.0, 1.5 and 2.0 M HCl. These concentrations were made by diluting 2.0 M HCl.

Here in Figure 2 we see evidence of clear planning in the three samples of varying particle size, and the diagram which illustrates the experimental set-up to be used to measure the amount of gases produced over time (collection by downward displacement of water).

Interestingly, for the dilution of the solutions, students showed a good understanding of the preparation of chemical solutions, and they were able to solve problems, albeit algorithmically. The formula $C_1V_1 = C_2V_2$ was generally used to calculate the

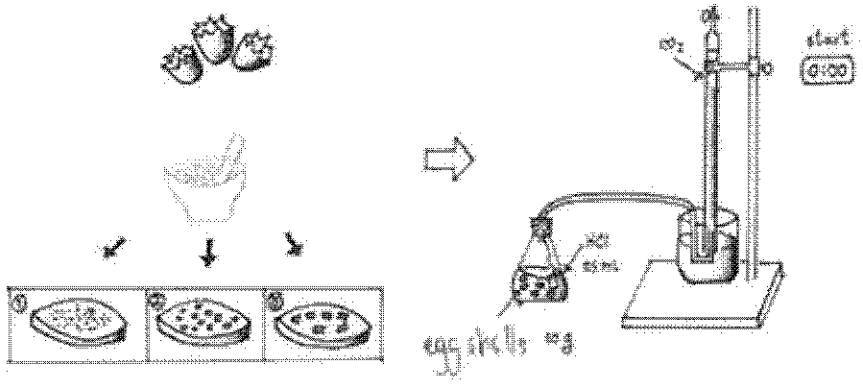

Figure 2. Students' experimental design for the preparation of eggshells and the collection of carbon dioxide.

acquired concentration of hydrochloric acid or vinegar. However, some students did not give any units of concentration when doing their calculations.

Student conceptual understanding of chemical kinetics concepts

One common issue in the teaching and learning of chemical kinetics is that students need to be able to explain the basic concept of rates of reaction, i.e. how variables (e.g. surface of the solid reactant, concentration, temperature and type of acid used) affect the rate of a chemical reaction. It is important not only to find out the students' conceptual understanding of chemical kinetics, but also to investigate their alternative conceptions of these ideas. The findings of this part of the study come from analysis of participants' laboratory documentation with respect to their understanding of chemical kinetics.

In this study, the students were introduced to the rates of reaction for different examples, and investigated the influence of different variables (i.e. surface of solid reactant, concentration of acid, temperature of a reaction and type of acid) on the rate of a reaction. The concept here then is first-order chemical kinetics, and the experiment involves students measuring the amount of gaseous carbon dioxide formed from the reaction of an acid with calcium carbonate (i.e. hydrochloric acid or vinegar and calcium carbonate in the form of an everyday material, eggshells) at different time intervals. The first stage of reporting the experiment is to present data using graphs or tables. In this way, when a variable is changed in an experiment, the data presented include the changes in the independent and dependent variables.

In general, here the students carried out the investigation of the influence of the surface area of eggshells for two different particle sizes (there is no standard particle size needed in the preparation of the solid sample – see above). Students in each group varied the particle size of eggshells themselves, and to explain the influence of surface area of the solid reactant and the rate of reaction, the students commonly reasoned that the change of the rate of a reaction is due to changes in physical dimensions of the solid reactant (Figure 3). A typical student response, reproduced here from a report, was that they concluded that:

> The rate of a reaction is dependent on the surface of the solid reactant (eggshells). If the size of eggshells is big, the rate of a reaction is slow. On the other hand, if the size of eggshells is small, the rate of a reaction is fast.

Interestingly, some students drew upon the analogy of a cube to explain the increase in the surface area of solid reactants. This was perhaps because it was simple for students to understand in their mind, an important feature of student-generated analogy (see Coll, France, and Taylor 2005): 'If we put four cubes together, the surface area is only 16 cm^2. However, if we separate all four cubes away from each other, the surface area is 24 cm^2.'

In a given experiment, the students generally carried out the reaction at four different concentrations of acid. In general, the students prepared the concentrations of both hydrochloric acid and vinegar at 0.5 M, 1.0 M, 1.5 M, and 2.0 M. To explain the increase in the rate of a reaction at higher concentrations, most said the effect of concentration of acid used was due to the number of particles in the solution. For example, some students carried out the experiment between 400 mg of eggshells, and 5 ml acid at a fixed temperature of 303K, and explained their observations thus: 'If

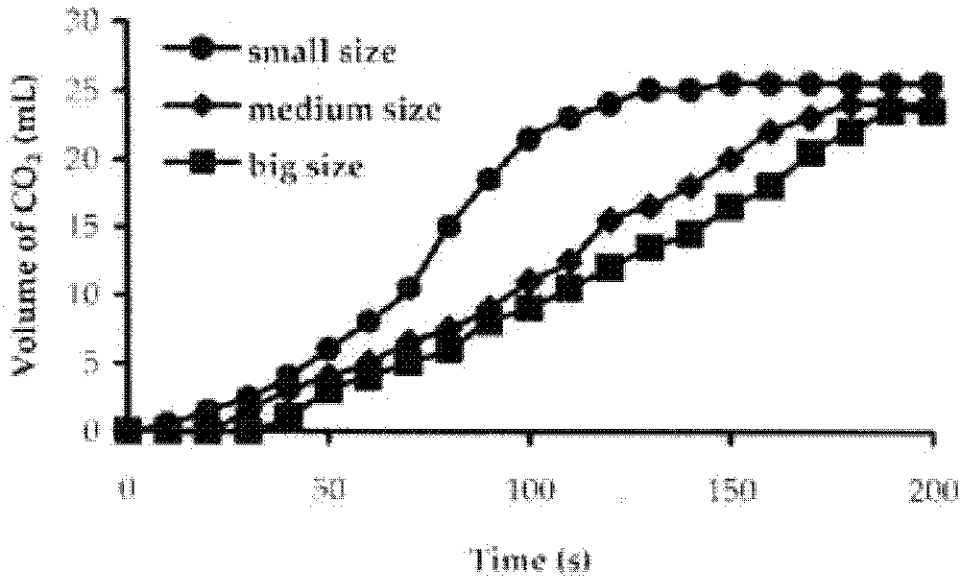

Figure 3. Students' laboratory data – the surface of the solid reactant (eggshells) and the volume of gaseous carbon dioxide formed.

the acid used is higher concentrations, the rate of a reaction increases, because higher concentrations have many molecules that can react more than low concentrations'.

To investigate the influence of temperature, the students carried out the reaction at least at two different temperatures (Figure 4). They started doing a reaction at a low temperature and then moved on to higher temperatures, although some started at higher temperatures and moved to lower temperatures. The students that changed from room temperature to higher temperature reasoned pragmatically that it was easier to increase the temperature using a water bath. To explain the influence of different temperatures on the rate of a reaction, students observed that 'the rate of a reaction increases at higher temperatures'. This they reasoned was due to increased kinetic energy of the reacting particles, in accord with the scientific view. For instance, some students carried out an experiment with 100 mg large surface area eggshells and 1.0 M HCl at three different temperatures:

> From the experiment, when increasing the temperature for a reaction, the kinetic energy of reactant molecules increases. So, molecules move faster and more collision. The rate of a reaction increases and then the reaction occurs quickly.

It is somewhat surprising that some students provided considerable detail in their descriptions, as seen in an excerpt from a student report reproduced below.

> The rate of a reaction is dependent on the temperature. So, when you also give the temperature, if the reaction is endothermic, the rate of a reaction increases. In contrast, if the reaction is exothermic, the rate of a reaction decreases.

Finally, the students investigated the influence of different types of acid – hydrochloric acid and vinegar – on rates of reaction. Here, the students retained the same

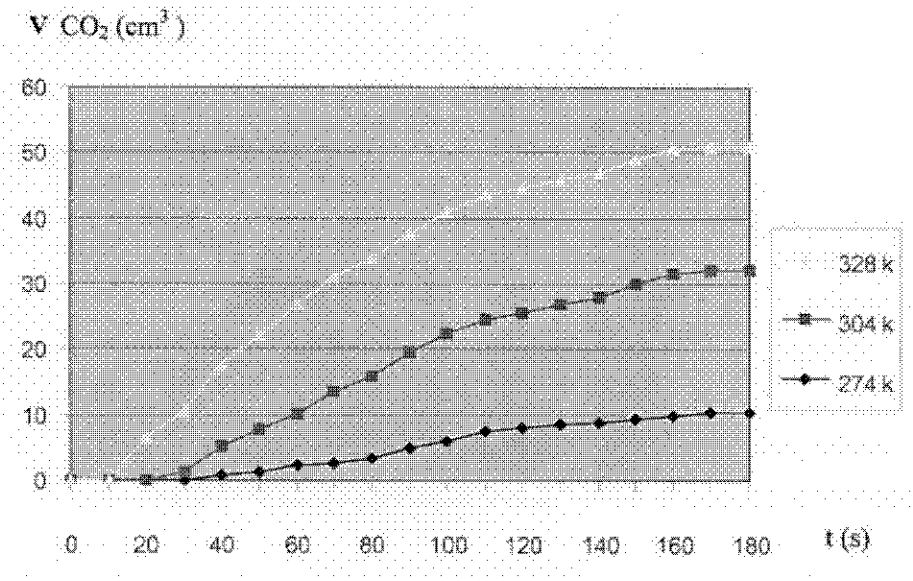

Figure 4. Students' laboratory data – the temperature of the reaction and the volume of gaseous carbon dioxide formed.
Note: the reaction has not at this early stage of the reaction gone to completion, at completion the reaction produces the same amount of gas.

conditions, other than the acid. To explain changes in the rate of a reaction as a result of the different acid used, most students explained it in terms of the 'strength' of the acids; again in accordance with the scientific view. For instance, some students carried out an experiment between 100 mg large surface of eggshells and 0.5 M HCl, and replaced the HCl with vinegar (acetic acid). Students again provided quite detailed responses, and concluded that:

> The rate of a reaction increases when using the strong acid [i.e. HCl]. On the other hand, the rate of a reaction decreases when using the weak acid. HCl is more active than vinegar. Hydrochloric, a strong acid, dissociates more completely when it dissolves in water and it is a good $H^{|}$ donor. On the other hand, vinegar, a weak acid, dissociates only slightly when it dissolves in water and it is also a poor $H^{|}$ donor.

After completing the experiment, in whole-class discussions, the experimental data from student investigations of chemical kinetics were analysed by the class to compare the rates of reaction by plotting the relationships between the amount of carbon dioxide produced and the variables over time using commonly available software (i.e. Solver Parameters in Microsoft Excel). Students typically explained their findings thus:

> At the beginning, the slope of graphs is very sharp, because the rate of a reaction is large. As the reaction progresses, the reaction becomes slower. The rate of a reaction decreases, eventually to zero when the reaction is completed.

Students were able to perform the calculation of the rate of a reaction correctly. However, a few students still had problems with the calculations, perhaps because it was the first time that they had done such calculations by themselves.

Findings from the survey

In this study, all first year undergraduate science students were familiar with the teaching and learning of chemical kinetics on a general chemistry laboratory course. Before allowing students to do the experiment, students (n = 129) in groups were randomly selected to perform a pre-test survey about variables which affect the rate of a reaction. After completing the experiment, students (n = 103) were then selected to complete a post-test survey. These tests, available from the authors, were similar in nature and contained questions deemed by a panel of experts to be suitable for this educational level. Students were provided with a balanced equation for the reaction of acid with carbonate and asked questions such as how particle size, temperature or other variables affect the rate of reaction. They were also asked to provide explanations for their answers. A comparison of the pre-test and post-test surveys is provided in Figure 5. The findings from the pre-test survey showed that 99 (76.7%), 55 (42.6%), 60 (46.5%) and 97 (75.2%) of the participating students provided a correct answer with respect to surface area of the solid reactant, concentration of acid, temperature of reaction and type of acid, respectively. Of the four variables, it was noted that students held a poor conceptual understanding of the effect of concentration and temperature on reaction rate. In order to investigate student understanding, the participating students again completed a post-test survey in groups after doing the experiment. From the post-test survey, scores of 95 (92.2%), 76 (73.8%), 91 (88.3%) and 89 (86.4%) correct responses were obtained for the surface area of the solid reactant, concentration of acid, temperature of reaction and type of acid, respectively.

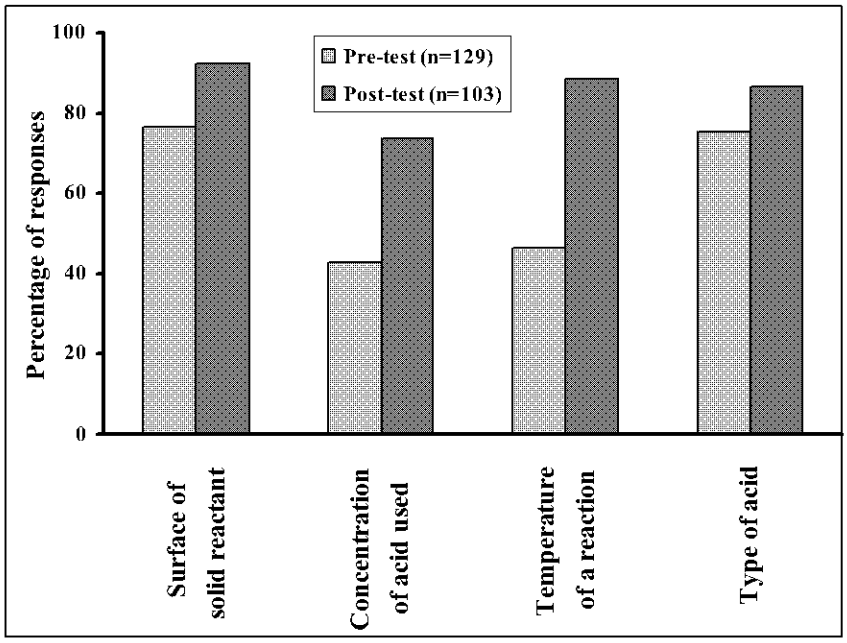

Figure 5. Comparison of pre-test and post-test survey of students' responses on the chemical kinetics laboratory before and after doing an inquiry-based practical chemistry class.

Student perceptions of the role of the teacher

The Thailand *National science education standards* (NRC 1996) state that active engagement of students in learning science is an importance aspect of effective science teaching. In this study, the role of the teacher was manifestly different to the norm, and it was of interest to see how this was perceived by the students. Here it was intended that the teachers would act as a facilitator of learning – consistent with social constructivism (see above). Hence, they had to pose problems to their students in the experiment, and to encourage useful discussion between students about the issues. In order to understand the role of teachers, students also provided their reflections on the role of the teacher in practical classes (see Table 1).

The students' responses to items 3, 4 and 5 are interesting in that the majority of students showed that the teachers in classes were friendly and attempted to help students when they found difficulties in class. This suggests the students enjoyed a different role of the teacher than they were used to. This is somewhat at odds with the normal situation in Thai classrooms (MOE 1996). However, some caution is needed in interpretation of this finding. As well as the fact that here the activities were likely perceived as more interesting and more exciting for teachers and students alike, the positive response noted in Table 1 also may be a result of the low ratio of teachers, including teaching assistants, to students of around 1:20 in classes – much less than is normal in Thai schools. Such a ratio would obviously allow for more student–teacher interaction and probably less stress on the part of the teachers, and thus more enjoyment on the part of the teachers and students alike.

Student perceptions of the POE technique

White and Gunstone (1992) proposed that the POE technique is a good teaching strategy in science education. In support of this proposition, the POE strategy has been reported as successful in a number of studies (see, for example, Kearney et al. 2001; Kearney 2004). Here, in a given experiment about chemical kinetics of acid–base reactions (i.e. hydrochloric acid or vinegar and calcium carbonate in eggshells), students were first asked to discuss their ideas and make predictions of the actual outcome, and to give their reasons. Then, they performed the observations and explanations of the evolution of carbon dioxide gas (CO_2) produced in the experiment, and finally sought reconciliation of any discrepancies between their predictions and observations after completing the task. Students' responses showed that the students enjoyed using the POE technique during the experiment sessions (see Table 2).

Table 1. Students' responses to questionnaire items relating to the role of the teacher (n = 389) in the inquiry-based experiment.

Item		SD	D	N	A	SA
3.	In this experiment, the teacher was friendly to me	0	8	56	184	141
4.	In this experiment, the teacher was interested in answering my questions	1	5	59	183	141
5.	In this experiment, the teacher helped me when I had trouble in the class	2	11	64	205	107
10.	In this experiment, the teacher encouraged me to discuss my ideas with other students	2	19	126	197	45

Note: SD = strongly disagree; D = disagree; N = neither agree nor disagree; A = agree; SA = strongly agree.

Table 2. Students' views of the value of the four POE tasks used in the inquiry-based experiment (n = 389).

Item		SD	D	N	A	SA
13.	In this experiment, I felt that the POE was a useful way to predict	2	13	112	211	51
14.	In this experiment, I felt that the POE is a useful way to explain	2	9	106	211	61
17.	In this experiment, I learned how to use data to support my conclusion for chemical kinetics	1	11	105	228	44
20.	In this experiment, I felt that I learned to do things in a way more like scientists do	0	41	84	193	93

Note: SD = strongly disagree; D = disagree; N = neither agree nor disagree; A = agree; SA = strongly agree.

Student responses to items 13 and 14 suggest that the students felt that the POE was a useful strategy to predict the actual outcome. The responses to the other items suggest that the participants felt the POE approach helped them to make connections between what they predicted and observed in the experiment of chemical kinetics, and that it helped them understand the basic concepts of chemical kinetics (item 17), and how to do things in the ways scientists do (item 20).

Group learning

The science education literature suggests group learning can be an important component of modern teaching approaches. A fundamental outcome of effective group learning is for students to be able to communicate, explain, and justify their understanding, argue from data, and defend their conclusions within their group (NRC 2000). Here, the rationale of implementing group learning in the laboratory was so that students could come to understand more about the nature of science, and how scientists actually worked, i.e. the fact that scientists seldom work alone, and that they socially negotiate knowledge. Students' responses about working in groups are provided in Table 3.

The responses suggest that the majority of students enjoyed learning in groups (item 21). The working in group situations seem to provide ways of helping students to understand the social and procedural rules in the experiment. It seemed that students appreciated this new way of working in their practical classes, and that the majority of students attempted to share their ideas with group members (items 23, 25 and 28). Group activities can be used to engage students in communicating and negotiating in class. Finally, most students believed that the group discussions among

Table 3. Students' views about learning in groups for the inquiry-based experiment (n = 389).

Item		SD	D	N	A	SA
21.	I worked cooperatively in this experiment	2	5	34	191	157
23.	I shared ideas with other students while doing this experiment	1	5	72	196	115
25.	I felt that working in a group stimulated my thinking	0	11	53	207	118
28.	I learned ideas from other students in my group	0	8	69	224	88
30.	I felt that the group discussion helped me to understand the concept of chemical kinetics	2	13	83	219	71

Note: SD = strongly disagree; D = disagree; N = neither agree nor disagree; A = agree; SA = strongly agree.

group members helped them a lot in understanding the basic concepts of chemical kinetics (item 30).

Summary

The research findings of this study suggest that engaging students in inquiry-based practical chemistry classes produces sound learning outcomes in terms of conceptual understanding of chemical kinetics, the ability to design and conduct experiments in chemical kinetics, and the nature of scientific inquiry. The students were also able to explain the changes in the rate of a chemical reaction based on kinetic theory and drew upon energy and particle theory to explain changes in rates of reaction. They seemed to be quite clear on how to conduct experiments, and the notion of investigating variables by changing each separately, while maintaining the others constant. Hence, overall analysis of students' laboratory documentation suggests that most students had a better conceptual understanding of chemical kinetics.

As noted above, inquiry-based practical classes in Thailand represent a very different teaching approach. However, in addition to sound conceptual understanding of chemical kinetics evidenced in their laboratory reports, the students' responses to the survey instrument suggests that they enjoyed this 'new' way of learning, they were comfortable about the very different role the teacher assumed, and they enjoyed working in groups. The new experiment here was conducted in order to allow science students to develop student-centred learning processes based on inquiry-based learning. Students had done things in the way that scientists do. As noted in the findings, they designed the experimental procedure themselves, and this seemed to help them gain a better understanding of the process of scientific inquiry. This can be seen from an analysis of their procedures, which consisted of the following steps for experimental design: state the problem, make hypotheses, make predictions, make observations, provide an explanation, and construct their own understanding from group discussions after completing the experiment. This is in marked contrast to the 'normal' situation for teaching chemical kinetics in Thailand, which more often simply involves following laboratory instruction or teacher demonstrations.

Discussion

Consistent with a case study approach, the data interpretation of this research was conducted within the interpretive paradigm described by Merriam (1988) and so the transferability of our findings is best judged by the reader. Here we attempt to interpret our findings in relation to other reports of research in the literature. The authors here have attempted to provide insights into the learning of chemical kinetics by first year science students in Thailand when using inquiry-based learning incorporating a series of POE activities. A number of themes have emerged from this research. The research findings reported here have some similarities to work by Hofstein and Lunetta, (2004), Wellington (1998), and Woolnough (1991), all of whom investigated laboratory science education at the tertiary level. The new experiment here placed a high value on 'hands-on' activities, and students were deeply engaged in the experiment in the form of student-centred learning as suggested in these reports (see also Tamir 1991).

The new experiment developed in this work was similar in nature to that of Choi and Wong (2004), who focused on acid–base reactions which demonstrated first-order

kinetics, but involving the application of a datalogger (i.e. a computer interfaced to one or more sensors, see above). However, datalogger experiments are expensive to set up, and are not generally suitable in the Thailand educational context, where teachers typically do not have access to such electronic instruments. One intention of this new experiment was to relate the laboratory class to daily life, since the chemicals used in the experiments were, sometimes, not purchased from a chemical company. This also introduced an element of student choice, with respect to research design and the conduct of the experiment – in a way that might not have been the case if they were given, say, a laboratory sample of calcium carbonate of uniform particle size. Another factor was that the solid reactant, calcium carbonate, was in a form (i.e. eggshells) that could be easily changed by grinding to different particle sizes. Moreover, students were also provided with opportunities to investigate other factors that might influence the rate of reaction, such as concentration of the acid used, temperature and the type of acid used.

As noted in the research findings, most of these Thai students seemed to have a better conceptual understanding of chemical kinetics after doing the experiments. A key feature was the move from passive to active learning, since the new experimental design was developed to enhance student-centred learning processes based on inquiry-based learning. Interestingly, one of the differences from other reported work is that, in these practical chemistry classes, the learning also comprised the development of the methodology to investigate the influence of some variables on rates of reaction, and specifically to use the POE strategy in small groups. The authors found that the POE tasks in the form of paper-based drawings on sheets seemed to help enhance student learning of chemical kinetics.

Finally, the research findings reported here suggest the students developed an understanding of inquiry that went beyond simply 'fair testing'. Hume and Coll (2007, 2008) noted that many so-called inquiry-based experiments are not much different in principle from conventional 'cookbook' style experiments, in that the former are also often rather formulaic in nature. However, the inquiry-based experiment as used here did provide these Thai students with some insights into how scientists conduct research. The students had to identify the problem, design an appropriate method, decide how to collect and record data, and perhaps most importantly, by drawing on the POE activities, predict the results and offer explanations. The use of interactive groups and whole-class discussions also sought to reinforce the socially-negotiated nature of scientific knowledge; more consistent with more holistic views of the nature of science and genuine inquiry-based learning (Hume and Coll 2007, 2008).

Conclusions and implications

Chemical kinetics is an important concept in introductory chemistry courses. From other reported work, instruction in chemical kinetics is typically teacher-dominated at both the secondary school and tertiary levels, and this also is the case in Thailand – the context for this inquiry. The research reported here seeks to shift undergraduate science students from passive learning to active learning, and involved some 413 first year students at Mahidol University in Thailand, of whom 389, consisting of 129 males and 260 females, completed a questionnaire about the experiment. A key feature needed to move students from passive to active learning was the use of the POE strategy, along with small group and whole-class discussions. Students who

participated were asked to design the experimental procedure themselves, in order to investigate the reaction of acids and bases. A number of variables were here investigated by changing each separately, while maintaining all others constant, including solid surface area, concentration, temperature and type of acid. Overall, the research findings suggest that most students had a better understanding of chemical kinetics, were able to explain the changes in the rate of a chemical reaction, and also developed a better conceptual understanding of chemical kinetics both qualitatively and quantitatively.

Hence, the authors suggest here that science teachers may wish to consider teaching chemical kinetics using simple chemical reactions and materials related to everyday processes, and based on inquiry learning. An additional advantage of the experiment used here is that it is not particularly hazardous, and so is convenient for science teachers to apply in class.

One feature of teaching chemical kinetics is that the calculations, particularly at the university level, and the concepts are more complex, and complex equations are often used to describe the kinetics of a reaction, such as differential equations. The authors observed that some of the first year students in this work did not know how the equations are derived, or how to use the equations for calculating the rate of a reaction. Therefore, in this research, the authors recommend the use of computers, and, as for example here, the experimental data from the experiments was easily analysed using Solver Parameters in the tool function of Microsoft Excel, which enable students to plot the relationship between the production of carbon dioxide and time. As shown in the findings, the students were able to see how the rate of a reaction changed for different experiments, and how to investigate the influence of variables (e.g. solid surface area, concentration, temperature and type of acid) on the rate of reaction.

Finally, the authors suggest that science teachers modify the experiments to suit their own needs and circumstances using, say, other variables, such as catalysts or the size of the reaction flask, for students to investigate how the rate of a reaction differs from others. Students here did not investigate the influence of catalysts because of limited time to carry out the experiments.

Acknowledgements

This work was supported by the Thailand Research Fund (TRF), the Postgraduate Education Research Program in Chemistry (PERCH), and the Department of Chemistry, Faculty of Science, Mahidol University, Bangkok, Thailand.

References

Billson, J.M. 1986. The college classroom as a small group: Some implications for teaching and learning. *Teaching Sociology* 14: 143–51.

Brown, A. 1989. *Group work.* Aldershort, UK: Gower.

Carin, A.A., J.E. Bass, and T.L. Contant. 2005. *Teaching science as inquiry.* Columbus, OH: Pearson Education.

Choi, M.M.F., and P.S. Wong. 2004. Using a datalogger to determine first first-order kinetics and calcium carbonate in eggshells. *Journal of Chemical Education* 81: 859–61.

Coll, R.K., B. France, and I. Taylor. 2005. The role of models and analogies in science education: Implications from research. *International Journal of Science Education* 27: 183–93.

Driver, R., H. Asoko, J. Leach, E. Mortimer, and P. Scott. 1994. Constructing scientific knowledge in the classroom. *Educational Researcher* 23: 5–12.

Duit, R., and D.F. Treagust. 1995. Students' conceptions and constructivist teaching approaches. In *Improving science education,* ed. B.J. Fraser and H.J. Walberg. Chicago, IL: International Academy of Education.

Duit, R., and D.F. Treagust. 1998. Learning in science – from behaviourism towards social constructivism and beyond. In *International handbook of science education,* ed. B.J. Fraser and K.G. Tobin. Dordrecht, The Netherlands: Kluwer.

Gabel, D.L., and D.M. Bunce. 1994. Research on problem solving: Chemistry. In *Handbook of research on science teaching and learning: A project of the National Science Teachers Association,* ed. D.L. Gabel. New York: Macmillan.

Hassard, J. 2004. *The art of teaching science: Inquiry and innovation in middle school and high school.* Oxford, UK: Oxford University Press.

Hart, C., P. Mulhall, A. Berry, J. Loughran, and R. Gunstone. 2000. What is the purpose of this experiment? Or can students learn something from doing experiments? *Journal of Research in Science Teaching* 37: 655–75.

Hegarty-Hazel, E. 1990. *The student laboratory and the science curriculum.* London: Routledge.

Hodson, D., and J. Hodson. 1998. From constructivism to social constructivism: a Vygotskian perspective on teaching and learning science. *School Science Review* 79: 33–41.

Hofstein, A., and V.N. Lunetta. 1982. The role of the laboratory in science teaching neglected aspects of research. *Review of Educational Research* 52: 201–17.

Hofstein, A., and V.N. Lunetta. 2004. The laboratory in science education: Foundations for the twenty-first century. *Science Education* 88: 28–54.

Hofstein, A., R. Shore, and M. Kipnis. 2004. Providing high school chemistry students with opportunities to develop learning skills in an inquiry-type laboratory: A case study. *International Journal of Science Education* 23: 47–62.

Hofstein, A., and H.J. Walberg. 1995. Instructional strategies. In *Improving science education,* ed. B.J. Fraser and H.J. Walberg. Chicago, IL: International Academy of Education.

Hume, A., and R.K. Coll. 2007. Student engagement in authentic scientific inquiry: The curriculum intent and the classroom reality. Paper presented at the annual meeting of the National Association for Research in Science Teaching, April, 15–18, in New Orleans, LA.

Hume, A., and R.K. Coll. 2008. Student experiences of carrying out a practical science investigation under direction. *International Journal of Science Education* 30, no. 9: 1201–28.

Johnson, D.W., and R.T. Johnson. 2005. Learning groups. In *The handbook of group research and practice,* ed. S.A. Wheelan. London: Sage.

Justi, R. 2003. Teaching and learning chemical kinetics. In *Chemical education: Towards research-based practice,* ed. J.K. Gilbert, O.D. Jong, R. Justi, D.F. Treagust and J.H. Van Driel. Dordrecht, The Netherlands: Kluwer.

Justi, R., and J.K. Gilbert. 1999a. A cause of a historical science teaching: Use of hybrid models. *Science Education* 83: 163–77.

Justi, R., and J.K. Gilbert. 1999b. History and philosophy of science through models: The case of chemical kinetics. *Science and Education* 8: 287–307.

Kaartinen, S., and K. Kumpulainen. 2002. Collaborative inquiry and the construction of explanations in the learning of science. *Learning and Instruction* 12: 189–212.

Kearney, M. 2004. Classroom use of multimedia-supported predict–observe–explain tasks in a social constructivist learning environment. *Research in Science Education* 34: 427–53.

Kearney, M., D.F. Tregust, S. Yeo, and M. Zadnik. 2001. Student and teacher perceptions of the use of multimedia supported predict–observe–explain tasks to probe understanding. *Research in Science Education* 31: 589–615.

Klopfer, L.E. 1990. Learning scientific enquiry in the student laboratory. In *The student laboratory and the science curriculum,* ed. E. Hegarty-Hazel. London: Routledge.

Laws, P.M. 1996. Undergraduate science education: A review of research. *Studies in Science Education* 28: 1–85.

Lazrowitz, R., and R. Tamir. 1994. Research on using laboratory instruction in science. In *Handbook of research on science teaching and learning: A project of the National Science Teachers Association,* ed. D. L. Gabel. New York: Macmillan.

McComas, W.F., M.P. Clough, and H. Almazroa. 1998. The role and character of the nature of science. In *The nature of science in science education: Rationales and strategies,* ed. W.F. McComas. London: Kluwer.

Merriam, S.B. 1988. *Case study research in education: A qualitative approach.* San Francisco, CA: Jossey-Bass.
Millar, R. 1998. Rhetoric and reality. In *Practical work in school science: Which way now?,* ed. J. Wellington. London: Routledge.
Ministry of Education (MOE). 1990. *The curriculum A.D. 1979 (revised A.D. 1990).* Bangkok: Ministry of Education.
Nakhleh, M.B., J. Polles, and E. Malina. 2002. Learning chemistry in a laboratory environment. In *Chemical education: Towards research-based practice,* ed. J.K. Gilbert, O.D. Jong, R. Justi, D.F. Treagust and J.H. Van Driel. Dordrecht, The Netherlands: Kluwer.
National Research Council (NRC). 1996. *National science education standards.* Washington, DC: National Academy Press.
National Research Council (NRC). 2000. *Inquiry and the national science education standards: A guide for teaching and learning.* Washington, DC: National Academy Press.
Office of National Education (ONE). 1997. *Education in Thailand 1997.* Bangkok: Office of the Prime Minister.
Office of the Prime Minister (OPM). 2000. *Thailand into the 2000's.* Bangkok: Office of the Prime Minister).
Ogborn, J. 1977. *Practical work in undergraduate science.* London: Heinemann.
Parkash, B., and A. Kumar. 1999. Chemical kinetics illustrated by an improvised experiment. *School Science Review* 80: 114–7.
Pinnell, G.S. 1984. Communication in small group settings. *Theory into Practice* 23: 246–54.
Pravalpruk, S. 1999. Learning and assessment in the science classroom in Thailand. *Assessment in Education* 6: 75–82.
Rivera, F.D. 2003. In Southeast Asia: Philippines, Malaysia, and Thailand: Conjunctions and collisions in the global cultural economy. In *International handbook of curriculum research,* ed. W.F. Pinar. London: Lawrence Erlbaum Associates.
Schwartz, R.S., N.G. Lederman, and B.A. Crawford. 2004. Developing views of nature of science in an authentic context: An explicit approach to bridging the gap between nature of science and scientific inquiry. *Science Education* 88: 610–45.
Tamir, R. 1991. Practical work in school science: An analysis of current practice. In *Practical science: The role and reality of practical work in school science,* ed. B.E. Woolnough. Buckingham, UK: Open University Press.
Tobin, K.G., and D. Tippins. 1993. Constructivism as a referent for teaching and learning. In *The practice of constructivism in science education,* K.G. Tobin. Washington, DC: AAAS Press.
Vygotsky, L.S. 1978. *Mind in society: The development of higher psychological processes.* Cambridge, MA: Harvard University Press.
Webb, N.M. 1982. Student interaction and learning in small groups. *Review of Educational Research* 52: 421–45.
Wellington, J. 1998. Practical work in school science. In *Practical work in school science: Which way now?* J. Wellington. London: Routledge.
White, R., and R. Gunstone. 1992. *Probing understanding.* London: Falmer Press.
Woolnough, B.E. 1991. *Practical science: The role and reality of practical work in school science.* Buckingham, UK: Open University Press.